COMPARATIVE STUDY ON THE EFFECT OF DIFFERENT RUBBER WASTE AS FILLER ON RECYCLED PVC

KEE YEE HANG

UNIVERSITI TUNKU ABDUL RAHMAN

COMPARATIVE STUDY ON THE EFFECT OF DIFFERENT RUBBER WASTE AS FILLER ON RECYCLED PVC

KEE YEE HANG

A project report submitted in partial fulfilment of the

requirements for the award of Bachelor of Engineering

(Honours) Petrochemical Engineering

Faculty of Engineering and Green Technology

Universiti Tunku Abdul Rahman

May 2024

DECLARATION

I hereby declare that this project report is based on my original work except for citations and quotations which have been duly acknowledged. I also declare that it has not been previously and concurrently submitted for any other degree or award at UTAR or other institutions.

Signature : _____

Name : Kee Yee Hang

ID No. : 19AGB02779

Date : 16/5/2024

APPROVAL FOR SUBMISSION

I certify that this project report entitled **"COMPARATIVE STUDY ON THE EFFECT OF DIFFERENT RUBBER WASTE AS FILLER ON RECYCLED PVC"** was prepared by **KEE YEE HANG** has met the required standard for submission in partial fulfilment of the requirements for the award of Bachelor of Engineering (Honours) Petrochemical Engineering at Universiti Tunku Abdul Rahman.

Approved by,

Signature : _____

Supervisor : Dr. Mathialagan a/l Muniyadi

Date : 16/5/2024

Signature : _____

Co-Supervisor : Dr.Yamuna a/p Munusamy

Date : 16/5/2024

Special dedicated to

My beloved parents, supervisors, lecturers, seniors, and friends.

ACKNOWLEDGEMENTS

I would like to express my gratitude to everyone who helped and supported me in successfully completing this research. I would especially like to thank my research supervisor, Dr. Mathialagan Muniyadi, for his unwavering support, expertise, experience, and guidance throughout my research.

On top of that, I would also like to express my gratitude to all the Petrochemical Laboratory officers for their valuable guidance in performing laboratory work and ensuring laboratory safety. Additionally, I am thankful to my research moderator, Dr. Yamuna Munusamy, for providing constructive comments that have significantly contributed to the improvement of this research.

Besides that, I also appreciated the care and support from my family and course mates, who were compassionate and encouraging. Lastly, I would like to express my heartfelt gratitude to CY-Handee Rubber Moulding Sdn. Bhd. for generously providing us with the essential research materials and facilities.

COMPARATIVE STUDY ON THE EFFECT OF DIFFERENT RUBBER WASTE AS FILLER ON RECYCLED PVC

ABSTRACT

The rising amount of rubber waste and the usage of polyvinyl chloride (PVC) has contributed to severe environmental issues, which can be tackled by recycling rubber waste and PVC into value-added products. This research aims to develop a new composite using recycled PVC (rPVC) from carpet backing material with different types of rubber waste, known as Almost Like Unvulcanized Material (ALUM), which is an industrial rubber scrap, and cryogenically grounded waste tire powder (LeHigh) for car floor mat application. Composites containing rPVC and different loading of ALUM and LeHigh ranging from 0 to 30 wt% have been produced through melt mixing using a Brabender internal mixer at a temperature of 165 °C. The rubber particles were characterized using Fourier Transform Infrared Spectroscopy (FTIR), Particle Size Analysis (PSA), Thermogravimetric Analysis (TGA) and Scanning Electron Microscopy (SEM) to evaluate their functional groups, particle size distribution, thermal stability and surface morphology, respectively. Besides that, the effect of different rubber waste on the characteristics and properties of rPVC composites has been evaluated through FTIR, TGA, SEM, processing torque, tensile test, swelling absorption and hardness test. FTIR analysis confirmed that there was no chemical interaction between rPVC and the rubber particles. Addition of ALUM showed a reduction in the thermal stability, whereas LeHigh showed increasing thermal stability of rPVC composites. The melt mixing of rPVC also becomes harder when increasing both ALUM and LeHigh loadings, as

depicted by the increased processing torque caused by the stiffening of the composite system. Furthermore, the tensile strength, elongation at break and water absorption of the rPVC composites have been reduced, whereas the elastic modulus and hardness were improved by increasing both the filler loading. The SEM morphological study of the tensile fractured surface revealed that both ALUM and LeHigh particles have fairly good dispersion in rPVC at low filler loading. However, the dispersion and interfacial interaction of rubber particles with rPVC become weaker with increasing filler loading up to 30 wt%, leading to reduced tensile strength. The evaluation of the suitability of both ALUM/rPVC and LeHigh/rPVC for car floor mat application was carried out. The standard specification values desired to produce a car floor mat include a minimum tensile strength of 5 MPa, minimum elongation at break of 25 %, maximum water absorption of 2.5 % and Shore A hardness of 90 ± 5. Upon evaluation, the optimum loading of ALUM and LeHigh in rPVC suitable for car floor mat application is 10 wt% and 20 wt%, respectively, to produce a composite with properties fulfilling the standard specification values. However, by comparing both the rubber particles, Lehigh is more preferred and suitable to be used as filler in rPVC to produce the car floor mat as compared to ALUM. LeHigh can be added up to 20 wt% as compared to only 10 wt% of ALUM in rPVC, and the smaller particle size of LeHigh could produce a better adhesion to rPVC matrix to provide a better overall property as desired for the car floor mat application.

TABLE OF CONTENTS

LIST OF TABLES

LIST OF FIGURES

LIST OF SYMBOLS / ABBREVIATIONS

°C	Degree Celsius
cm	centimeter
g	Gram
J	Joule
K	Kelvin
kV	kilovolt
m	Meter
m_f	Final Mass
m_i	Initial Mass
min	Minute
ml	Milliliter
mm	millimeter
MPa	Megapascal
N	Newton
Nm	Newton-meter
psi	Pounds per square inch
rpm	Revolution Per Minute
$T_{50\%}$	Temperature at 50 % Mass Loss
W	Watt
wt %	Weight Percent
Ω m	Ohm-meter
μm	micrometer

ALUM	Almost Like Unvulcanized Material
AP	Acidification Potential
ATO	Antimony Trioxide
ATR	Attenuated Total Reflectance
C	Carbon
$CaCO_3$	Calcium Carbonate
CB	Carbon Black
CBS	Cyclohexyl Benzothiazole Sulfenamide
Cl	Chlorine
CO_2	Carbon Dioxide
CPVC	Chlorinated PVC
CR	Chloroprene Rubber
DINP	Diisononyl Phthalate
DIDA	Diisodecyl Adipate
DOP	Dioctyl Phthalate
DOTP	Dioctyl Terephthalate
DSC	Differential Scanning Calorimetry
DTG	Derivative Thermogravimetry
EDC	Ethylene Dichloride
EI	Emissions Intensity
ENR	Epoxidized Natural Rubber
EPDM	Ethylene-Propylene-Diene Monomer
FA	Fly Ash
FDA	Food and Drug Administration
FTIR	Fourier Transform Infrared Spectroscopy
GTR	Ground Tire Rubber
GWP	Global Warming Potential
H	Hydrogen
HCl	Hydrogen Chloride
HTP	Human Toxicity Potential
IIR	Butyl Rubber

IR	Infrared Radiation
IRSG	International Rubber Study Group
KBr	Potassium Bromide
NBR	Acrylonitrile Butadiene Rubber
NMF	NonMetallic Fractions
NR	Natural Rubber
O	Oxygen
PCBs	Printed Circuit Boards
POCP	Photochemical Ozone Creation Potential
POPs	Persistent Organic Pollutants
PP	Polypropylene
PPE	Personal Protective Equipment
PSA	Particle Size Analysis
PVC	Polyvinyl Chloride
PVC-M	Modified PVC
PVC-O	Molecularly Oriented PVC
rPVC	Recycled Polyvinyl Chloride
rPVC/ALUM 10	rPVC/ALUM Composite with 10 wt % ALUM
rPVC/ALUM 20	rPVC/ALUM Composite with 20 wt % ALUM
rPVC/ALUM 30	rPVC/ALUM Composite with 30 wt % ALUM
rPVC/LeHigh 10	rPVC/LeHigh Composite with 10 wt % LeHigh
rPVC/LeHigh 20	rPVC/LeHigh Composite with 20 wt % LeHigh
rPVC/LeHigh 30	rPVC/LeHigh Composite with 30 wt % LeHigh
SR	Synthetic Isoprene Rubber
TGA	Thermogravimetric Analysis
TOTM	Trioctyl Trimellitates
UHP	Ultra-High Pressure
US	United States
UV	Ultraviolet
VCM	Vinyl Chloride Monomer
WTP	Waste Tire Powder

ZnO	Zinc Oxide
ZnS	Zinc Sulfide

LIST OF APPENDICES

CHAPTER 1

INTRODUCTION

1.1 Background of Research

Nowadays, pollution due to plastic waste has become one of the most significant environmental issues in the world due to the increasing of disposable plastic products for conveniences, such as plastic bags, food wrappers and coffee cups, especially during the pandemic Covid-19 that augmented the demand of the plastic products for packaging purposes. Increasing demand for plastic throughout the world in various industries for a diverse range of applications, such as packaging, agriculture, automobile parts and electronic applications, also causes the accumulation of hundreds of millions of tons of plastic waste in the world after use, which leads to plastic pollution (Valavanidis, 2023). Plastic pollution can affect habitats and natural processes, reducing the ability of ecosystems to adapt to climate change and directly altering millions of people's livelihoods, food production capabilities and social well-being (Valavanidis, 2023). Thus, a proper management of plastic waste to reduce the impacts of plastic waste becomes a big concern in the world, besides reducing plastic consumption to decrease the amount of plastic waste. Recently, most of the plastic waste is managed by landfilling and incineration, while a small amount of the plastic waste is recovered through recycling and energy recovery processes (Comanita et al., 2020). However, the

plastic waste management method of landfilling and incineration poses a significant threat to the environment and public health, which are not the preferred options for plastic waste management. Hence, to achieve the goal of zero plastics in landfills with increasing environmental awareness in the public nowadays, implementation of the 3Rs, which includes reduction, reuse and recycling, and energy recovery through incineration, should be intensified and applied in a complementary manner to reduce the plastic production and negative impacts of plastic waste effectively.

Polyvinyl chloride (PVC) is one of the most widely used thermoplastic polymers, which is a synthetic plastic polymer with an amorphous structure produced by the polymerization of the vinyl chloride monomer. PVC is used in the manufacturing of packages, pipes and fittings, bottles, cables, toys, film and sheets and others due to its various properties of easy to process, UV stability and recyclability potential, which contributes to its high demand in the global market compared to other plastics. Although PVC acts as a universal polymer due to its relatively low cost and high performance, the production process of PVC by the polymerization of vinyl chloride monomer (VCM) produced by the thermal cracking of ethylene dichloride is very harmful to the environment and human health (Comanita et al., 2020). During the production of PVC, chlorine-based toxins and dioxins will be released into the surroundings due to the use of chlorine, with hazardous impacts on the environment and human health (Osmanski, 2020). Besides that, the applications of PVC now are mainly focused on single-use applications such as rubber mats, hose pipes, sealants and so on, which produce a high amount of disposal. In order to reduce the negative environmental impacts of PVC production with a high amount of plastic waste, the used PVC products have to be recycled; PVC can be recycled and reprocessed into other value-added applications nowadays, such as anti-slip bathroom mats and car floor mats.

On the other hand, the constant increase of rubber waste has also become a major environmental problem for countries in the world due to the high demand for rubber products, such as conveyor belts, rubber bearings, pipe seal rings, protective clothing

and footwear, hoses and so on and rising of rubber usage in the household, healthcare, industrial, military, automotive, civil and outer space applications (Nuzaimah et al., 2018). Among the various sources of rubber waste, tires of automobiles, trucks and motorcycles contribute to the majority of rubber waste to produce a hundred million scrap tires in the world due to the large volume produced with the high demand of vehicles (Chittella et al., 2021). Besides tires, other rubber waste, such as inner tubes, discarded and rejected rubber gloves, balloons, rubber bands and hoses, also contributed to the rubber waste numbers globally (Nuzaimah et al., 2018). Due to the rising numbers of discarded rubber products with the accumulation of rubber waste, the management of rubber waste becomes a worldwide problem as the current waste management method through landfilling and incineration poses negative impacts on the environment and public health. Therefore, in line with raising environmental concerns, reuse, recycling, recovery, and pyrolysis are widely used in the sustainable management of rubber wastes (Nuzaimah et al., 2018). Recently, the recycling method includes grinding the waste rubber and then incorporating the rubber particles into matrices such as concrete or polymer to develop into brand-new products, such as athletic tracks and playground surfaces, and as filler for polymer composites to create a new sustainable material with enhanced properties, which has been studied in the past few decades, is continued to expand and applied widely to ensure sustainable management of rubber waste products (Nuzaimah et al., 2018). However, this method is challenging to utilize waste rubber tires as a reinforcement material or filler in the polymeric material to form a composite to improve its properties and applications. One of the limitations is the coarse structure of the mechanically grinded rubber waste results in agglomeration issues and reduces the mechanical properties of the polymer system.

In this research, in order to solve the issues of accumulation of PVC and rubber waste throughout the world effectively in a sustainable way in line with raising environmental concerns and implementation of 3Rs, the used PVC or the recycled PVC is melt-mixing with the rubber waste through Brabender Internal Mixer to develop a new composite with new properties. The research will mainly focus on utilizing rubber waste

as a filler in recycled PVC from carpet backing material to form a composite and improvements contributed by the waste rubber on the properties of the composite. Two different types of rubber waste are used as filler in recycled PVC to produce the new composites in the research, which included the industrial rubber scraps from scuba diving products known as Almost Like Unvulcanized Material (ALUM). The second type of rubber waste is the waste tyre powder produced through the cryogenic grinding of tires, known as LeHigh. This research work will be carried out in collaboration with the rubber-producing company in Malaysia, CY Handee Rubber Mouldings Sdn. Bhd..

The first rubber waste used as filler for the recycled PVC from carpet backing material to produce a composite is the waste from the production of scuba diving products obtained from CY Handee Rubber Mouldings Sdn. Bhd., known as industrial rubber scrap or Almost Like Unvulcanized Material (ALUM). The rubber scrap was mechanically ground into granular particles and shredded before being incorporated into the polymer as the filler. Meanwhile, the second filler used in recycled PVC is the micronized waste tire powder obtained through cryogenic grinding of truck tires or known as LeHigh. In the earlier study by Ooi (2019), the cryogenic grinded LeHigh was added as filler in PVC to develop a new thermoplastic elastomer and study its characteristics and mechanical properties. The result showed that cryogenic grinded LeHigh as filler in PVC improved the thermal properties, hardness and elastic modulus of PVC. However, the agglomeration of cryogenic grinding LeHigh in PVC caused the produced PVC/LeHigh blends to have poor absorption resistance in water and solvent and reduced tensile strength of the PVC/LeHigh blends. Besides that, in the earlier study by Wong (2020), the cryogenic grinded ALUM was added as filler in PVC to form composites to study the processability and feasibility of the composite for its application with its characteristics and mechanical properties. The result proved that cryogenic grinded ALUM as filler in PVC improved the thermal stability, elastic modulus and hardness but reduced the tensile strength and elongation at break. ALUM agglomeration also lowered the water absorption resistance of composites with the tensile and water resistance properties.

Different from the previous studies, this research aims to develop a new composite by using two different types of rubber waste with dissimilar mechanical treatment processes to grind the rubber waste as filler in the recycled PVC from carpet backing material and study the characterizations and improvements contributed by the two different types of rubber waste on the composite properties. The new composites produced from the two rubber wastes as fillers in the recycled PVC from carpet backing material will be evaluated, whether they obey the minimum property specifications for car floor mat application, with the minimum ultimate tensile strength of 5 MPa, minimum elongation at break of 25 %, maximum water swelling of 2.5 % and Shore A hardness of 90 ± 5. The rubber waste particles (ALUM and LeHigh) were characterized by the refractive index test and Particle Size Analysis (PSA) to evaluate their characteristics, such as the mean diameter, specific surface area, particle size distribution, granulometric properties and the polydispersity of the particles. Other characterizations of ALUM and LeHigh include Fourier Transform Infrared Spectroscopy (FTIR), Thermogravimetric Analysis (TGA) and Scanning Electron Microscopy (SEM), were carried out to evaluate their functional groups, thermal stability and surface morphology respectively. In addition, the composites produced from recycled PVC, recycled PVC/ALUM and recycled PVC/LeHigh were characterized and tested via TGA, SEM, processing torque, tensile test, hardness test and swelling test to evaluate the effects of the two types of rubber waste as filler in recycled PVC (rPVC). The characterization of composites also was carried out by FTIR to evaluate any potential chemical interaction between the filler and rPVC. The optimum loading of the fillers (ALUM and LeHigh) in rPVC was determined after conducting all the characterizations and tests. The rubber waste filler that is most suitable and capable of enhancing the properties of rPVC and achieving the minimum property specification for car floor mat application from the new composite produced compared to rPVC will then be suggested with concrete justification to the industry.

1.2 Problem Statements

1.2.1 Increase in Rubber Waste with Low Recycling Rate

Recently, the high demand of rubber products and rubber usage in worldwide applications ranging from household, healthcare, industrial, military, automotive, civil and outer space applications have contributed to a large amount of rubber waste becoming a major environmental problem. International Rubber Study Group (IRSG) has predicted that the world's total rubber consumption will rise annually at an average of 2.8 % per annum from 2017 to 2025, with 28.05 million tonnes of world total rubber consumption in 2017, which indicates that more rubber waste will be generated throughout the world in the future (Nuzaimah et al., 2018). The typically used rubber for producing numerous types of products includes natural rubber (NR), styrene-butadiene rubber (SBR), nitrile, ethylene-propylene-diene monomer (EPDM) rubber and fluorocarbon rubber. These rubbers will then generate diverse sources of rubber waste that lead to excessive accumulation of rubber waste in the world, such as scrap tires, inner tubes, discarded and rejected rubber gloves, balloons, rubber bands, shoe soles, mattresses, hoses, seals, gaskets and diaphragms (Nuzaimah et al., 2018).

The global demand for rubber products is experiencing a significant increase year after year. According to statistics, the total amount of natural rubber produced worldwide in 2018 was almost 13.9 million metric tonnes. Asia Pacific created 91 % of the natural rubber consumed worldwide in 2018, whereas Europe, the Middle East and Africa combined to manufacture only 6.5 % of the world's natural rubber. Natural rubber is primarily used in manufacturing gloves, while synthetic rubbers are used mainly in the transportation industry to produce tires. By 2018, the global demand for tires for cars and trucks is anticipated to have surpassed 1.6 billion units, and by 2022, it reached 3.2 billion units (Chittella et al., 2021). The amount of discarded tires produced has increased rapidly due to the rise in automobile production. The worn-out natural and synthetic rubber material that accumulates into piles and takes years to disintegrate

organically will directly lead to the excessive accumulation of rubber waste. Figure 1.1 shows the consumption of natural and synthetic rubber worldwide from 2009 to 2022.

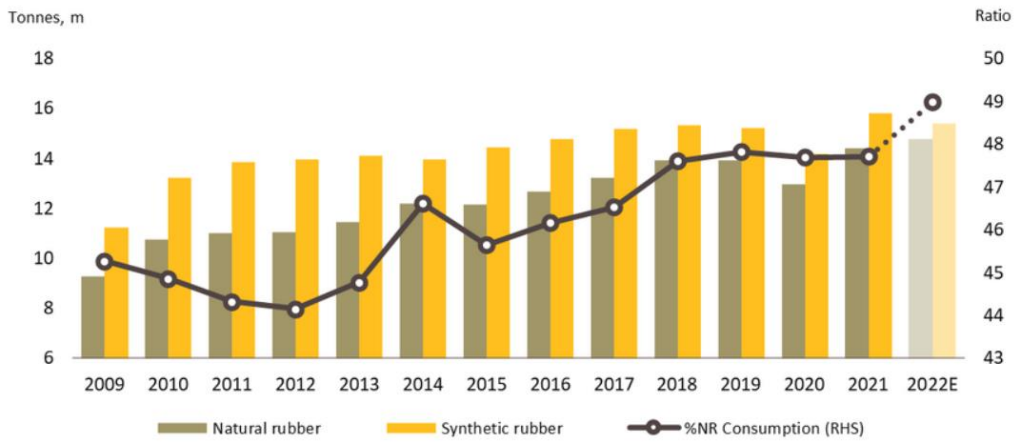

Figure 1.1: Consumption of Natural and Synthetic Rubber Worldwide from 2009-2022 (Sowcharoensuk, 2023)

Besides the growing global demand for rubber products that contribute to the high amount of rubber waste, the traditional rubber waste management methods of landfill disposal, open dumping, grinding the rubber waste into powder and incineration with a low recycling rate also cause the rubber waste cannot be processed or managed effectively and directly lead to the accumulation of rubber waste in the world. These waste management methods have limited the growth of integrated waste management techniques, such as recycling and recovery, aiming to reduce the source's waste and bring several negative impacts on the environment (Chittella et al., 2021). For instance, it was discovered that the United States produced 9.2 million tonnes of rubber and leather waste in 2018. Tires from cars, trucks, and motorbikes account for the majority of rubber waste produced. Clothing, shoes, gaskets, and furniture are additional sources of leather and rubber. Out of 9.2 million tonnes of rubber waste generated, only 1.7 million tonnes were determined as recyclable, which amounted to only 40 % of total tire waste produced, excluding its application for energy recovery and landfills (Chittella et al., 2021). Rubber products, especially synthetic ones, are challenging to recycle and

naturally degraded due to the vulcanization process to form the sulfur crosslinks between the polymer chains with the complex three-dimensional structure. Additionally, fillers, antioxidants, and other chemicals in rubber products increase their resistance to biodegradation and make them hard to reprocess into new products during recycling (Leong et al., 2022). Hence, developing multiple efficient waste management techniques besides improving present recycling techniques is crucial to reduce the amount of global rubber waste, as the current waste disposal measures are inefficient and will cause land, water and air pollution. In line with the rising environmental concerns of the public nowadays, sustainable management of rubber waste through reuse, recycling, recovery, and pyrolysis should be applied widely around the world to reduce the accumulation of rubber waste efficiently with less negative impacts on the environment.

1.2.2 Environmental Issue of PVC

The invention of plastics is one of the incredible technological achievements of the 20th century to manufacture diverse plastic products to be used broadly in various fields for packaging, building and construction, agriculture, and many other applications, due to their properties of lightweight, long life, low price and malleability (Lu et al., 2023). High global demand for plastic products causes plastic production to continuously increase annually from 2020 to 2023 and is predicted to rise until 2030, as shown in Figure 1.2. Among different types of plastics produced worldwide, polyvinyl chloride (PVC) accounted for 9.6 % of all plastics in 2020, ranking in fourth place compared to other plastics, as shown in Figure 1.3 (Lu et al., 2023). Polyvinyl chloride is an extensively used thermoplastic polymer throughout the world that is widely used in building and construction, automotive, packaging, piping and cable industries with various applications due to its long lifespan, strong, durable, lightweight, versatile and excellent mechanical, electrical, chemical, and thermal resistance properties (Miliute-Plepiene et al., 2021). Due to the high demand for PVC in the global market for various

worldwide applications, the high amount of used PVC from different streams, such as the construction and demolition sector, end-of-life vehicles and cables, contributed to the accumulation of large amounts of PVC waste in the world with negative impacts on the environment.

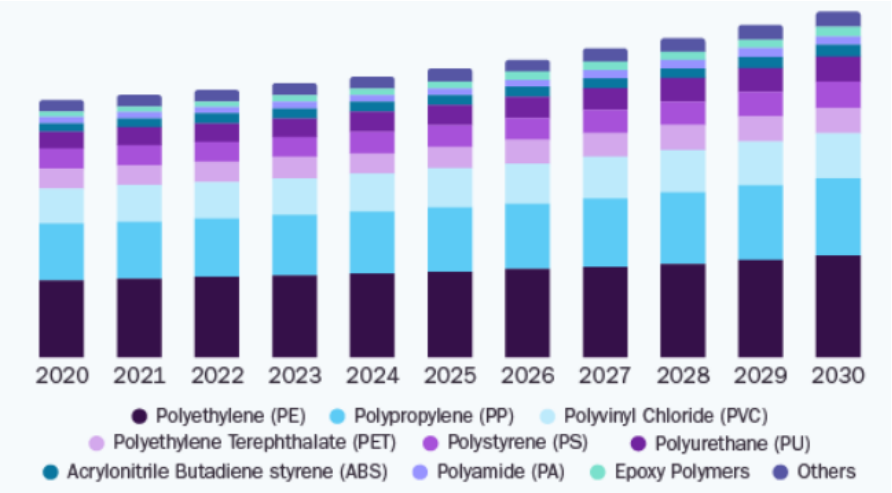

Figure 1.2: Global Production of Plastics from 2020-2030 (Waghmare, 2023)

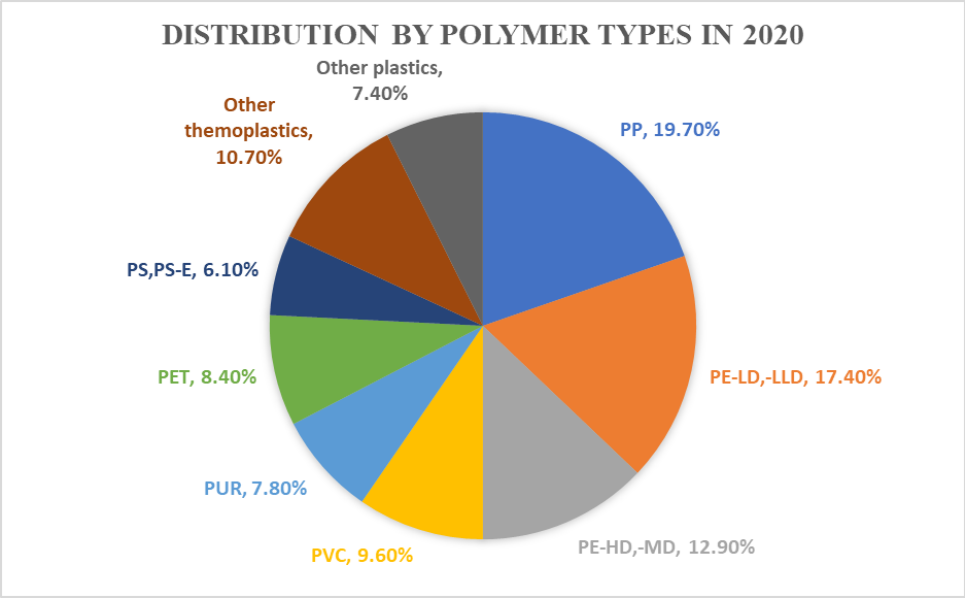

Figure 1.3: Distribution By Polymer Types in 2020 (Lu et al., 2023)

In order to manage the accumulation of a large amount of PVC waste, several PVC waste management methods of landfills, incineration and recycling are widely used to reduce the amount of PVC waste. However, these waste management methods will also bring several harmful effects on the environment. Firstly, PVC waste can be dumped as plastic waste in sanitary landfills, a preferred method in China and the United States (US) to manage PVC waste due to the availability of large land areas and economic feasibility. However, landfill space is limited in many countries, and the landfill disposal of PVC waste can cause hazardous additives from PVC, such as heat stabilizers, plasticizers, lubricants and fillers, to be released as leachate and contaminate soil and groundwater to cause water pollution, land pollution and soil pollution (Lu et al., 2023). Uncontrolled dumping of PVC wastes on the outskirts of towns and cities will also create overflowing landfills that lead to groundwater pollution and contributes to global warming (Behl et al., 2014). Additionally, managing PVC waste through incineration can help to reduce the volume of PVC waste besides using the produced energy for heating or generating electricity. Nevertheless, incineration of PVC waste emits excessive CO_2 and may generate hazardous substances, such as polychlorinated biphenyls, dioxins, furans and persistent organic pollutants (POPs), which leads to air pollution and poses a severe threat to the environment (Lu et al., 2023).

Furthermore, PVC waste also can be recycled to produce secondary materials, chemicals, feedstock, fuels and value-added polymers through mechanical and chemical recycling. Theoretically, primary mechanical recycling, secondary mechanical recycling, tertiary recycling and quaternary recycling are the four recycling types for managing PVC waste. PVC waste can be treated by primary mechanical recycling or closed-loop recycling to create new products (Lu et al., 2023). Yet, problems of selective collection and manual sorting may occur during the mechanical recycling. Secondary mechanical recycling requires sorting the rigid and uncontaminated PVC waste, reducing the waste size and extrusion to produce low-value materials. Tertiary recycling or chemical recycling is used to convert flexible, commingled and contaminated PVC waste into small molecular chemicals, fuels and feedstock. However, tertiary recycling will

produce HCl and chlorinated organic compounds as by-products. Meanwhile, quaternary recycling refers to the incineration of PVC waste with energy recovery, but it emits CO_2 and hazardous substances with adverse effects on the environment (Lu et al., 2023). In short, mechanical recycling helps to convert PVC waste into lower-value materials but does not address the environmental problems as it only delays the final disposal. By contrast, chemical recycling intends to convert PVC waste to plastic monomers, chemicals, fuels, feedstock and value-added polymers while recovering energy through chemical reactions to handle the PVC waste more effectively. Nevertheless, chemical recycling of PVC waste is limited to be applied due to the high energy costs, the lack of high-efficient and low-energy catalysts, and the high chlorine content with various additives of PVC (Lu et al., 2023). Other treatment methods for PVC waste, such as pyrolysis, hydrodechlorination and solvothermal carbonization also commonly used to handle the accumulation of PVC waste. However, these methods also have their drawbacks, in which pyrolysis will generate large amounts of corrosive HCl, while hydrodechlorination and solvothermal processes can produce inorganic salts to increase the burden of post-processing and decrease the process economics (Feng et al., 2023).

Besides the environmental impacts of the accumulation of PVC waste with its management methods, the production process of PVC will also lead to several hazardous effects on the environment. Generally, PVC is manufactured by polymerization of vinyl chloride monomer (VCM) produced by the thermal cracking of ethylene dichloride. During the production of 1,2-dichloroethane from ethylene and chlorine, which can decompose by thermal cracking in VCM, dioxins are formed with a high contribution to human toxicity potential (HTP) (Comanita et al., 2020). Exposure to dioxins can affect human health, which causes reproductive and fertility problems, liver damage and even developmental problems in children. The processing of crude oil during the production of PVC also leads to emissions of volatile organic compounds, contributing to a high photochemical ozone creation potential (POCP) (Comanita et al., 2020). The high value of photochemical ozone creation potential indicates high concentrations of ozone that can directly affect human health, causing eye irritation, respiratory tract and lung

irritation and ecosystem disruption due to its toxic nature (Farinha et al., 2021). Ethylene and chlorine production processes associated with PVC manufacturing also required high energy consumption with emissions of CO_2 and SO_2, which contributed to great global warming potential (GWP) and acidification potential (AP) impacts (Comanita et al., 2020). GWP is the EI responsible for the emission of greenhouse gases into the atmosphere to increase the global medium temperature of the Earth as they reflect or trap part of the radiation emitted by the Earth's surface (Farinha et al., 2021). The increment in temperature can result in several climate changes that can affect human health and ecosystems. High AP refers to the acid deposition of acidifying contaminants emitted from the production of PVC on soil, groundwater, surface waters, biological organisms and ecosystems (Dincer & Bicer, 2018). In a nutshell, the public should pay more attention to the adverse environmental issues of PVC to reduce the consumption of PVC with the development of better PVC waste management methods and increase the recycling possibilities for PVC material. Bioprocessed organic waste instead of petroleum-based raw materials may be used as the raw materials in the production of PVC to produce biopolymers or bioplastics, which are biodegradable with less harmful impacts on the environment.

1.3 Research Objectives

i. To characterize the industrial rubber scrap and waste tire powder.
ii. To develop different rubber waste based recycled polyvinyl chloride composites through melt mixing method.
iii. To evaluate the characteristics and mechanical properties of the recycled polyvinyl chloride/rubber waste composites.
iv. To justify the most suitable type of rubber waste material that can be used as filler for recycled polyvinyl chloride.

CHAPTER 2

LITERATURE REVIEW

2.1 Polyvinyl Chloride (PVC)

2.1.1 Introduction

Polyvinyl chloride, popularly known as PVC, is one of the most commonly used versatile thermoplastic polymers worldwide and is ranked as the world's third-largest thermoplastic by production volume after polyethylene and polypropylene (Staff, 2016). PVC is a naturally white and very brittle solid thermoplastic available in powder form or granules with properties of being durable, lightweight, low cost and easy to process (PVC properties, 2019). PVC mainly consists of resin produced from the polymerization of the vinyl chloride monomer that is unstable due to its low thermal stability and high melt viscosity, which needs to be modified by additives during processing to enhance PVC's stability and obtain specific groups of properties for different applications, such as heat additives, UV stabilizers, plasticizers, impact modifiers, fillers and flame retardants (Industrial Quick Search, 2023). PVC was first synthesized by German chemist Eugen Baumann in the year 1872 and commercially used by the Russian chemists Ivan Ostromislensky and Fritz Klatte later in the 20th century (Staff, 2016). However, they found that the rigid polymer was hard to process, and thus in 1926, the

method of processing PVC was proposed by Waldo Semon and the B.F. Goodrich Company to obtain a flexible PVC by the addition of various additives (Comprehensive guide on polyvinyl chloride (PVC), 2023). With the critical properties of PVC of low cost, durability, chemical resistance, flame retardancy, good dielectric strength and good machinability, PVC is widely used in various industries for a diverse range of applications, such as films for packaging, construction products of pipes and fittings, conservatories, window and door profiles, healthcare products of blood bags and tubing, electric cable coverings, automotive applications of exterior side moulding, interior door panels and pockets, sporting products and leisure products (Industrial Quick Search, 2023).

Polyvinyl chloride is widely available in two broad categories, which are flexible PVC and rigid PVC. Besides these broad groups, there are smaller groups, which include chlorinated PVC (CPVC) or perchloro vinyl, molecularly oriented PVC (PVC-O) and modified PVC (PVC-M). Each group of PVC comes with its own set of benefits and ideal uses for different industries. Flexible PVC or known as plasticized PVC, with a density between 1.1 and 1.35 g/cm^3, is synthesized by adding compatible plasticizers to pure PVC to lower the crystallinity, such as phthalates and diisononyl phthalate or DINP (Amobonye et al., 2023). These plasticizers play a lubricating role in flexible PVC to produce a more transparent and flexible plastic. Flexible PVC is a soft and elastic material that ranges in appearance from transparent to opaque to be commonly used for a wide range of applications, such as wire and cable jacketing, pool liners, flooring, electrical cable insulation and inflatable products due to its properties of low-cost, flexibility, high impact strength, chemical resistance and good electrical insulation properties (Comprehensive guide on polyvinyl chloride (PVC), 2023). Besides that, rigid PVC or unplasticized PVC, with a density of 1.3-1.45 g/cm^3, is a relatively stiff plastic with high resistance to impact, chemicals, corrosion, water, and weather (Amobonye et al., 2023). High density, lightweight, excellent thermal properties and stability and incredibly robust rigid PVC make it an ideal option for water and waste pipes, conservatories, gutters, cladding, window frames and so on (Staff, 2016). Rigid PVC is

also commonly found as a building material and replacement for copper and aluminium piping for waste lines, irrigation systems, and pool circulation systems since it is easy to form and cut (Industrial Quick Search, 2023). Furthermore, chlorinated PVC is prepared by chlorinating PVC resins with high chlorine content to impart the properties of chemical stability, flame retardancy, high durability and high thermostability to the polymer. The forces of attraction between the molecular chains can be reduced by the chlorination of PVC and become essentially amorphous, which allows CPVC to be stretched easily and to a greater extent than PVC above its glass transition temperature. Molecular-oriented PVC is produced by reorganizing the amorphous structure of rigid PVC into a layered form so that the produced PVC can be stiffer, more lightweight and resistant to fatigue. Meanwhile, modified PVC is a composite material created by combining PVC and other modifying agents, such as metals, salts and nanoparticles, resulting in enhanced toughness and impact properties (Amobonye et al., 2023). The advantages and disadvantages of rigid and flexible PVC are shown in Table 2.1.

Table 2.1: Advantages and Disadvantages of Rigid PVC and Flexible PVC (Comprehensive guide on polyvinyl chloride (PVC), 2023)

Advantages	Disadvantages
Unplasticized or Rigid PVC	
Low cost and high stiffness	Difficult to melt process
Intrinsic flame retardant	Limited solvent stress cracking resistance
FDA compliant and also suitable for transparent applications	Becomes brittle at 5 °C when not modified with impact modifiers or processing aids
Better chemical resistance than plasticized PVC	Low continuous service temperature of 50 °C
Good electrical insulation and vapor barrier properties	
Good dimensional stability at room temperature	
Plasticized or Flexible PVC	
Low cost, flexible and high impact strength	Properties can change with time due to plasticizer migration
Good resistance to UV, acids, alkalis, oils and many corrosive inorganic chemicals	Attacked by ketones; some grades swollen or attacked by chlorinated and aromatic hydrocarbons, esters, some aromatic ethers and amines and nitro-compounds
Good electrical insulation properties	Tends to degrade at high temperatures
Non-flammable and versatile performance profile	Non-suitable for food contact with some plasticizers
Easier to process than rigid PVC	Lower chemical resistance than rigid PVC

Polyvinyl chloride is a synthetic resin made from vinyl chloride monomer with the chemical formula of $H_2C=CHCl$ through polymerization. During the process of polymerization, individual vinyl chloride monomers are combined to create long polymer chains, ultimately resulting in the formation of PVC that is composed of multiple repeating units of vinyl chloride monomers with the chemical structure of $(H_2C–CHCl)$ n, where n is the degree of polymerization or the number of repeating units in the polymer chain. The carbon-carbon double bond in the vinyl chloride monomer is replaced by a single bond when the monomer joins with another monomer to form the polymer chain (Bajaj, 2023). The single bond indicates that all the carbon atoms in the chain are bonded to two other atoms, either hydrogen or chlorine, with the PVC chain becoming saturated. The molecular weight and degree of polymerization of PVC vary depending on the manufacturing process and the planned application of the material. The molecular weight of PVC generally falls within a range of 50000 to 150000 g/mol, while the degree of polymerization can span from 700 to 2000. Figure 2.1 shows the chemical structure of vinyl chloride monomer, while Figure 2.2 shows the chemical structure of polyvinyl chloride.

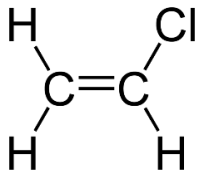

Figure 2.1: Chemical Structure of Vinyl Chloride Monomer, C_2H_3Cl (Comprehensive guide on polyvinyl chloride (PVC), 2023)

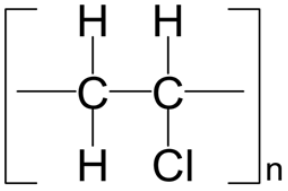

Figure 2.2: Chemical Structure of Polyvinyl Chloride, (C_2H_3Cl) n (Comprehensive guide on polyvinyl chloride (PVC), 2023)

The chemical structure of PVC can affect its physical, mechanical, thermal and melting properties. Firstly, the degree of polymerization and molecular weight of PVC can influence its melting point, in which higher degrees of polymerization and molecular weights typically result in higher melting points with a higher degree of crystallinity (Bajaj, 2023). Moreover, the chemical composition, degree of crystallinity and molecular weight of PVC can affect its physical properties, including its density, transparency and hardness. Generally, PVC has a low density and high transparency when not pigmented, which can be blended with plasticizers, such as phthalates, adipates and trimellitates, to modify PVC's hardness and the degree of crystallinity besides enhancing the flexibility and workability of PVC. The mechanical properties of PVC, such as strength, elasticity and toughness, are also affected by the structure of the polymer chain of PVC. PVC with a high degree of polymerization and molecular weight commonly exhibits greater strength and rigidity than PVC with a lower degree of polymerization and molecular weight, which tends to be more flexible and elastic. The thermal properties of PVC, such as thermal stability, thermal conductivity and heat resistance, are also impacted by its chemical structure and any added additives. PVC resin obtained from polymerization is usually unstable, with low thermal stability and high melt viscosity, which requires the addition of stabilizers to enhance its heat resistance (Bajaj, 2023). However, the thermal conductivity of PVC is relatively low, contributing to its good electrical and thermal resistance. Table 2.2 shows the key properties of PVC.

Table 2.2: Properties of PVC (Amobonye et al., 2023)

Property	Value
Crystalline melting temperature	100 - 260 °C
Density	1.1 - 1.4 g/cm^3
Glass transition temperature	60 - 70 °C
Notched impact strength	20 - 40 J/M
Percentage crystallinity	9 % - 11 %
Resistivity	1012 - 1016 Ω m
Surface resistivity	1011 - 1014 Ω
Tensile strength	75 MPa
Thermal coefficient of expansion	8.0×10^{-7}
Thermal conductivity	0.14 - 0.28 W/m K
Vicat	65 - 140 °C
Young's modulus	2.9 - 3.4

The production process of PVC generally involves five steps, which are the extraction of hydrocarbon resources and the extraction of salt, the production of chlorine and ethylene, the manufacturing of the vinyl chloride monomer (VCM) through the combination of chlorine and ethylene, the polymerization of the VCM to produce polyvinyl chloride, and the blending of the polymer (PVC) with different types of additives that provide a broad range of physical properties to meet various end application requirements (Industrial Quick Search, 2023). At first, the petrochemical or upstream industries supply ethylene derived from natural gas or naphtha via the thermal cracking process, while the chlor-alkali industry yields chlorine via electrolysis using industrial-grade salt as the primary raw material. Ethylene dichloride (EDC), the principal precursor for vinyl chloride monomer, is then produced by the chlorination of ethylene via one of two processes, direct chlorination process using pure chlorine and ethylene or oxychlorination process in which ethylene reacts with chlorine in hydrogen chloride. EDC produced will then be cracked by a thermal cracker into vinyl chloride monomer, the basic building block of polyvinyl chloride. VCM produced is then sent to undergo the polymerization process to link all the VCM molecules to form PVC resin.

Currently, there are four types of vinyl chloride polymerization techniques to link the vinyl chloride monomers produced together to form chains of PVC in the form of a white powder, which includes suspension polymerization, emulsion polymerization, bulk polymerization and solution polymerization. The most widely used polymerization process to manufacture PVC resins is known as suspension polymerization, which accounts for 80 % of PVC production worldwide. During the suspension polymerization, the pressurized and liquefied raw material VCM is fed into the polymerization reactor containing water and suspending agents, such as polyvinyl alcohol, to obtain small droplets of VCM through high-speed agitation within the reactor. PVC is then produced in the reactor with the feeding of an initiator under a few bars at 40-60 °C. PVC obtained in slurry form is then discharged from the reactor, followed by stripping of residual monomer, dehydrating and drying to yield PVC in the form of a white powder (The PVC production process explained, 2023). The unreacted VCM is recovered through a stripping process and recycled as raw material for reuse after being purified. The suspension polymerization process provides the advantages of high productivity per unit reactor volume, flexibility in polymer composition for high plasticizer absorption and the granular nature of its product. Besides that, emulsion polymerization and bulk polymerization are alternative technologies to manufacture PVC, which are much less extensively employed than suspension polymerization. During the emulsion polymerization, surfactants or soaps are used to disperse the VCM in water to trap the monomer inside soap micelles and carry out the polymerization using water-soluble initiators. The process can be either continuous or batch to produce finer resin grades with much smaller particles in water. The polymer particles produced are then dried with excess monomer recovered and recycled. The PVC resins from the process are commonly used for a wide range of specialty applications, such as coating, dipping or spreading (Comprehensive guide on polyvinyl chloride (PVC), 2023).

In addition, bulk or mass polymerization is the process that involves the charging of vinyl chloride monomer and initiator to a first stage polymerizer to convert about 10 % of the monomer to polymer. Then, the batch is transferred to a second stage polymerizer

with additional monomers and initiators to continue converting about 80-85 % of the container monomer to polymer. The finished resin product is sent to storage bins for later shipment to fabricating plants, while unreacted VCM is removed by heat and vacuum (Wheeler, 1981). The absence of water in the polymerization stage eliminates the need for the drying step to reduce capital and operating costs during the process. Although the bulk process provides the benefits of the uniformity of the resin particle size, the high porosity of the resin particles and the purity of the polymer, it also provides the disadvantages of less flexibility in the product mix and poorer removal of residual VCM. Lastly, solution polymerization is a process that accounts for about 2 % of the total resin produced, which involves a continuous reactor system consisting of VCM, comonomer, solvent and initiator (Wheeler, 1981). The polymer formed is then soluble in the reacting mass of the reactor to create a viscous resin solution as the reactor product. The resin solution is purified to remove the unconverted VCM, while the resin product is recovered by treating the resin solution with water and drying the product. The resin particles formed are very porous with good dissolving qualities and widely used as a coating material, such as paints and lacquers (Wheeler, 1981). After the production of PVC through one of the polymerization techniques, PVC is mixed with various types of plasticizers, stabilizers, and modifiers to formulate vinyl compounds that are rigid and flexible and promote the attainment of diverse properties, such as UV resistance, scuff and mar resistance, weather ability, texturing capability and so on.

Polyvinyl chloride commonly exhibits white coloration with extreme brittleness and susceptibility to environmental damage in its natural state due to its low thermal stability and high melt viscosity. Thus, PVC is added with various additives to modify its properties and fulfil the properties for specific applications. The most popular types of additives that can affect the properties of PVC include plasticizers, heat stabilizers, flame retardants, fillers, lubricants and pigments. Plasticizers are generally used as softening agents to soften the rigid PVC to become more flexible and pliable by decreasing the attraction between polymer chains (Alban, 2023). The rheological properties of vinyl products also can be enhanced and increase the mechanical

performance of the PVC, such as toughness and strength. Some examples of plasticizers are diisononyl phthalate (DINP), dioctyl terephthalate (DOTP), diisodecyl adipate (DIDA), trioctyl trimellitates (TOTM) and epoxy fatty acid monoesters. Besides that, heat stabilizers help in every PVC formulation with low thermal stability to prevent the decomposition of the PVC by heat and shear during processing. They can also enhance the resistance of PVC to daylight, heat ageing and weathering (Industrial Quick Search, 2023). Several factors to evaluate when selecting heat stabilizers are the technical requirements of the polymer products, regulatory approval and cost. Furthermore, flame retardant additives, such as antimony trioxide (ATO), decabromodiphenyl ethane and zinc borate, are used to increase the flame retardance of PVC and protect the structural integrity of the plastic material (Alban, 2023). Moreover, fillers, such as calcium carbonate, titanium dioxide and calcined clay, are added to PVC to increase its stiffness and strength, improve impact performance and add colour, opacity and conductivity. Two types of lubricants are also typically used to enhance the properties of PVC, which are the external lubricants that aid in the smooth passage of PVC melt through processing equipment by reducing friction and the internal lubricants used for lowering melt viscosity, preventing overheating and ensuring the good colour of the product (Comprehensive guide on polyvinyl chloride (PVC), 2023). Pigments that include naphthol red 210, zinc oxide (ZnO) and zinc sulfide (ZnS) are used to customize the material colour and allow differentiation of various PVC compounds for different applications by colour (Alban, 2023). Other additives of processing aids and impact modifiers also can be added to PVC to improve the mechanical and surface properties of the PVC. Table 2.3 describes the common types of additives used in PVC productions and their functions in PVC.

Table 2.3: Common Types of Additives and Their Functions in PVC (Fråne et al., 2019)

Additives	Property of PVC article affected
Stabilizer	Prevents decomposition during processing, imparts light and weather resistance
Colorant Colour	Colour, weather resistance
Plasticizer	Mechanical properties, burning behavior
Impact modifier	Impact strength and other mechanical properties
Lubricants	Rheology of the PVC melt, transparency, gloss, surface finish and printability
Fillers	Electrical and mechanical properties
Flame retardants	Burning behavior
Antistatic agents	Electrical properties
Blowing agents	Processing to expanded products

2.1.2 Properties and Applications of PVC

Polyvinyl chloride is widely used in various applications nowadays due to its several main properties of good electrical and thermal insulation, excellent corrosion and weather resistance, durability, fire and mold resistance, high chemical resistance, high impact strength, lightweight and biocompatibility. Firstly, about 70 % of PVC output is utilized in the construction industry as an excellent alternative to traditional materials of wood, metal, rubber and glass, to be used as window and door profiles, water and sewage pipes, cable insulations, gutters, floor lining and roof membranes, aided by the excellent properties of PVC of high chemical resistance, advantageous mechanical properties with a long life span and low maintenance, as well as resistance to water and

weather conditions (Lewandowski & Skórczewska, 2022). PVC is perfect for window profiles due to its high strength-to-weight ratio, durable, lightweight and versatile features. It is also ideal for cabling applications because of its excellent electrical insulation and inherent flame-retardant properties (Industrial Quick Search, 2023). Strong moisture resistance, long lifespan, easier installation with maintenance, and abrasion properties of PVC also allow its use for roofing and cladding, fencing, decking, wallcovering and flooring (Fråne et al., 2019).

Besides that, PVC is primarily used as outdoor plumbing and drainage pipes in the construction industry due to its various benefits. The PVC pipes offer the benefits in the construction industry of good mechanical strength with high abrasion resistance, lightweight with a lower cost of transportation and labour charges, flexibility, ease of installation, long lifespan with zero maintenance, non-toxic, fire resistance and corrosion resistance when exposed to harsh chemicals or UV rays (Oriplast, 2022). PVC pipes stand out among other materials as they are highly energy-efficient during production and offer a cost-effective option due to their unparalleled durability and maintenance-free service life (Fråne et al., 2019). Furthermore, PVC is also employed in many lifesaving and healthcare products owing to its biocompatibility, chemical stability, low cost and resistance to sterilization (Lewandowski & Skórczewska, 2022). It can be used to manufacture flexible blood containers, urine ostomy bags, flexible tubes for blood transfusions, heart-lung bypasses, inhalation masks, oxygen masks, or PPE such as gloves and footwear. PVC is also widely utilized in the packaging industry as a food wrap, which delivers good oxygen barrier properties with a long shelf life of the food, with its properties of lightweight, flexibility, dependability and durability (Lewandowski & Skórczewska, 2022). Rigid vinyl film is also used in blister and clamshell packaging to protect medicines, personal care products and other household goods. Last but not least, PVC is applied in the automotive industry for automotive applications, such as interior door panels, instrument panels, seat coverings, headlining, weather strips, window sealing profiles and so on due to its properties of lightweight, long lifespan, being affordability and durability (Industrial Quick Search, 2023). The use of PVC in

vehicle components, such as soft dashboards, is beneficial for reducing the risk of injuries during accidents owing to its impact absorption properties. Additionally, PVC-coated fabrics are utilized for their flame resistance to make thermal protection systems for space vehicles, blood pressure cuffs for medical uses and liquid storage tanks, besides used to produce airbags for the automotive industry due to their mechanical properties (Fråne et al., 2019).

2.1.3 Sources of Recycled PVC

Nowadays, polyvinyl chloride (PVC) is one of the most widely used thermoplastic materials concerning worldwide polymer consumption and is the second most popular material in terms of volume in the plastics sector, trailing only polyethene, with annual demand exceeding 35 million tonnes on a global scale. Due to the excellent properties of PVC with low cost and high performance, PVC has become a universal polymer that can be manufactured into a wide variety of short-life products, such as PVC packaging materials used in food, textile, beverage packaging bottles and medical devices, and also long-life products, such as pipes, window frames and cable insulation (Sadat-Shojai & Bakhshandeh, 2011). As a result of the rising consumption of PVC-made products with the rapid growth of PVC products in recent years, the amount of used PVC items entering the waste stream as PVC waste has gradually increased. Besides the increasing global demand for PVC that leads to the accumulation of large amounts of PVC waste, the ineffective traditional treatment methods of PVC waste with harmful impacts on the environment, such as landfills, incineration, pyrolysis, hydrodechlorination and solvothermal carbonization, also causes the PVC waste to increase rapidly in the world (Feng et al., 2023). Although different types of recycling methods, such as mechanical recycling, feedstock recycling and chemical recycling, are widely introduced in the world to recycle PVC into a variety of products, secondary materials, chemicals and value-added polymers with less environmental problems to reduce the PVC waste, only

a small amount of PVC waste is now recycled in the world due to the high costs, the feasibility of a recycling system that requires a minimum quantity of wastes and the difficulties in the separation process of PVC from waste stream, which contributes to continue increasing of PVC waste.

PVC waste can be classified into two main types, pre-consumer and post-consumer. Pre-consumer waste is the garbage produced by manufacturers, facilities or organizations but not delivered to consumers. Pre-consumer wastes of PVC are generated from the final production of PVC and intermediate products as production wastes, and installation wastes from the handling or installation of PVC products (Plinke et al., 2000). The production process for PVC end products requires more than three distinct steps, which may be distributed among multiple companies. For example, the process of creating PVC packaging that begins with producing PVC films from PVC compounds, followed by thermoforming of the films to packaging, will yield the production wastes of cut-offs during the calandaring of films. Cut-offs from the laying of cables or floorings are examples of installation wastes. The pre-consumer waste is recycled at the PVC processors in-house after mechanical treatment of installation wastes or recycled in closed loops internally at the PVC production plants (Plinke et al., 2000). Production waste that cannot be managed within the production facility can be collected or treated by waste management companies outside the facility. It is easy to recycle PVC pre-consumer waste as it can be gathered in specific amounts and used effectively in practical applications.

In addition, post-consumer waste is waste that comes to be at the end of the consumer lifecycle. Recycling PVC pre-consumer waste can be challenging as it often comes in the products like pipes, windows and packaging that have reached the end of their life and can be part of mixed waste fractions or composite materials (Plinke et al., 2000). PVC can exist in waste material as a relatively pure fraction, which can be separated from the waste stream through sorting, depending on the products involved. Alternatively, PVC can form a part of composite products or materials, such as windows,

car components, floorings and cables, which must be subjected to disassembling or mechanical treatment processes to extract PVC. There are various PVC product groups for post-consumer waste with specific waste flows, such as construction products which end up in construction and demolition wastes, consumer and technical products that arrive as municipal solid wastes or packaging wastes, vehicle components of dashboard elements, cables and coatings that end up in the shredder residues, electronic products as electronics waste and other products ending up in unique waste flows, such as hospital and agricultural wastes (Plinke et al., 2000).

The sources of recycled PVC can be attained from various industries of building and construction, automotive, packaging, piping and cable industries, including numerous household goods. Due to the features of PVC of high strength, durability, lightweight, versatility, long life span and resistance to oil, weather and UV radiation, more than 75 % of the total PVC is used in industrial applications, especially in the building and construction sector, to produce piping for plumbing and draining applications, electric wiring and cables, flooring, roofing, door profiles and window profiles (Miliute-Plepiene et al., 2021). These PVC products generally end up as construction and demolition wastes to undergo further sorting and separation processes to extract the recycled PVC for other uses (Prestes et al., 2011). Hence, the primary sources of recycled PVC can achieve from the used products of construction industries, especially from the profiles, flooring, pipes and fittings. Besides that, recycled PVC can be obtained from wire insulation from waste electrical and electronic equipment, household appliances and cars. Due to PVC's excellent insulating qualities, outstanding mechanical and ageing properties, ease of use during manufacture and high fire resistance, PVC is frequently utilized in cable insulation (Fråne et al., 2019). Recycled cable insulation PVC materials can be processed into other technical products, including composites with recycled fillers, besides acting as an additive to cement and bituminous masses (Plinke et al., 2000). In addition, packaging waste from packaging industries also can be a source of recycled PVC, as PVC is mainly used to produce bottles, containers, labels, cling film for meat, fish, cheese and vegetables, pharmaceutical tablets blisters

and packaging for toiletries. Last but not least, recycled PVC can be acquired from the waste of automotive industries or shredder residues as PVC is widely used in automotive applications for manufacturing underbody coatings, sealants and floor modules, wire harnesses, passenger compartment parts and exterior parts of body side protection strips, weather strips and window sealing profiles (Fråne et al., 2019). Other sources of recycled PVC are the after-use of coated fabrics, rigid film, rigid plates, and flexible film and sheets (Miliute-Plepiene et al., 2021). Figure 2.3 shows the sources of recycled PVC from different applications in various industries.

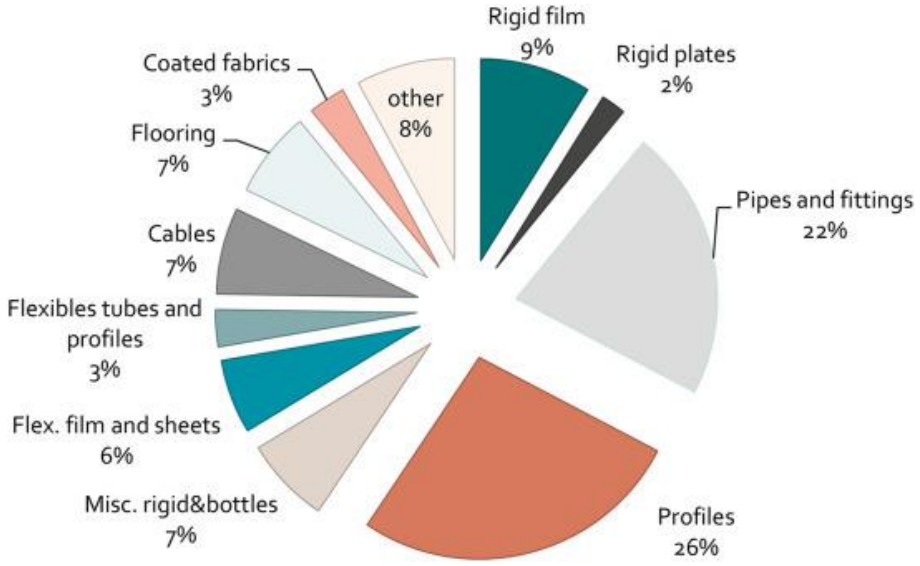

Figure 2.3: Sources of Recycled PVC from Different Applications (Miliute-Plepiene et al., 2021)

2.2 Rubber

2.2.1 Introduction

A thermosetting rubber, latex, or acrylic, also known as a thermoset, is a polymer that transforms a soft, rigid, or viscous liquid prepolymer or resin into a permanently hardened material (Bin Bakri et al., 2022). Rubber is a natural polymer referred to as an elastomer in the raw state, which is produced from the emission of some tropical plants as natural rubber or extracted from petroleum and natural gas as synthetic rubber. Rubber is a distinctive material that possesses both elastic and viscous properties. It can return to its original shape after being deformed due to its low modulus of elasticity with very high elongation at break (J. Schaefer, 2018). At room temperature and without being stretched, rubber is typically amorphous. Rubber is given a permanent shape through a process of crosslinking or vulcanization, in which the molecules are bonded together by a few chemical bonds. Before crosslinking, rubber is a very viscous and elastic liquid, but after the process, it becomes a soft, highly elastic solid (kadum abd-ali, 2017). Compared to fibers and plastics, rubber exhibits significantly less interchain interaction. Rubber also has a glass transition temperature lower than the ambient temperature, at which the glass transition temperature is the temperature above which a rubber becomes rubbery in nature, whereas, below this temperature, it becomes glassy (Introduction to rubber, 2021). Besides that, rubber also can be molded into various shapes and attached to metal inserts or mounting plates (J. Schaefer, 2018). It also can be combined with different compounds to obtain diverse properties. Rubber is preferred over other materials for a diverse range of applications in the world, especially for the manufacturing of surgical gloves, aircraft and car tires, due to its various properties of low density, less energy-intensive fabrication, amenable to high-speed production, resistance to corrosion and related electrochemical action and low thermal and electrical conductivity (Introduction to rubber, 2021).

Generally, there are two main types of rubber, natural rubber and synthetic rubber. Natural rubber is the type of rubber obtained naturally from the milky liquid or latex from the rubber tree of Hevea brasiliensis, native to the Amazon basin (Kim & Jung, 2022). The natural rubber molecule is a linear, unsaturated, long-chain aliphatic hydrocarbon polymer specified chemically as cis-1, 4-polyisoprene with the monomer of isoprene or 2 methyl-1, 3-butadiene. The crucial mechanical properties of cis-polyisoprene are its softness and elasticity. The hydrocarbon content of raw natural rubber is about 94 %, besides containing small quantities of proteins, fats, fatty acids and carbohydrates, which can affect its physical, chemical and mineral properties (Ibrahim et al., 2019). In addition, natural rubber also has high regularity in its backbone structure to align and crystallize when a strain is applied, which resulting high tensile properties. Natural rubber possesses general benefits of outstanding resilience, high tensile strength, superior resistance to tear and abrasion, good flexibility at low temperatures and excellent adhesion to fabrics, metals and other rubber. Due to the superior properties of natural rubber, it is widely used in different applications, such as airplane or big truck tires, surgical gloves, medical gadgets, aircraft, mattresses, shoe soles, rubber boots and toys. Natural rubber is extensively utilized in tires due to its ability to reduce rolling resistance, lower heat generation, better adhesion properties and higher hot tear strength (Introduction to rubber, 2021). It is also widely used in shock and vibration isolators because of its remarkable elasticity, durability, and economical price (J. Schaefer, 2018). Yet, natural rubber also has the limitations of poor resistance to heat, ozone, sunlight, oil and gasoline. Thus, natural rubber can be cured by sulphur, peroxides and other vulcanizing agents through the vulcanization process to improve the properties of natural rubber and possess specific properties.

Synthetic rubber is known as a polymer that is artificially created by humans. It is commonly made of raw materials derived from petroleum, coal, natural gas, oil and acetylene. Synthetic isoprene rubber (SR) is a polymer with physical properties similar to natural rubber and 98-99 % purity composed primarily of cis-isoprene units linked together by 1,4-linkages and 10 % trans-isoprene units with 3,4-linkages (Ali Shah et al.,

2013). Nevertheless, synthetic polyisoprene's stress stability, processability, and other parameters do not better than those of natural rubber. Synthetic rubber comes in various types, such as neoprene, Buna rubbers, and butyl rubbers. These rubber variants are designed with specific features to cater to niche applications. Styrene-butadiene rubber (SBR) is one of the examples of synthetic rubber, a copolymer of styrene and butadiene. SBR is widely used in car tires due to its excellent impact strength, good resilience, high tensile strength, high abrasion resistance and flexibility at low temperatures. SBR is often blended with natural rubber and cured by sulphur to enhance its properties. Other examples of synthetic rubber include butadiene rubber for tire manufacture, chloroprene rubber used for weather-resistance products and butyl rubber used for inner tubes. Besides natural rubber and synthetic rubber, there are also other types of rubbers utilized for different purposes with different strengths and weaknesses, such as ethylene vinyl acetate rubber, fluorocarbon rubber, acrylic rubber, polyurethane, epichlorohydrin rubber, silicone rubber, and more (Introduction to rubber, 2021).

Although rubber naturally possesses various outstanding properties, it also has some inherent deficiencies, which need to undergo compounding with several additives or compounding ingredients to improve its physical and processing properties. Elastomer is the primary component of a compound that is chosen based on the end-use application and desired physical properties. The elastomer may be a single rubber, a blend of two polymers, or a rubber-black master batch (Introduction to rubber, 2021). One of the compounding ingredients added to rubber is the vulcanizing agents, such as sulfur, peroxides and metal oxides, used for the chemical crosslinking of different parts of rubber chains to prevent rubber flow and gain strength during the vulcanization process by which the elastomer molecules become chemically crosslinked to form three-dimensional structures with dimensional stability (J. Schaefer, 2018). The mechanical properties of the rubber, such as tensile strength, fatigue strength, tear strength and static modulus, can be improved through the vulcanization process with increasing crosslinking density. Furthermore, accelerators, such as cyclohexyl benzothiazole sulfenamide (CBS), are used with accelerator activators inside the rubber to increase the

vulcanization rate along with vulcanizing agents and further improve the physical properties of rubber (Introduction to rubber, 2021). Reinforcing fillers of carbon blacks of various particle sizes also can be added to strengthen rubber, reduce cost and modify physical properties. A reinforcing filler's particle size and surface area can affect the reinforcement degree at which smaller particle size of carbon blacks with a higher surface area promotes a better reinforcing effect to increase tensile, modulus, hardness, abrasion resistance, tear strength and electrical conductivity. Moreover, the processing aid of oils is used in compounding rubber to retain a given hardness when increased carbon black or other fillers are added, besides improving the mixing and flow properties (J. Schaefer, 2018). Antidegradant of phenolic, amine, and phosphite chemicals are employed to prevent the ageing process in rubber vulcanizates and enhance long-term stability and function by different chemical mechanisms. Other ingredients include retarders, blowing agents, abrasives, odorants, flame retardants, coloring agents and so on, are used for specific purposes with desirable properties (Introduction to rubber, 2021).

2.2.2 Properties and Applications

Rubber plays a vital role in worldwide applications owing to its distinctive and excellent properties, much like other polymer materials that provide various uses to humankind. Rubber exhibits exceptional behavior with high elasticity properties that can stretch up to a few hundred per cent and return to its original shape when pressure is released due to its remarkably low Young's modulus and high yield strain resulting from the vulcanization process. Rubber also possesses highly durable properties and high resistance to environmental agents because of its thermoset cross-linked structure. Rubber also has a low density and design flexibility that can be processed into various shapes. Rubber also is resilient and exhibits internal damping to dampen or reduce vibration. Besides that, rubber also has a high resistance to acids, alkalis and chemical

solutions, resistance to corrosion and relative resistance to gas and water permeability with reduced swelling in hydrocarbon oils, which makes rubber widely applied in many critical environments, including healthcare, food processing, chemical manufacturing, refining, automotive, electronics and semiconductor manufacturing, pharmaceutical and research laboratory (Nuzaimah et al., 2018). Rubber also held another beneficial characteristic, such as a better-wet grip, lower temperature processing compared to metals, low energy-intensive fabrication, low thermal and electrical conductivity and high-speed production (Introduction to rubber, 2021). Rubber also often be compounded with vulcanizing agents and several additives to have widely varying properties, enhance physical properties, affect vulcanization, prevent long-term deterioration and improve processability. These exceptional properties of rubber make it frequently chosen over other materials to be widely used in worldwide applications ranging from household, healthcare, industrial, military, automotive, civil and outer space applications. However, these properties have a drawback that causes rubber tough to degrade due to its intricate structure and composition (Nuzaimah et al., 2018).

Generally, there are over 25 different types of rubber available such as natural rubber (NR), styrene-butadiene rubber (SBR), nitrile rubber, butyl rubber (IIR), ethylene-propylene-diene monomer (EPDM) rubber, fluorocarbon rubber, chloroprene rubber (CR), silicon rubber and so on being utilized to manufacture numerous types of products besides possessing different properties. Natural rubber with lower heat generation, higher hot tear strength, excellent resilience, high tensile strength, superior resistance to tear and abrasion and good flexibility at low temperatures is extensively used to produce automobile tires, aircraft tires and surgical gloves (Introduction to rubber, 2021). It also can be used to manufacture flooring for gyms, commercial kitchens and animal shelters, which prevents fatigue, provides padding, is slip-resistant and waterproof, besides easy to maintain and long-lasting. Natural rubber is also employed for producing airbags, seals and padding for automobile parts, tight-fitting and expandable clothing of wetsuits and cycling shorts, gaskets, nozzles, adhesives and coatings. In addition, chloroprene rubber that possesses the properties of good chemical

resistance, high resistance to ageing and ozone, better wear resistance than natural rubber, excellent adhesion and abrasion resistance, is widely used for footwear, athletic gear, cable jackets, tubing, tire-sidewalls and gasoline hoses (Kanny & Mohan, 2017). Styrene-butadiene rubber with excellent abrasion and fatigue resistance, high impact strength, good resilience and better tire tread traction properties is used for lightweight vehicle tires, electrical insulation, hoses, seals, haul-off pads and shoe soles. Butyl rubber of outstanding impermeability to gases, high energy absorption, excellent resistance to heat, oxygen, ozone and sunlight and superior resistance to alkalis, water, steam, and oxygenated solvents, is utilized in the production of stoppers, gas masks, sealants, gasket, hoses, O-rings, chewing gum base and waterproof liners. Last but not least, nitrile rubber is used for engine hoses, seals, gloves, waterproof fabrics, adhesives and pigment binders due to its excellent oil and solvent resistance, high green strength, low flexibility and good chemical resistance (Boon et al., 2022).

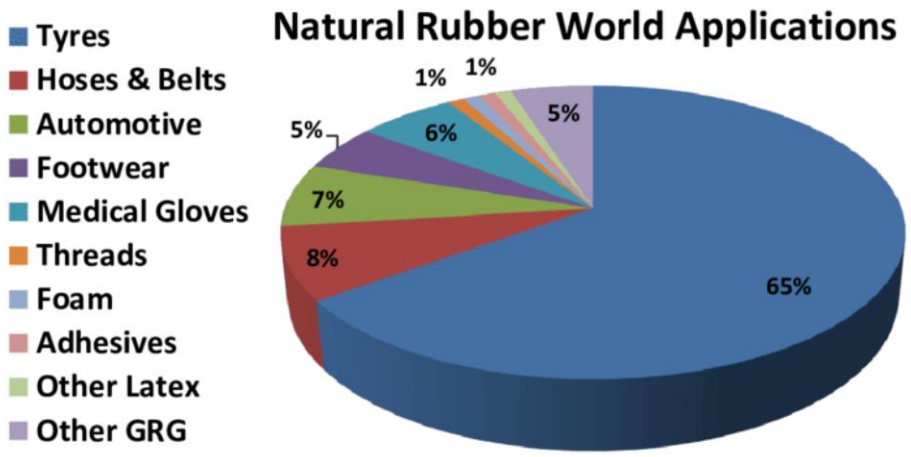

Figure 2.4: Distribution of the World Natural Rubber Applications (Blengini et al., 2017)

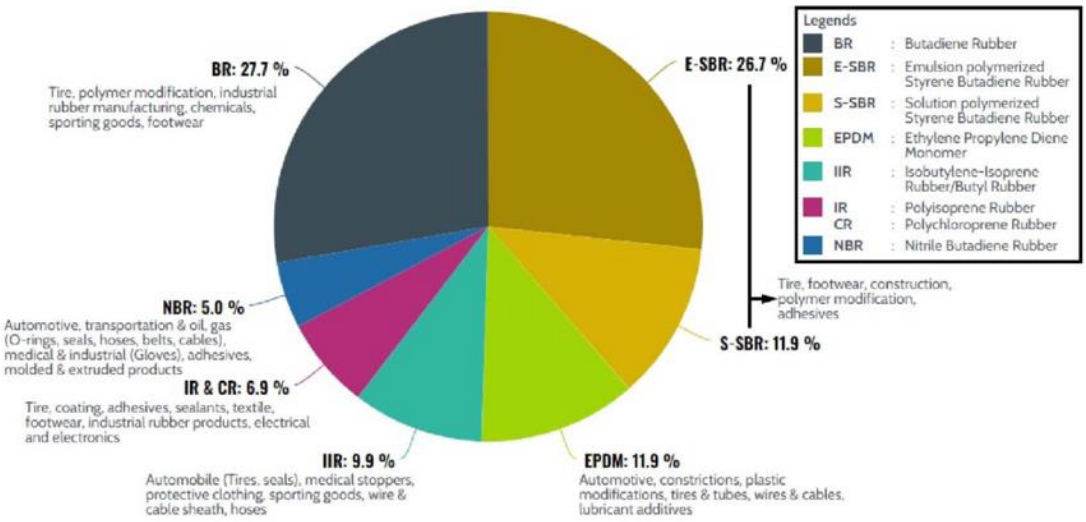

Figure 2.5: Demand for Synthetic Rubber in 2020 according to Rubber Types and Their Respective Applications (Boon et al., 2022)

2.3 Rubber Waste

2.3.1 Sources of Rubber Waste

Rubber waste has become a global challenge due to the rapid growth of rubber consumption in various industries, including automotive, construction and manufacturing. This escalating demand has led to a significant increase in rubber waste generation worldwide, and this study projects that by 2050, the globe will consume 25 million metric tons of rubber yearly, further intensifying the problem of handling rubber waste. Improper handling or processing of rubber waste also leads to the accumulation of rubber waste and could harm the environment. There are several sources of waste generated from different types of rubber, such as scrap tires, inner tubes, discarded and rejected rubber gloves, rubber bands, seals, gaskets, diaphragms and so on. Among the different sources of rubber waste, tires are one of the largest sources due to the large

volume produced by a rapidly growing population with transportation development and the challenge to process after use owing to their durability. The increasing global demand for vehicles with commercial vehicle tires due to the growth of the automotive industry contributes to approximately 1.4 billion tires being sold in each year to generate a significant amount of scrap tires as rubber waste in the world (Nuzaimah et al., 2018). The amount of discarded waste tires is predicted to reach 1.2 billion pieces by 2030 due to the large production of the tires. These large numbers of end-of-life tires commonly remain untreated and end up as illegal dumps or landfills with a negative impact on the environment that leads to the leaching of toxic substances and heavy metals into the groundwater to pollute the water source, affecting the soil fertility and contaminate nearby streams, ponds and lakes (Leong et al., 2022). The disposed tires also can act as a breeding ground for various mosquitoes, causing the spreading of various deadly diseases, such as malaria, dengue, and chikungunya, besides serving as a home to disease-carrying rodents and snakes (Chittella et al., 2021). Waste tires are also being burned for disposal in addition to landfilling and stockpiles, which lead to air pollution.

Moreover, waste rubber gloves also contributed to the large amount of rubber waste generated worldwide. The rising health awareness among the public on safety and hygienic issue nowadays to take extra cautions on self-protection, such as wearing gloves in food preparation, humanitarian activities, gardening and so on, leads to the increasing demand for rubber gloves in the world with the increment of waste rubber gloves. In addition to the higher production of rubber gloves producing a large number of waste rubber gloves, the high reject rate during the production process of rubber gloves due to its strict production specifications and the unstable nature of the latex also causes the number of waste rubber gloves to rise rapidly. Rubber gloves with the properties of high strength, excellent chemical resistance and elasticity owing to the highly cross-linked thermoset structure, causing them hard to degrade naturally and will pollute the soil and water source indirectly when disposing of the gloves at the landfills due to the possibility of leaching out (Nuzaimah et al., 2018). Furthermore, other primary sources of rubber waste are automotive scraps from styrene-butadiene rubber,

waste rubber condoms, footwear, mattresses, hoses, industrial rubber waste, automotive components of shock absorbers and conveyor belts, and municipal solid waste, such as clothing, shoe soles, sofas, cushions, electric wires and insulations (Leong et al., 2022).

2.3.2 Industrial Rubber Scraps

Generally, industrial rubber scraps are obtained from rubber goods other than used automobile tires, such as medical gloves, adhesives, gaskets, tubes, hoses, conveyor belts, airbags, rubber seals, rubber mats, footwear and so on, that undergo the reclaiming process followed by shredding and grinding process to achieve ground rubber scrap. These rubber scraps or known as recycled rubber, typically be used to manufacture new tires, hospital floors, surgical gloves, asphalt roadbeds, agriculture hoses, vegetation protectors and windbreaks, sheds, livestock mats, bumpers, feeders, truck bed liners, basketball courts, new shoes, indoor and outdoor running tracks, fitness mats and so on. By utilizing industrial rubber scraps in various industries for different applications and downsizing the rubber scraps for the production of composite materials or blending, rubber waste generation can be reduced effectively, besides lowering the utilization of rubber resources as the rubber manufacturing and production remain strong throughout the years due to high market demand for various niche applications (Leong et al., 2022).

Industrial rubber scraps of used automobile tubes, hoses, conveyor belts and other rubber products commonly undergo two different types of reclaiming processes before shredding and grinding, which are physical reclaiming processes of mechanical, thermo-mechanical cryo-mechanical, microwave and ultrasonic, and chemical reclaiming processes by organic disulfides and mercaptans, inorganic compounds and miscellaneous chemicals to convert the rubber scraps into a state that can be mixed, processed and vulcanized again (Sathiskumar & Karthikeyan, 2019). The basis behind

rubber reclamation and devulcanization is the disassembly of crosslinks within the rubber's polymeric chains. Reclamation is the breaking of carbon bonds or refers to the scission of both the crosslinks and the primary chain bonds, whereas devulcanization is the cleavage of sulphur bonds in the molecular structure or refers to the scission of crosslinks, such as C-S and S-S bonds (Leong et al., 2022). Reclaiming goods also entails converting a thermoset polymer that is three-dimensionally interconnected, insoluble, and infusible into a two-dimensional, pliable, processable polymer with the same qualities as virgin rubber (Sathiskumar & Karthikeyan, 2019). Yet, in reality, the main chain scission could still occur in the devulcanization process since the carbon-carbon bonds are present in higher abundance than the crosslinking bonds (Leong et al., 2022).

There are several standard techniques of rubber reclamation, such as thermomechanical devulcanization, microwave treatment, ultrasonic method, chemical method, biological method and supercritical devulcanization. In thermomechanical devulcanization, the breaking of crosslinks of the C-S and the S-S bonds is achieved to ensure the bond energies of crosslinks are lower than that of the C-C bonds building the rubber backbone using a combination of high temperature and shear force with equipment of mills and extruders (Chittella et al., 2021). A twin-screw extruder is the most practical equipment used for thermomechanical devulcanization in the polymer industry. Numerous known pieces of equipment and methods for thermomechanical devulcanization have been reported, such as Formela et al. in 2014 discovered that an increase in the treatment temperature reduces the screw torque required to reclaim ground tire rubber (GTR) and the properties of the recycled rubber are also affected by the temperature used (Leong et al., 2022). The one produced at 60 °C out of three treatment temperatures of 60, 120, and 180 °C had the best mechanical properties with the least main chain scission, while GTR reclaimed at 180 °C mixes better and more homogeneously in other polymeric matrices, such as in styrene-butadiene rubber (SBR) blend to provide better mechanical properties. Thermomechanical reclamation or devulcanization provides the advantages of high selectivity for crosslink scission and

easy to scale up for industrial application with the disadvantages of potential main chain scission due to the high abundancy of C-C bond (Leong et al., 2022).

Besides that, the microwave method utilizes the heating effect of the microwave to cleave the crosslinks in the rubber as the rubber is sufficiently polar to absorb the microwave radiation. Polar fillers that absorb microwave radiation, such as silica and CB, could be added to rubber with low radiation absorption, like natural rubber, styrene-butadiene rubber and ethylene-propylene-diene rubber (EPDM), to speed up the devulcanization procedure (Leong et al., 2022). Microwave devulcanized rubber displays increased fluidity and improved reusability of the rubber (Chittella et al., 2021). These characteristics make it simple to remold and revulcanize the devulcanizates. The microwave method provides the benefit of environmentally friendly homogenous heating with promising properties of the resulting devulcanized rubber and the drawback of being restricted to polar rubber molecules that absorb microwaves besides requiring suitable additives. Furthermore, the ultrasonic method uses the vibrations induced by wave energy to achieve the scission of crosslinks of C-S and S-S bonds in vulcanized rubber (Leong et al., 2022). Ultrasound devulcanization is an efficient process that can take place within a few seconds but requires high energy input and is costly. Microwave and ultrasonic devulcanization are the most explored physical techniques due to the lack of harmful substances or chemicals involved in the process.

Moreover, the chemical approach of rubber reclamation uses chemicals to disassemble crosslinks between rubber chains and prevent sulfur linkages between polymer chains from successfully recombining. Psulfides, peroxides, amines, deep eutectic solvents and ionic liquids are some of the chemicals that are reported to serve as effective devulcanizing agents (Leong et al., 2022). Most of the elastomeric qualities are preserved during the chemical devulcanization so that the devulcanized product can be utilized to create new rubber products again (Chittella et al., 2021). Although the chemical method provides a wide selection of devulcanizing chemicals and high efficiency, it harms the environment with secondary pollution. The biological

degradation of rubber polymer offers a safer alternative to the chemical technique since the devulcanization process is catalyzed by enzymes made by microorganisms, as opposed to the chemical method, which uses a variety of hazardous chemical solvents. The microorganisms either attach to the surface of the rubber or secrete enzymes that help with the devulcanization and breakdown of the rubber. Biological devulcanization provides high selectivity for crosslink bonds by desulfurization enzymes, but the microbial degradation is very slow and the devulcanization only happens on the rubber surface. Last but not least, supercritical devulcanization technology utilizes CO_2 at a supercritical state ($scCO_2$) as the reaction medium for devulcanization, which is known for its non-flammability, non-toxicity and chemical inactivity to ensure the safety of the process. Additionally, it was said to have a critical point that is simple to reach with good diffusivity that aids in the swelling process for the devulcanization agent's diffusion into the rubber material (Leong et al., 2022).

After reclamation, the rubber scraps will undergo the primary reduction or ambient shredding down to a manageable form with smaller pieces by the guillotine, the cracker mill, the high-impact hammer mill and the rotary shear shredder. Then, all the steel and polyester fragments are removed by a magnetic separator and a fiber separator. The rubber scraps can be further reduced using ambient ground mill or ground into fine particles while frozen using cryogenic grinding (Isayev, 2013). Dry ambient grinding is a relatively simple process of grinding the rubber physically at room temperature to produce crumbs with a high surface area to volume ratio. Yet, the friction between the rubber surface and the grinder generates a lot of heat, which causes the rubber surface to oxidize. Cryogenic grinding is a method for obtaining fine-mesh rubber by cooling rubber scraps in liquid nitrogen below their glass transition temperature and then pulverizing the brittle material in a hammer mill to produce ground rubber particles besides avoiding surface oxidation on the rubber (Leong et al., 2022). Due to the high liquid nitrogen consumption in the grinding process, it is highly costly. Other grinding methods of wet ambient grinding can produce ground particles with a high surface area to volume ratio but require a long post-grinding drying period, while a high-water

pressure jet is an environmentally friendly and cost-effective grinding way but needs highly trained personnel to ensure smooth operation of the process. Berstoff's process also works well for creating rubber particles with fine grain sizes, but it requires expensive equipment, including an industrial miller and a twin-screw extruder (Leong et al., 2022).

The downsizing industrial rubber scraps can then be utilized as a reinforcement material or filler in polymeric material to form a composite, besides being used by manufacturers in various industries for a wide variety of applications. For example, fillers from waste rubber gloves can improve the composite properties, in which filler from waste acrylonitrile butadiene rubber (NBR) gloves can be blended with epoxidized natural rubber (ENR 50) to produce a composite with improvement of tensile strength, modulus and elongation at. NBR waste gloves can be used as a filler to provide additional value to the newly developed material or composite as they possess excellent puncture and tear resistance with good chemical resistance, besides reducing the cost of the material and are also easy to handle. The waste condoms can also compound with styrene-butadiene rubber (SBR) after grinding into polydisperse particles to improve the thermal conductivity of the composite with increased rubber content. Besides that, SBR scraps from automotive extruded can be utilized as filler in styrene-butadiene rubber (SBR) composite to provide better tensile strength and elongation as the devulcanized SBR scraps promote better interfacial adhesion with the SBR matrix. Moreover, waste latex products can also act as a filler in epoxidized natural rubber (ENR) to decrease the stickiness of ENR and provide better processability during the mixing process, besides reducing mixing time and enhancing product resistance towards ageing. In addition, latex foam waste can be incorporated into natural rubber compounds to produce rubber mats with improved tensile strength and elongation (Nuzaimah et al., 2018). Without impairing the primary characteristics of the vulcanizates, the surface-treated scrap rubber powder can also replace 20-40 % of the carbon black and enhance the physicomechanical properties of rubber vulcanizates. The road pavement performance is

also significantly improved by asphalt that is chemically treated with fine waste rubber powder (Yehia, 2004).

2.3.3 Production of Waste Tire Powder with Usage

Recently, the global expansion of the automotive industry with the rising use of cars as the primary mode of transportation has tremendously boosted tire production, with approximately 1.4 billion new tires sold globally each year. These tires will become solid waste at the end of their life span or when damaged to generate massive stockpiles of used tires or scrap tires. The ineffective recycling or random piling of scrap tires can seriously harm the environment with human health by destroying vegetation, causing soil erosion and polluting the water supply, besides acting as a breeding ground for various mosquitoes, causing the spreading of various deadly diseases (Li et al., 2020). The piling of the waste tires also can form enormous dumpsites. These dumpsites may cause an inextinguishable fire with air pollution as the rubber can act as excellent fuel to support the combustion (Leong et al., 2022). The incineration of waste tires to manage the number of waste tires will also contribute to the emission of greenhouse gases (GHGs) and hazardous air pollutants, such as carbon dioxide and sulfur dioxide, that lead to air pollution (Leong et al., 2022). Thus, an ideal waste tire management strategy without harming the environment and conserving natural resources by utilizing fewer raw materials, as well as developing industrial applications with added economic value, should be introduced and improve the typical waste tire management methods. Recycling waste tires is also growing important as the complete degradation of a tire in natural conditions requires hundreds of years and the chemical composition of tires contains harmful components like leachable heavy metals. However, traditional recycling techniques, including retreading, burning for energy recovery or pyrolysis to obtain gas and carbon black, typically result in low-quality recovered goods or will emit toxic gases that contribute to secondary pollution (Li et al., 2020).

In recent years, preparing rubber powder or waste tire powder has gained popularity as a promising recycling technique to recycle waste tires for further applications, besides reducing the large volume of waste tires for more storage space. The smaller rubber powder provides additional value and is suitable for more extensive applications, which can be utilized as a modifier for asphalt pavement and cement concrete mixtures, as a raw material to produce reclaimed rubber and for manufacturing new tires with a particle size less than 0.075 mm (Li et al., 2020). Grinding waste tires into rubber powder also can increase the surface area of the rubber particles and facilitate its vulcanization mixing with matrix rubber to make more stable products (Peng et al., 2011). Various grinding approaches have been designed to obtain scrap tire rubber powder from tires according to the difference in grinding conditions, which include ambient grinding, cryogenic grinding, wet grinding and so on (Li et al., 2020).

Grinding is a complex process to shred and grind tires with a high mechanical strength to a suitably small size and at a great degree of purity using specialized mechanical equipment (Rowhani & Rainey, 2016). The first method to grind the scrap tires into waste tire powder is known as ambient grinding, which is a method in which scrap tire rubber is ground or processed at or above ordinary room temperature (Lo Presti, 2013). It is the most popular and economical way of processing end-of-life tires. Ambient processing is generally carried out using rotating blades and knives to produce irregularly shaped and torn rubber particles with rough surfaces and relatively large surface areas to promote interaction with the paving bitumen (Lo Presti, 2013). The waste tires will first pass through the nip gap of a shear mill or two-roll mill to decrease the particle size by breaking the tires into chips (Fazli & Rodrigue, 2020). During this milling step, the temperature may increase to 130 °C. The chips will then feed into a granulator to break them into small pieces while removing metal and polymer fibers from the tire chips by separator and electromagnetic equipment. Once separated from the metallic material, the remaining rubber particles are sent for further size reduction via secondary granulators, cracker mills and micro mills (Fazli & Rodrigue, 2020). Ambient grinding can produce rubber powder with particle sizes ranging from 5 to 0.5 mm (Lo

Presti, 2013). Waste tire powder produced by ambient grinding with unevenly shaped sheared particles and comparatively large surface area improved interaction with composite matrix besides possessing higher mechanical strength than cryogenically granulates. However, ambient grinding requires a cooling system due to heat generation that contributes to the high energy consumption of the process (Okafor et al., 2020).

Besides that, cryogenic grinding is a process that employs liquid nitrogen to freeze the scrap tire rubber at a temperature typically between -87 to -198 ℃ until it becomes brittle, followed by using a hammer mill to shatter the frozen rubber into smooth particles (Lo Presti, 2013). Generally, cryogenic grinding works by transforming elastic rubber to a brittle material known as embrittle in the presence of liquid gases to eliminate the rubber degradation due to the heat build-up associated with shearing at ambient conditions (Fazli & Rodrigue, 2020). Cryogens-liquid nitrogen or supercritical carbon dioxide CO_2 are commonly used as the coolant to cool rubber tires below glass transition temperature (-80 ℃), besides functioning to avoid oxidization of the material during crushing grinding by the hammer mill. The brittle nature of the material makes it simple to separate the metal and fibers in a hammer mill. The waste tire powder particles acquired from the cryogenic process with size less than 50 μm have lower surface roughness and specific surface area. Compared to ambient grinding and solution processes, cryogenic grinding has a higher production rate and uses less milling energy. Nevertheless, the pre-granulation and drying process is required for cryogenic ground rubber, which increases the production cost (Okafor et al., 2020). The high consumption of coolant in the freezing process also increases the production cost, which can be solved by modification treatment before rubber grinding. The rubber waste tires can be modified by soaking with polar solvents, such as benzene, cyclohexanone, cyclohexane and toluene, to achieve a superfine level of the particle size of the ground product (Li et al., 2020). The cryogenic grinded granulated bind poorly with polymer matrices when blended and will cause the mechanical properties of the composite tends to fail due to its smooth surface (Fazli & Rodrigue, 2020). Cryogenic-treated crumb rubbers are ideally suited for usage in new tires as they have a high value and are simple to process into

smaller mesh sizes (Okafor et al., 2020). The number of grinding cycles and residence time inside the grinding process determines the final particle size (Fazli & Rodrigue, 2020).

On the other hand, wet grinding is a patented grinding process based on circular grinding plates rotating simultaneously and lubricated by water that acts as a liquid medium and is also used to adjust the temperature (Fazli & Rodrigue, 2020). Wet grinding also requires a water jet with pressure above 2000 psi to strip the rubber. With a high surface area, high volume and less granulate degradation, wet grinding can produce very finely comminuted grain (Rowhani & Rainey, 2016). The fine waste tire powder obtained from wet grinding is mostly utilized as a bitumen modifier (Lo Presti, 2013). Moreover, solution grinding is frequently used to produce tire powders of less than 1 mm by dissolving the rubber chips in a solvent such as aromatic or chlorinated hydrocarbons before feeding them into the gap of the grinding plates (Fazli & Rodrigue, 2020). Last but not least, ultra-high pressure (UHP) water jet grinding is a method of processing large-sized rubber tires into finer granulates by pressurized water without initial shredding of the tires. High operating pressure of about 55,000 psi of water jets revolves in high-speed arrays to shred a whole tire into clean, wire-free narrow strips. The different parts of a tire of thread, sides and interior are treated separately to recover segregation of the various rubber compounds. The unprocessable wastes may be sold as scrap metal. UHP produces the best rubber crumb with fine particle size distribution to possess better mechanical properties in which composites of waterjet-produced crumb had enhanced tensile and shear strength. The granulates are also free of metal and textile materials with a very high surface volume ratio and a high degree of purity (Okafor et al., 2020). UHP is an energy-saving and environmentally friendly method to process a whole tire with good separation to produce granulates without oxidation (Rowhani & Rainey, 2016). Yet, the cost of UHP is very high and high technological expertise is required.

Crumb and granulated rubber made from end-of-life tires can be employed to produce molded rubber goods, such as furniture, signposts, dustbins, wheels, lawnmowers and so on. It also can be utilized for playground flooring, shock-absorbing mats, roofing material, courtyard tile and turf for artificial football fields. The end-of-life tire granules also can be used for rubber concrete, rubberized asphalt and railway and tram tracks due to rubber's possibility to mitigate noise and vibration (Okafor et al., 2020). There is some research or development on waste tire powder as a filler in composites after conducting surface modification on the ground rubber tires either physically or chemically and also by devulcanization or reclamation process to improve adhesion between the rubber particles with the polymer matrix. For example, the waste tire powder was filled in polyester-based composite to be used as an insulating material. Waste rubber crumbs of 40 % were added into the polyester-based composite and characterized for the insulation properties of the composite, such as thermal conductivity, water retention, density and thermal stability. The addition of waste rubber tire particles into the polyester matrix decreased the thermal conductivity and the water retention of the composite, besides improving the tensile strength and compressive strength of the composite to be utilized as a thermal insulator (Nuzaimah et al., 2018).

Furthermore, the waste tire powder (WTP) also can be used as a polypropylene (PP) property enhancer in the plastic composite. The surface morphology of PP/WTP was moderately smooth without any visible impurities, which indicated better adhesion between PP and WTP. PP/WTP at 40% WTP displayed the highest strength value for elongation break and impact testing as the tire rubber powder reduced the stiffness of the composites and improved their impact absorption capacity (Ruey Ong et al., 2021). By utilizing waste tire powder, PP/WTP plastic composite had a tremendous potential to be employed in plastic manufacturing industries and maintain a green environment. The performance of the road pavement was also substantially enhanced by the addition of fine waste rubber powder into the asphalt concrete mixture as the combination was resistant to crack tip separation with good compatibility and interaction between waste rubber particles with the asphalt mixture binder (Nuzaimah et al., 2018). Last but not

least, waste rubber tire powder can be employed to improve the mechanical properties of cement-clay composites. The addition of waste tire powder in the composite showed ductile behavior with the advantage of reflection cracking on roads due to the cement-stabilized base, besides eliminating the need for chip seal, geotextile, or unbound granular layer between the stabilized base and surface to provide stress relaxation. The waste tire powder also improved cemented clays' strength and stiffness characteristics with the final composites can be used in diverse structural and non-load bearing applications, such as a base, sub-base, embankments, rammed earth and retaining walls (Al-Subari et al., 2021).

2.4 Recycled PVC and Composites

Recycled PVC (rPVC) or used PVC from different sources or applications in various industries can be recycled through mechanical recycling, chemical recycling and feedstock recycling. Mechanical recycling is the best method to recycle PVC material directly in the production plant, where waste is produced during start-up and shutdown, mechanical processing of completed goods, or trash resulting from production faults. After mechanical milling, PVC waste can be added to the original material as an admixture (Lewandowski & Skórczewska, 2022). The mechanical approach to PVC recycling is commonly used in cases where clean PVC with a known composition and track record is accessible and has been used to handle post-consumer PVC trash for many years. Meanwhile, chemical recycling is used to convert plastic into its original constituent chemicals for use in polymerization or other chemical processes (Sadat-Shojai & Bakhshandeh, 2011). Besides that, another approach to managing PVC waste is through feedstock recycling. Energy recovery is a relatively simple method of feedstock recycling, which involves burning fuel directly in specialized thermal utilization units or gasifying it. Notably, PVC can exist as a proportion combined with other waste kinds in energy recovery. A slightly more advanced method of feedstock

recycling is converting PVC into valuable raw materials for the chemical industry (Lewandowski & Skórczewska, 2022).

Nowadays, PVC recyclates have been widely used to produce various composites with a high degree of filling, which also acts as an effective method to recycle PVC waste. The minor contamination of PVC with incompatible polymers will not affect the characteristics of these composites to achieve a material with acceptable mechanical properties. Additionally, the blend's composition in terms of its rheological qualities can be optimized through PVC modification using a wide range of process grease and fillers (Lewandowski & Skórczewska, 2022). There are some studies or developments on rPVC utilized as a filler in other materials or blended with other materials to form a composite to improve the properties for further applications, besides resulting in sustainable waste reduction and reuse. One of the research projects studied the mechanical properties and durability of wood plastic composites manufactured from commercially available and rPVC grades. The research project showed that the mechanical properties of PVC drastically decreased, indicating limited compatibility between the wood fibers and the matrix. The tensile strength of the composites from both PVC sources decreased by as much as 64 %, indicating poor durability. However, the composite samples made from rPVC showed superior resistance to weathering than the composites made of plain PVC (Irina & Timo, 2020).

Besides that, rPVC can combine with NonMetallic Fractions (NMF) of printed circuit boards (PCBs) to form PCB-PVC composites. The NMF of paper fabric PCB that acted as a reinforcing filler in rPVC had barely improved the thermal stability of PCB-PVC composites over its pure PVC composite counterpart. When the NMF percentage increased to a specific limit or threshold value of 20 wt % NMF, there was a noticeable improvement in the mechanical properties, such as tensile strength and modulus, bending strength and modulus. Comparing the usage of this threshold quantity of NMF to the pure rPVC, the tensile and bending strength increased by 10 MPa and 7 MPa, respectively. The mechanical strength qualities decreased as the NMF % increased

further. The study concluded that adding a certain percentage of NMF of PCBs as reinforcing filler in the rPVC can efficiently enhance the rPVC's mechanical and thermal qualities for other usage, besides leading to an effective waste resource reusing (Soomro & Sohaib, 2015).

In addition, the development of composite materials employing rPVC recovered from waste electrical and electronic materials (E-waste) and waste fly ash (FA) acquired from thermal power plants has been studied. The mechanical test showed that the tensile strength and elongation at the break of the rPVC/fly ash composite increased up to 30 wt % loading of fly ash, after which the tensile strength decreased. Yet, the impact strength decreased as the fly ash level in the rPVC matrix increased. The morphological characteristics of the composites also demonstrated the filler's good dispersion inside the recycled matrix. Differential scanning calorimetry (DSC) and thermogravimetric analysis (TGA) studies also indicated the thermal properties of rPVC improved with the incorporation of fly ash. The inclusion of fly ash in the rPVC matrix also increased water uptake, according to the results of the water absorption test (Gohatre et al., 2020). With the improved tensile strength, elongation at the break, water absorption and thermal properties at the optimum loading of fly ash incorporated within the rPVC matrix, the composite produced can be applied in further usage to reduce the amount of rPVC effectively.

Last but not least, the waste rPVC was used as an alternative fine aggregate in eco-friendly composite mortars to replace natural sand, which aimed to enhance the brittle behavior of cementitious materials in high acidity environments and the thermal insulation performance. Tests on density, compressive and flexural strengths, thermal conductivity and ultrasonic pulse velocity were used to assess the characteristics of recycled PVC-mortar composites. The results indicated that although values of compressive and flexural strengths and ultrasonic pulse velocity decreased with an increase in rPVC content, it is possible to use up to 70 % rPVC in lightweight ductile mortars. The resistance of mortars against strong acids also increased significantly with

the introduction of PVC aggregates in place of natural sand. Mortars with higher rates of rPVC aggregates also improved the thermal insulation of composite mortars, according to the thermal conductivity results (Senhadji et al., 2019).

In this research, recycled PVC from the carpet backing materials of floor mats was used to mix with two types of rubber waste as fillers, which were the industrial rubber scraps from the scuba diving products or known as ALUM and the micronized rubber tire powder or known as LeHigh, to develop a new composite for car floor mat application that meet industry standards and regulatory requirements. Currently, the typical rubber car floor mats are made from a combination of raw materials of kaolin, recycled rubber, natural rubber, rubber aromatic oil, zinc oxide, sulphur and zinc stearate (ÖRÜCÜ & ATILGAN TÜRKMEN, 2022). Meanwhile, the PVC leather car floor mats are made from a combination of raw materials of PVC artificial leather, imitation fur, sponge, XPE or other anti-slip materials and non-woven fabric (Benson, 2024). Thus, the usage of recycled PVC with rubber waste as filler to produce a new composite for car floor mat application is trusted to be more cost-effective and sustainable, besides reducing the usage and production of PVC and increasing the recycling rate of rubber waste.

CHAPTER 3

MATERIALS AND METHODOLOGY

3.1 Introduction

This chapter includes the source and details of raw materials used, recycled PVC (rPVC), recycled PVC/ALUM (rPVC/ALUM) and recycled PVC/LeHigh (rPVC/LeHigh) composites preparation method with specified parameters, characterization of the fillers used (ALUM and LeHigh) and characterization of rPVC, rPVC/ALUM and rPVC/LeHigh composites as well as the testing of the composites. The overall experimental process is shown in Figure 3.1.

3.2 Raw Materials

3.2.1 Recycled PVC

Recycled PVC (rPVC) was obtained from the recycled backing materials of floor mats from Entex Carpet Industries Sdn. Bhd.. The rPVC contains 70 % plasticized PVC and 30 % calcium carbonate ($CaCO_3$).

3.2.2 Almost Like Unvulcanized Material (ALUM)

Almost Like Unvulcanized Material (ALUM) was obtained from the CY-Handee Rubber Mouldings Sdn. Bhd. located at Parit Buntar, Perak, Malaysia. It is a scrap from latex thread that was produced from in-house industrial scrap of scuba diving products. The production of ALUM included cryogenic grinding of rubber scrap under liquid nitrogen flow into granulates.

3.2.3 Micronized Waste Tire Powder (LeHigh)

LeHigh is a micronized rubber tire powder produced through the cryogenic grinding of truck tires supplied by the company of CY-Handee Rubber Mouldings Sdn. Bhd. located at Parit Buntar, Perak, Malaysia. It has a vulcanized rubber odor and a relative density of 1.14 g/cm^3. The flash point and auto-ignition temperature of LeHigh were measured to be 246.11 °C and 371.11 °C.

3.3 Preparation of Composites

In the recycled PVC (rPVC) composites preparation, the rPVC was pre-dried using an oven at 80 °C for 24 hours to remove any possible moisture content. Next, a mass of 50.0 g of rPVC composite was produced through the melt blending method via a rheometer Brabender® Plastograph® EC 815652. The melt mixing of only rPVC was performed at a temperature of 165 °C for 4 minutes, with a mixing speed of 60 rpm. The melt mixing process of rPVC was performed three times to produce three samples of rPVC composites. The graphs of processing torque against mixing time were obtained from the Brabender Internal Mixer for every run. Afterwards, the rPVC composites were compressed into 0.5 mm thickness sheets via a hydraulic hot and cold press machine (GT-7014-A30C, GOTECH Testing Machines INC., Taichung, Taiwan) at a temperature of 170 °C for a total of 15 minutes, including 8 minutes of pre-heat followed by 4 minutes of hot compression and 3 minutes of cooling. The compressed sheets were then used for further characterization and testing. The same steps above were repeated for rPVC/ALUM and rPVC/LeHigh composites preparation based on the compounding formulations shown in Table 3.1. The melt mixing of rPVC with ALUM and rPVC with LeHigh was also performed three times for every compounding formulation.

Table 3.1 Compounding Formulations of Composites

Composites	Composition (wt %)		
	rPVC	ALUM	LeHigh
1	100	-	-
2	90	10	-
3	80	20	-
4	70	30	-
5	90	-	10
6	80	-	20
7	70	-	30

3.4 Characterization of Raw Materials and Composites

3.4.1 Fourier Transform Infrared Spectroscopy (FTIR)

Fourier Transform Infrared Spectroscopy (FTIR) was performed on the fillers used (ALUM and LeHigh) and composites of recycled PVC (rPVC), rPVC/ALUM and rPVC/LeHigh to determine the types of chemical bonds and functional groups in the fillers used, besides identifying any possible chemical interaction between rPVC with ALUM and rPVC with LeHigh via Perkin Elmer Spectrum ex1. The FTIR analysis was carried out to evaluate the absorption band with wavelength within the range of 4000 cm^{-1} to 400 cm^{-1} with 16 scans at a resolution of 4 cm^{-1}. FTIR method was conducted on the ALUM and LeHigh particles, whereas the ATR method was performed for the composites of rPVC, rPVC/ALUM and rPVC/LeHigh in thin films. For ALUM and LeHigh, the particles were pre-mixed with KBr powder and then finely pulverized before being put into a pellet-forming die to compress into pellets. The pellets were then placed on the disk holder in the spectrometer for analysis.

3.4.2 Particle Size Analysis (PSA)

Before conducting the particle size analysis of the fillers used for ALUM and Lehigh, the refractive index test was carried out to measure the refractive index of ALUM and LeHigh using a digital refractometer (300034, Sper Scientific Ltd., Scottsdale, AZ, USA). Particle size analysis (PSA) was performed to determine the physical characteristics of ALUM and LeHigh particles, such as mean diameter, specific surface area and particle size distribution via Mastersizer 2000, Hydro2000 MU (A). The granulometric properties and the polydispersity of the particles were also evaluated

through the analysis. Distilled water with a refractive index of 1.330 was used as the dispersant for the analysis.

3.4.3 Thermogravimetric Analysis (TGA)

Thermogravimetric analysis (TGA) was conducted to study the Derivative Thermogravimetry (DTG) and thermal stability from weight loss percentage of ALUM, LeHigh, recycled PVC (rPVC) composites, rPVC/ALUM composites and rPVC/LeHigh composites. The decomposition of the composites was also studied at their processing and surface temperature. The analysis was performed by Mettler Toledo TGA SDTA851 E under 50 ml/min flow rate of nitrogen and oxygen flow with a heating rate of 20 °C per minute from 30 °C to 900 °C.

3.4.4 Scanning Electron Microcopy (SEM)

The morphology of ALUM and LeHigh particles, including their shape, surface roughness and any pores on their surfaces, was ascertained through scanning electron microscopy (SEM) analysis. SEM analysis was also conducted on the tensile fractured surface of the rPVC, rPVC/ALUM and rPVC/LeHigh composites to determine the dispersion of ALUM and LeHigh in the rPVC matrix, the surface roughness of the composites as well as the interfacial adhesion between ALUM and LeHigh with the rPVC matrix. SEM analysis was performed using a JOEL JSM 6701F SEM machine at an accelerating voltage of 4 kV. Before the commencement of SEM analysis, the samples were placed on a disc and held in place by double-sided carbon tape, followed by sputter coating with platinum particles to prevent electron charging of the samples.

3.5 Testing of Composites

3.5.1 Tensile Test

According to ASTM D638, a tensile test was performed under room temperature to study the mechanical properties of recycled PVC (rPVC), rPVC/ALUM and rPVC/LeHigh composites, including elastic modulus, ultimate tensile strength and elongation at break using a light-weight universal tensile tester (Tinius Olsen, Model: H10KS-0748, Salfords, UK). Before the testing, the compressed composite sheets were cut into dumbbell shapes using a dumbbell presser and cutter (Leader Technology Scientific (M) Sdn.Bhd., Balakong, Malaysia). For each compounding formulation, five dumbbell-shaped samples were prepared and labelled. A micrometer was used to measure the thickness from three different points for every dumbbell-shaped sample and recorded the average values. The samples with gauge lengths of 26 mm and 3 mm width were then subjected to the tensile tester with 1200 mm of extension range and a load cell of 500 N at a crosshead speed of 50 mm/min. The minimum specification values set by the industry are a minimum of 5 MPa of the ultimate tensile strength and a maximum of 25 % of elongation at break for car floor mat application.

3.5.2 Swelling Test

According to ASTM D471-79, the swelling test was performed to evaluate the resilience of recycled (rPVC), rPVC/ALUM and rPVC/LeHigh composites towards swelling in water. Before the testing, the compressed composite sheets were cut into dumbbell shapes using a dumbbell presser and cutter (Leader Technology Scientific (M) Sdn.Bhd., Balakong, Malaysia). The initial mass (m_i) of the samples was measured using an electronic balance in grams and recorded before being immersed in a constant volume of

water for 72 hours at an ambient temperature of 25 °C and stored under a dark environment. After 72 hours of immersion, the samples were taken out and pressed lightly against tissues, followed by measuring their final mass (m_f). The swelling percentage of the composites in water was determined by Equation 3.1 below. A lower swelling percentage indicated higher swelling resilience of the composites in water, and vice versa. The requirement specification value set by the industry for car floor mat application is a maximum of 2.5 % of the swelling percentage.

$$\text{Swelling Percentage} = [(m_f - m_i) / m_i] \times 100\ \% \quad (3.1)$$

where

m_i = Initial mass of samples, g

m_f = Final mass of samples, g

3.5.3 Hardness Test

According to ASTM D2240, a hardness test using a Trusize brand Durometer with Shore A scale was conducted to determine the hardness value of recycled PVC (rPVC), rPVC/ALUM and rPVC/LeHigh composites at different rPVC compositions through penetration of a stress loaded metal sphere into the rubber. Cylindrical-shaped samples with a diameter of 16 mm and thickness of 8 mm were prepared from the composites via compression moulding before the test. The indentation level of the samples in the durometer indicated their hardness value, whereas a value of 100 showed that the sample had no indentation. The minimum specification value set by the industry for car floor mat application is a Shore A hardness of 90 ± 5.

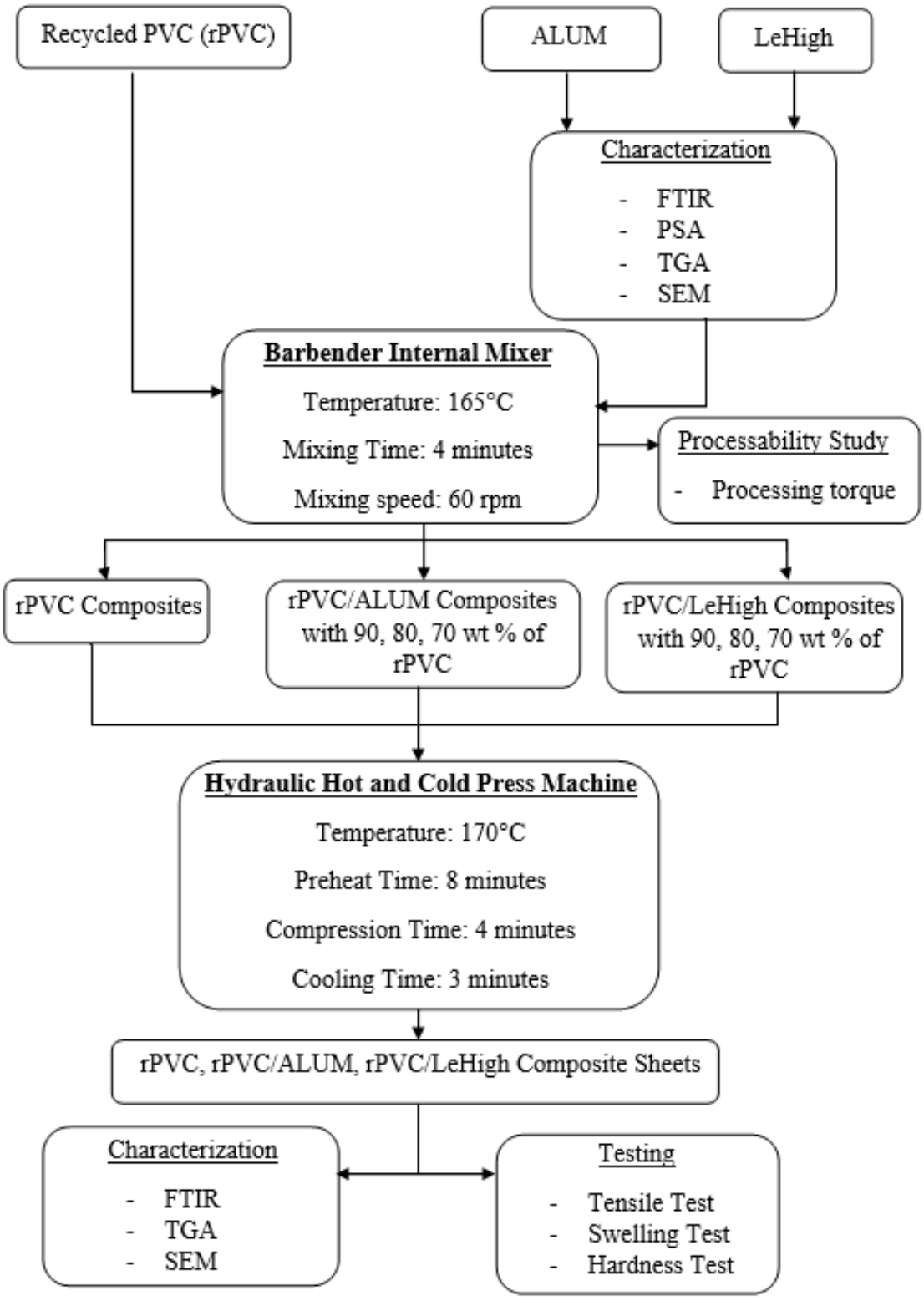

Figure 3.1: Flowchart of Experimental Process

CHAPTER 4

RESULTS AND DISCUSSIONS

4.1 Introduction

This chapter includes the results and analysis of the characterization of the fillers used (ALUM and LeHigh), characterization and testing of recycled PVC (rPVC), recycled PVC/ALUM (rPVC/ALUM) and recycled PVC/LeHigh (rPVC/LeHigh) composites, such as Fourier Transform Infrared Spectroscopy (FTIR), Thermogravimetric Analysis (TGA), Scanning Electron Microscopy (SEM), tensile test, hardness test, swelling test, etc. The characterization of the fillers was carried out for ALUM and LeHigh in the powder form, while the characterization and testing of the composites were carried out by using the composite sheets produced through the hydraulic hot and cold press machine. Significance findings from the results were interpreted and discussed based on past research work.

4.2 Characterization of Fillers

4.2.1 Fourier Transform Infrared Spectroscopy (FTIR)

Fourier Transform Infrared Spectroscopy (FTIR) was an effective analytical instrument for detecting functional groups and identifying chemical bonds of ALUM and LeHigh samples by measuring their absorption of infrared radiation over a range of wavelengths between 4000 and 400 cm^{-1}. The FTIR analysis applied infrared radiation to the ALUM and LeHigh samples to produce an infrared absorption spectrum by absorbing infrared radiation of different wavelengths through different types of chemical bonds and various functional groups. An IR spectrum is a plot of wavenumber, cm^{-1}, (X-axis) vs transmittance or absorbance percentage (Y-axis) that acts as a fingerprint of a specific molecular structure and chemical bonding (Nandiyanto et al., 2022).

For the FTIR analysis of ALUM, Table 4.1 tabulated the characteristic infrared bands of ALUM with the wavelengths, functional groups and vibration types based on its chemical structure and functional groups similar to that of natural rubber as shown in Figure 4.1 as ALUM is mainly composed of natural rubber (NR). Referring to the FTIR spectrum of ALUM displayed in Figure 4.2, the narrow and sharp peak observed at about 3677 cm^{-1} corresponded to the O-H stretching vibration of the hydroxyl group in alcohols, in which the range of wavelengths for O-H stretching vibration of the hydroxyl group in alcohols varied from 3550 cm^{-1} to 3670 cm^{-1} (Nandiyanto et al., 2022). The presence of the hydroxyl group of alcohols in ALUM may be due to the contaminant of isopropanol during the cleaning process of the ATR crystal for the FTIR analysis. Besides that, the asymmetric stretching vibration of C-H in the methyl group can be observed at the absorption peak of 2960 cm^{-1}, while the narrow peaks of 2921 cm^{-1} and 2853 cm^{-1} indicated the asymmetric stretching vibration of C-H in the methylene group as the chemical structure of natural rubber contains a tri-substituted C=C bond with two CH_2 substituents and one CH_3 substituent (Smith, 2022). The medium to intense peak

observed at wavenumber 1663 cm^{-1} indicated the stretching vibration of the alkene double bond (Rahmah et al., 2019).

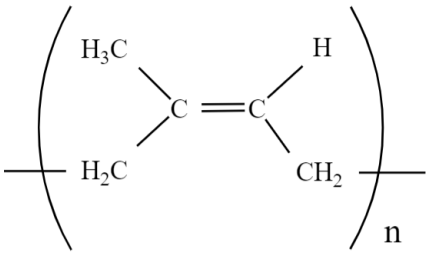

Figure 4.1: Chemical Structure of Natural Rubber (cis-1,4-polyisoprene) (Surya et al., 2018)

Furthermore, the sharp peak observed at 1447 cm^{-1} indicated the deformation vibration of methylene groups ($-CH_2$), while the sharp peak at 1376 cm^{-1} indicated the asymmetric deformation vibration of methyl groups ($-CH_3$) as in the chemical structure of natural rubber (Intapun et al., 2021). The absorption peaks at 1189 cm^{-1} and 1012 cm^{-1} corresponded to the stretching vibration of C-C in the natural rubber chains. Moreover, the peak at a wavenumber of 836 cm^{-1} corresponded to the out-of-plane bending vibration of =C-H in the natural rubber chains, and the band appeared at 753 cm^{-1} assigned to the rocking vibration of C-H in the methylene group (Rahmah et al., 2019). In addition, the low absorption peaks of 669 cm^{-1} and 610 cm^{-1} indicated the stretching vibrations of the C-S and S-S disulfide bonds, which may be due to the traces of sulfur from vulcanization with sulfur as a curing agent to crosslink the rubber matrix and improve the properties of natural rubber (Sisanth et al., 2017). Lastly, the sharp peaks at 532 cm^{-1}, 464 cm^{-1}, 451 cm^{-1} and 424 cm^{-1} are attributed to the stretching vibration of zinc oxide (ZnO) as the range of wavelengths for stretching vibration of zinc oxide varied from 400 cm^{-1} to 600 cm^{-1} (Luna et al., 2019). Zinc oxide is commonly used as an activator or accelerator in the vulcanization process of rubber to promote the crosslinking of rubber polymer chains to improve the mechanical properties of rubber (Paulthangam et al., 2022).

Table 4.1: FTIR Analysis of ALUM

Wavelength (cm^{-1})	Functional group	Vibration mode
3677	O-H alcohol	Stretching
2960	C-H alkyl group (methyl)	Stretching
2921, 2853	C-H alkyl group (methylene)	Stretching
1663	C=C alkene	Stretching
1447	C-H alkyl group (methylene)	Bending
1376	C-H alkyl group (methyl)	Bending
1189, 1012	C-C	Stretching
836	Out of plane =C-H alkene	Bending
753	C-H alkyl group (methylene)	Rocking
669	C-S	Stretching
610	S-S	Stretching
532, 464, 451, 424	Zn-O	Stretching

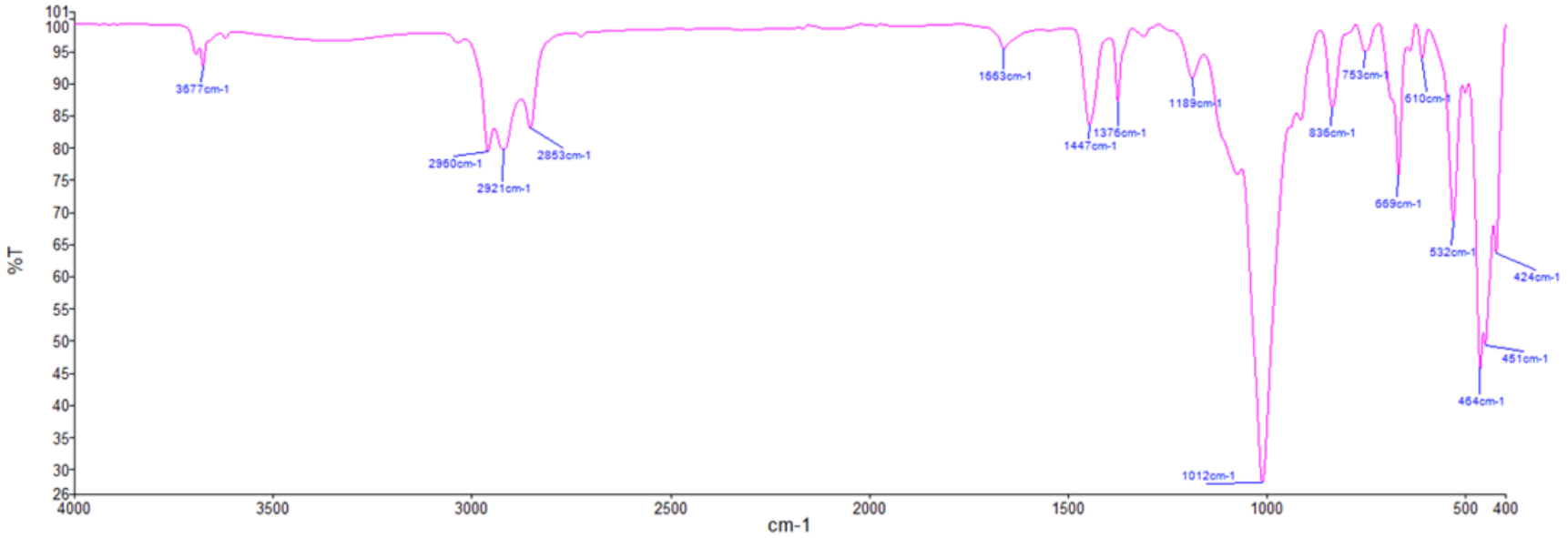

Figure 4.2: FTIR Spectrum of ALUM

For the FTIR analysis of Lehigh, LeHigh is known to be mainly composed of natural rubber (NR), styrene-butadiene rubber (SBR), butadiene rubber (BR) and ethylene-propylene-diene monomer or EPDM rubber with their chemical structures shown in Figure 4.3. Table 4.2 tabulated the characteristic infrared bands of LeHigh with the wavelengths, functional groups and vibration types. Referring to the FTIR spectrum of LeHigh displayed in Figure 4.4, the narrow and sharp peaks observed at 3853 cm^{-1}, 3747 cm^{-1}, 3673 cm^{-1}, 3649 cm^{-1} and 3615 cm^{-1} corresponded to the O-H stretching vibration of the hydroxyl group in alcohols, which may be due to the contaminant of isopropanol during the cleaning process of the ATR crystal for the FTIR analysis. Besides that, the absorption peaks at 2915 cm^{-1} and 2848 cm^{-1} indicated the asymmetric stretching vibration of C-H in the methylene group as the chemical structures of NR, SBR, BR and EPDM contained the CH_2 substituents (Intapun et al., 2021). The sharp peak observed at wavenumber 1536 cm^{-1} indicated the stretching vibration of the C=C-C bond in the aromatic ring as consisted in the chemical structure of SBR (Nandiyanto et al., 2022).

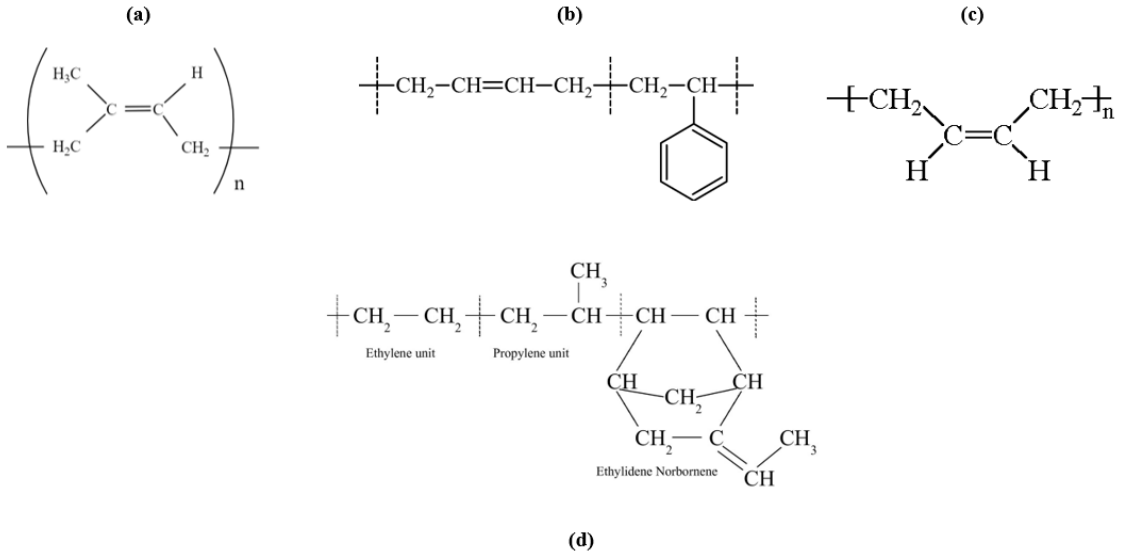

Figure 4.3: Chemical Structure of (a) Natural Rubber (b) Styrene-Butadiene Rubber (c) Butadiene Rubber (d) EPDM Rubber (Fazli & Rodrigue, 2020)

In addition, the sharp and intense peaks at 1432 cm^{-1} and 1372 cm^{-1} are attributed to the asymmetric deformation vibration of methyl groups ($-CH_3$) as in the chemical structures of NR and EPDM (Intapun et al., 2021). The peaks at 1432 cm^{-1} and 1372 cm^{-1} also can be assigned to the bending of the C-C bond of the SBR backbone structure (Khan et al., 2022). Moreover, the prominent peaks noted at 1074 cm^{-1} and 960 cm^{-1} corresponded to the in-plane bending vibration of C-H bond in the aromatic ring, while the absorption peaks at the wavenumber of 819 cm^{-1}, 720 cm^{-1} and 694 cm^{-1} assigned to the out-of-plane bending vibration of C-H bond in the aromatic ring as the chemical structure of SBR consisted of the aromatic ring functional group (Nandiyanto et al., 2022). Lastly, the narrow and sharp peaks at 563 cm^{-1}, 448 cm^{-1} and 412 cm^{-1} indicated the stretching vibration of zinc oxide (ZnO) as the range of wavelengths for stretching vibration of zinc oxide varied from 400 cm^{-1} to 600 cm^{-1} with zinc oxide is commonly used as an accelerator in the vulcanization process to reduce curing time besides enhancing the efficiency of the vulcanization process (Luna et al., 2019).

Table 4.2: FTIR Analysis of LeHigh

Wavelength (cm^{-1})	Functional group	Vibration mode
3853, 3747, 3673, 3649, 3615	O-H alcohol	Stretching
2915, 2848	C-H alkyl group (methylene)	Stretching
1536	C=C aromatic ring	Stretching
1432, 1372	C-H alkyl group (methyl)	Bending
1074, 960	In plane C-H aromatic ring	Bending
819, 720, 694	Out of plane C-H aromatic ring	Bending
563, 448, 412	Zn-O	Stretching

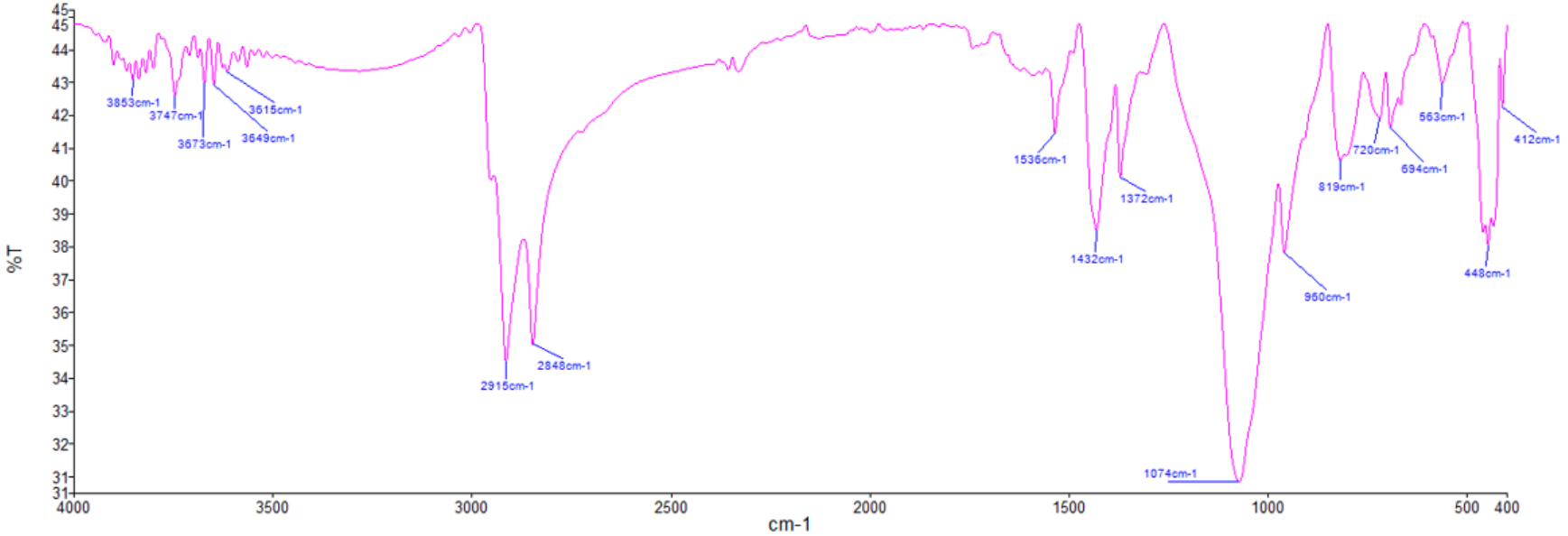

Figure 4.4: FTIR Spectrum of LeHigh

4.2.2 Particle Size Analysis (PSA)

Particle Size Analysis (PSA) was an efficient technique to determine the particle size and particle size distribution (PSD) of the fillers (ALUM and LeHigh) with various parameters as their particle size plays a vital role in affecting physical and mechanical properties, processing and performance of polymer blends. Generally, the finer particle size of the filler particles will provide more surface area to contact with the polymer matrix for better mechanical reinforcement and enhance filler-matrix physical interaction and interfacial adhesion, leading to improved mechanical properties, such as tensile strength, as the specific surface area is inversely proportional to the particle size (Sun et al., 2023). Besides enhancement in the strength and increased compactness of a polymer composite by the smaller filler particle size, it also reduces particle projection at the surface, which improves wear resistance and increases the matrix viscosity (Siraj et al., 2022). Moreover, fillers with smaller particle sizes can also enhance flexural strength and compressive strength due to high specific surface area and strong interfacial bond formation, which results in high surface energy at the filler-matrix interface (Elfakhri et al., 2022). Finer particles also tend to disperse more uniformly within the polymer matrix, resulting in better homogeneity and distribution. Improved dispersion can minimize agglomeration and enhance the effectiveness of the filler in reinforcing the polymer blend (Zhu et al., 2021).

On the contrary, larger particle sizes with lower specific surface area will have lower contact surface area with the polymer matrix, leading to poorer interfacial adhesion of the filler with the matrix. Besides that, large filler sizes also will lead to some drawbacks, such as poor wear resistance due to crack propagation at the filler or resin interface and loss of filler particles, resulting in poor polish-ability, as well as early discoloration and staining due to roughness (Elfakhri et al., 2022). The flexural strength will also decrease, which can be due to the higher stress concentration at the filler-polymer matrix contact as a result of bigger particles, poor interaction between the matrix and filler or the presence of interfacial flaws and inadequate stress distribution

caused by the formation of the stress concentration points resulted from the filler clusters (Elfakhri et al., 2022). However, large filler particles can enhance fracture toughness by improving crack propagation resistance through diverse toughening processes, including crack deflection, crack pinning or bowing, matrix-filler interactions and crack bridging.

For the particle size analysis of ALUM, based on the particle size distribution curve depicted in Figure 4.5, it can be observed that ALUM exhibits a mono-modal (single peak) and narrow particle size distribution. The mono-modal particle size distribution of ALUM with only one dominant peak indicated that most of the particles in the sample are clustered around a single size range with a narrow spread of particle sizes, resulting in a sharp and well-defined peak on the distribution curve in which the peak represented the particle size at which the highest number or volume of particles are present in the sample (Hlobil et al., 2022). Furthermore, the particle size distribution width can be characterized by the span value with the formula of (D90-D10)/D50, in which the wider the distribution, the larger the standard deviation and span value. The D90 value for ALUM was 1215.305 µm, which indicated that 90 % of the sample particles were smaller than 1215.305 µm, 50 % of the sample particles were smaller than 500.722 µm with the D50 value of 500.722 µm and D10 value of 166.154 µm, indicating that 10 % of particles were smaller than 166.154 µm. Through the values of D90, D50 and D10, the span value obtained is 2.095, which was slightly higher but still deemed a narrow particle size distribution. The particle size of ALUM that ranges from 6.181 µm to 2046.612 µm with a distribution broadness of 2040.431 µm in Table 4.3 also implied that ALUM would have irregularity in shapes due to cryogenic grinding, which contributed to deviation in their sizes with a high particle size distribution broadness and slightly higher span value. The irregularity in the shape of ALUM particles was further proven by the SEM images of ALUM shown in Figure 4.9.

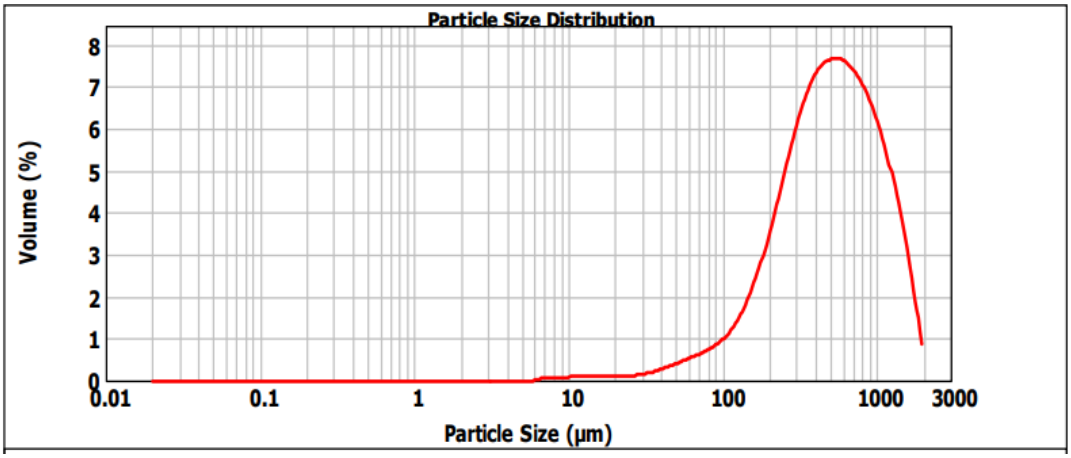

Figure 4.5: Particle Size Distribution of ALUM

Since the ALUM displayed a narrow particle size distribution from the mono-modal particle size distribution curve and the lower particle size distribution width, it suggested that ALUM may have a good uniformity or homogeneity in the particle sizes with moderate variation of particle sizes for less prone to segregation during blending with rPVC to form composite in the melt mixing process besides achieving better surface quality and desired quality (Tuladhar et al., 2020). Without segregation during the melt mixing process, it will ease the processability of ALUM blending with the rPVC with better dispersion and result in more homogeneous blends with improved mechanical properties and product performance. Besides that, it was worth noting that the distribution curve of ALUM was asymmetrical and left-skewed (negatively skewed) as it had a lower tail that created an asymmetry in the distribution by extending far to the left (Green et al., 2023). The left-skewed distribution curve of ALUM indicated that the skewness is less than zero and the sample mean is typically smaller than the sample median with a conclusion that more fine ALUM particles in the sample as compared to coarse particles (Borah & Verbruggen, 2022).

Although ALUM is said to consist of more fine particles in the sample, the particle size of ALUM was considerably coarse as it had a mean diameter of 500.722 µm with a specific surface area of 0.0218 m^2/g from Table 4.3. The large mean particle

size with a relatively small specific surface area of ALUM could cause poor distribution and poor interfacial adhesion between ALUM and the rPVC matrix, leading to the deterioration of the mechanical properties of the composite produced (Elfakhri et al., 2022). Although increasing the filler loading can help enhance the mechanical properties of the composite produced, excessive filler loading will cause filler agglomeration with poor interfacial bonding between the polymer matrix and the filler and poor dispersion of filler particles within the polymer matrix that leads to a reduction in mechanical properties and poor surface quality (Cionita et al., 2022).

For the particle size analysis of LeHigh, based on the particle size distribution curve depicted in Figure 4.6, it can be observed that LeHigh also exhibits a mono-modal (single peak) and narrow particle size distribution. The span value obtained for LeHigh was 1.368, with a D90 value of 95.304 µm, a D50 value of 51.879 µm and a D10 value of 24.309 µm, which was considerably lower and deemed a narrow particle size distribution. Although both ALUM and LeHigh displayed a mono-modal and narrow particle size distribution in the curves, the ALUM seemed to have a broader particle size distribution than LeHigh by comparing the particle size distribution curves in Figure 4.5 and Figure 4.6. The narrow particle size distribution of LeHigh from the mono-modal particle size distribution curve and the lower particle size distribution width or span value indicated that LeHigh has a high degree of uniformity or homogeneity in the particle sizes within the sample with lower variation of particle sizes to facilitate better dispersion within the polymer matrix during blending with less segregation besides promoting increased surface area for stronger interfacial adhesion and bonding, leading to improved mechanical properties and surface quality (Kundie et al., 2018). The particle size that ranges from 4.084 µm to 148.264 µm with a distribution broadness of 144.180 µm in Table 4.3 proved that LeHigh has a higher uniformity of particle size with a lower deviation in their sizes as it still has some irregularity in shapes due to cryogenic grinding. The irregularity in the shape of LeHigh particles was further proven by the SEM images of LeHigh shown in Figure 4.9.

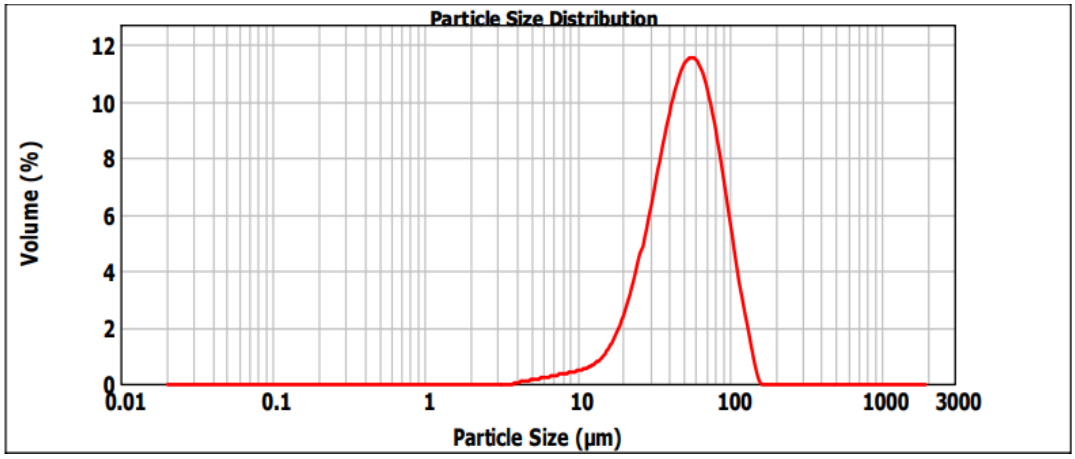

Figure 4.6: Particle Size Distribution of LeHigh

In addition, it was worth noting that the distribution curve of LeHigh was also asymmetrical and left-skewed as it had a lower tail that created an asymmetry in the distribution by extending far to the left, which indicated that there are more fine LeHigh particles in the sample as compared to coarse particles (Borah & Verbruggen, 2022). The particle size of LeHigh was considerably fine as it had a mean diameter of 51.879 µm with a specific surface area of 0.147 m^2/g from Table 4.3. The smaller specific surface area of LeHigh particles also tends to cause poor interfacial interaction and bonding between the polymer matrix and the filler and poor dispersion and distribution of fillers within the polymer blend, affecting the mechanical properties of the composite produced (Kundie et al., 2018). Although fine particles of LeHigh can enhance the surface quality and mechanical properties of the polymer blend, it can show an increased tendency towards agglomeration with the increase of the filler content and introduce a lubrication action on the molecular mobility (Zhu et al., 2021). The filler particle's agglomeration around the polymer matrix at a higher percentage of filler will result in a reduction in the flexural and tensile behavior of the composites and more voids in the surface of the composites due to poor dispersion and poor interfacial bonding between the polymer matrix and the filler (Cionita et al., 2022).

Table 4.3: Physical Properties of ALUM and LeHigh

Physical Properties	Values	
	ALUM	**LeHigh**
Mean diameter (µm)	500.722	51.879
Specific surface area (m^2/g)	0.0218	0.147
Particle size distribution (µm)	6.181 – 2046.612	4.084 – 148.264
Distribution broadness (µm)	2040.431	144.180

4.2.3 Thermogravimetric Analysis (TGA)

Thermogravimetric Analysis (TGA) is known as a widely used thermal analysis technique to study the thermal stability and decomposition behavior of materials, which is usually performed either as a function of temperature rise with constant heating rate or as a function of time by considering the mass loss and temperature constant. In other words, TGA measures a sample's weight as it is heated or cooled in a furnace or measures the amount and rate (velocity) of change in the mass of a sample as a function of temperature or time in a controlled atmosphere. The measurements will then be used to determine the thermal and oxidative stabilities of materials with their compositional properties. The TGA can also analyze materials that exhibit either mass loss or gain due to various factors, such as decomposition, degradation, oxidation and loss of volatile compounds. Overall, TGA is a powerful technique for studying the thermal behavior, stability and composition of polymeric materials, including thermoplastics, thermosets, elastomers and composites, providing valuable insights into their properties, processing and performance in a variety of applications (Parameshwaran et al., 2018).

According to Figure 4.7, the TGA analysis of ALUM indicated that the mass loss of ALUM occurred in a single-stage decomposition process, which can be supported by

the appearance of a single peak in the DTG curve of ALUM provided in Appendix A. Based on Figure 4.7, the single-stage decomposition process of ALUM happened between the temperature of 311.80 °C to 467.61 °C, in which the decomposition of natural rubber with the highest mass loss generally occurred in a single step with temperature ranging from 310 °C to 470 °C (Dobrovská et al., 2024). The general decomposition temperature range of natural rubber implied that ALUM can still exist as a thermally stable compound without much mass loss when below the temperature range of 310 °C to 470 °C, in which the total mass loss of ALUM showed only a lower value of 0.96 % when at the lower temperature of 165 °C as displayed in Table 4.4. The lower value also pointed out that ALUM has a high thermal stability of up to 99.04 % at the blend processing temperature of 165 °C, which is considerably thermally stable to blend with the rPVC to form a composite without losing its elasticity and properties.

Upon thermal decomposition of ALUM at temperatures of between 311.80 °C to 467.61 °C, the ALUM consisting mainly of natural rubber will undergo intense mass loss due to β-scission of rubber chains from the low bond-dissociation energy and lead to the formation of allylic radicals on the natural rubber (Yamamoto et al., 2018). The thermal decomposition of natural rubber will then produce decomposition products of dipentene accompanied by the appearance of isoprene monomer due to the Diels-Alder addition reaction between two isoprene molecules or the back-biting reaction of the pyrolysis product of polyisoprene (Wan et al., 2020). Certain decomposition products, such as CH_4, C_2 hydrocarbons, C_3 hydrocarbons, C_4 hydrocarbons, etc., also produced and increased in quantity when the temperature rose above 330 °C, while other products, such as toluene, dipentene, trimeric isoprene, etc., decreased (Wan et al., 2020). According to Fan et al. (2016), the pyrolysis of latex in the temperature ranges of 250 °C to 420 °C also produced various volatile and char. As for the remaining 23.98 % of the residue of ALUM at the temperature of 900 °C with a total mass loss of 76.02 %, it was mainly attributed to the carbonaceous material in ALUM with superb thermal stability that would not further decompose even at a high temperature of 900 °C. Besides that, the temperature at 50 % mass loss of ALUM of 329.73 °C from Table 4.4 indicated the

thermal stability index of ALUM, in which a lower $T_{50\%}$ temperature meant lower thermal stability as the material will degrade at lower temperatures, while a higher $T_{50\%}$ temperature suggested higher thermal stability as the material can withstand higher temperatures before significant decomposition occurs.

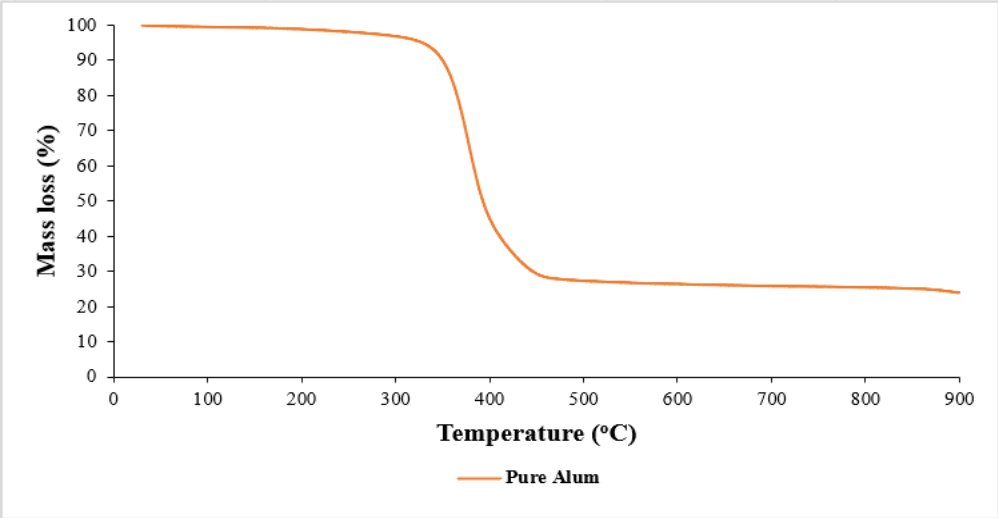

Figure 4.7: Thermogravimetric Analysis of ALUM

According to Figure 4.8, the TGA analysis of LeHigh indicated that the mass loss of LeHigh occurred in a two-stage decomposition process, which can be confirmed by the presence of two peaks in the DTG curve of LeHigh provided in Appendix A. By referring to Figure 4.8, the first stage decomposition process of LeHigh happened between the temperatures of 285.92 °C to 413.73 °C, while the second stage decomposition process occurred at the temperature ranges of 413.73 °C to 493.49 °C. The first stage decomposition process of LeHigh at temperatures of 285.92 °C to 413.73 °C may be related to the decomposition of additives and volatile compounds in the rubber compounds contained in LeHigh (Ammineni et al., 2022). Furthermore, as LeHigh consists of natural rubber and styrene-butadiene rubber, the natural rubber will decompose at a temperature range of 300 °C to 350 °C, while styrene-butadiene rubber will decompose at a temperature range of 350 °C to 450 °C, which are in the temperature ranges of the first stage and second stage decomposition process of LeHigh

(Tsipa et al., 2023). The butadiene rubber and EPDM rubber in LeHigh also decomposed under the second stage decomposition process of LeHigh, in which the thermal degradation process of EPDM rubber occurs in the temperature range of 400 °C to 450 °C (Tang et al., 2013). The decomposition products of CH_4, C_2 hydrocarbons, C_3 hydrocarbons, C_4 hydrocarbons, dipentene, trimeric isoprene, volatile compounds, char and so on also will be produced during the decomposition process with the scission of rubber chains (Wan et al., 2020). As for the remaining 33.75 % of the residue of LeHigh at the temperature of 900 °C with a total mass loss of 66.25 %, it was mainly attributed to the carbon black reinforcing filler generally found in waste tires that would not further decompose into smaller volatile fragments even at a high temperature of 900 °C. In addition, LeHigh with a lower total mass loss of 1.25 % at the blend processing temperature of 165 °C from Table 4.4 showed that LeHigh has a high thermal stability of up to 98.75 % to blend with the rPVC to form a composite without losing its elasticity and properties. The temperature at 50 % mass loss of LeHigh of 432.63 °C from Table 4.4 indicated the thermal stability index of LeHigh and the temperature is higher than that of ALUM, which implied that LeHigh has higher thermal stability than ALUM to withstand higher temperatures for decomposition due to the presence of carbon black reinforcing filler in LeHigh.

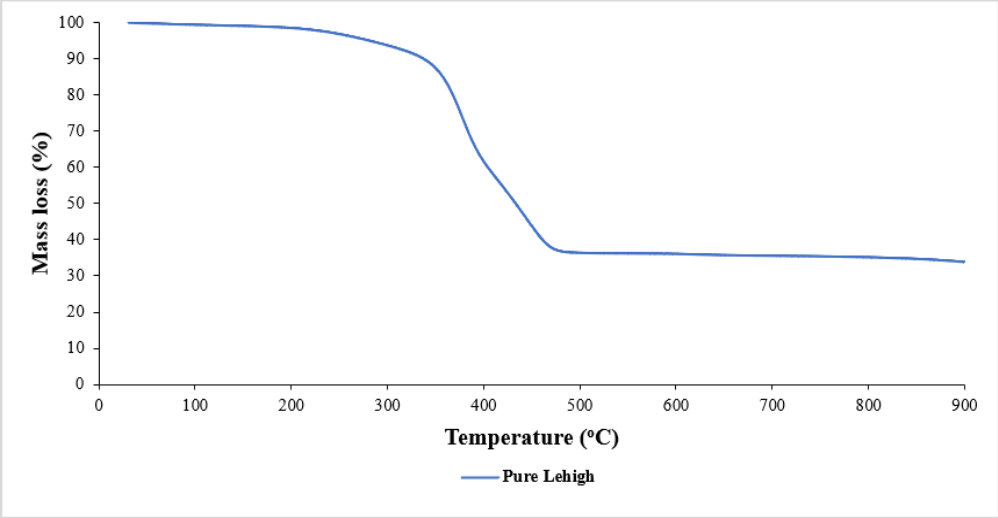

Figure 4.8: Thermogravimetric Analysis of LeHigh

Table 4.4: Thermogravimetric Analysis of ALUM and LeHigh

Component	Temperature at 50 % mass loss, $T_{50\%}$ (°C)	Total mass loss at 165 °C (%)	Total mass loss at 900 °C (%)
ALUM	392.73	0.96	76.02
LeHigh	432.63	1.25	66.25

4.2.4 Scanning Electron Microscopy (SEM)

Scanning Electron Microscopy (SEM) is a powerful imaging technique used to observe the surface morphology and composition of materials at high magnification by scanning a focused beam of electrons across the surface of a sample and detecting the interactions between the electrons and the sample. SEM provides detailed three-dimensional and high-resolution images of the surface of a sample with a high depth of field, making it valuable for a wide range of scientific and industrial applications (Ahmad et al., 2021).

Figures 4.9 (a) and (b) showed the SEM images of ALUM particles at 1000x and 5000x magnification, while Figures 4.9 (c) and (d) displayed the SEM images of LeHigh particles at 1000x and 5000x magnification. As illustrated in Figures 4.9 (a) and (c) of the SEM images of ALUM and LeHigh particles under 1000x magnification, ALUM particles and LeHigh particles both possessed irregular particle shapes due to the cryogenic grinding process during the production of the particles. Generally, there are several typical shapes of filler particles, such as spherical, cubic, tabular, flake, elongated, tubular and irregular, which can affect rubber processing and performance reinforcement. Each particle shape has its advantages, such as spherical particles providing the best packing density, a uniform distribution of stress and lower viscosity, cubic and tabular shapes delivering better reinforcement and packing density, and

elongated particles giving superior reinforcement, reducing shrinkage and thermal expansion and promoting thixotropic properties (Wypych, 2016). Irregular particles may not possess unique advantages with a less uniform distribution of stress that allow stress concentration, but they are generally more uncomplicated to produce and inexpensive (Nagrale et al., 2023).

Besides that, from Figures 4.9 (a) and (c), it also can be observed that ALUM particles had a larger particle size than LeHigh particles, which indicated that ALUM particles had a lower specific surface area than LeHigh particles. Smaller particle sizes of LeHigh with a higher specific surface area also implied that LeHigh particles had a larger interfacial contact area with the rPVC matrix compared to ALUM particles, which can result in stronger physical interaction to enhance the interfacial adhesion with the matrix and better mechanical reinforcement (Barrera & Cornish, 2022). The smaller size of filler particles also tends to provide high surface quality for the composite produced with improved wear resistance, besides generating high surface energy at the filler-matrix contact to improve flexural strength and compressive strength (Elfakhri et al., 2022). On the contrary, larger particle sizes of filler will have lower contact surface area with the polymer matrix, leading to poorer interfacial adhesion of the filler with the matrix with poor dispersion, besides degrading the properties of the composite by acting as flaws that concentrate stress and contribute to the breakage of the polymer chains and initiation of cracks (Barrera & Cornish, 2022).

Furthermore, the surface morphology of ALUM and LeHigh particles based on the SEM images under 1000x magnification showed that both ALUM and LeHigh particles possessed rough surfaces with a small amount of voids observed on their surfaces due to entrapped air and moisture. Theoretically, the rough surfaces of filler particles provide more surface area for better interfacial adhesion between the filler and the polymer matrix, resulting in improved mechanical properties and load transfer within the composite material (Hilal, 2021). In other words, the roughness of filler particles can affect the mechanical properties of the composite produced by increasing the actual

interface bonding area, besides improving the mechanical interlocking action between the polymer matrix and the filler particles at the interface (Hilal, 2021). Irregularities on the surface can also help prevent crack propagation, resulting in more robust and fatigue-resistant bonds. Although ALUM and LeHigh particles seem to possess the same surface roughness from the SEM images under 1000x magnification, it can be noted that LeHigh particles had a higher surface roughness than ALUM particles with more voids on the surface from the SEM images of ALUM and LeHigh particles under 5000x magnification displayed in Figures 4.9 (b) and (d), which indicated that LeHigh particles tend to have better physical interaction with the rPVC matrix via chain interlocking with better interfacial adhesion as compared to ALUM particles to improve the tensile properties of the composite produced. Hence, from all the SEM images, it can be concluded that LeHigh particles will have more contact surface area with the rPVC matrix to form stronger interfacial adhesion and show better physical interaction via chain interlocking due to their smaller particle size with irregular shape and higher surface roughness.

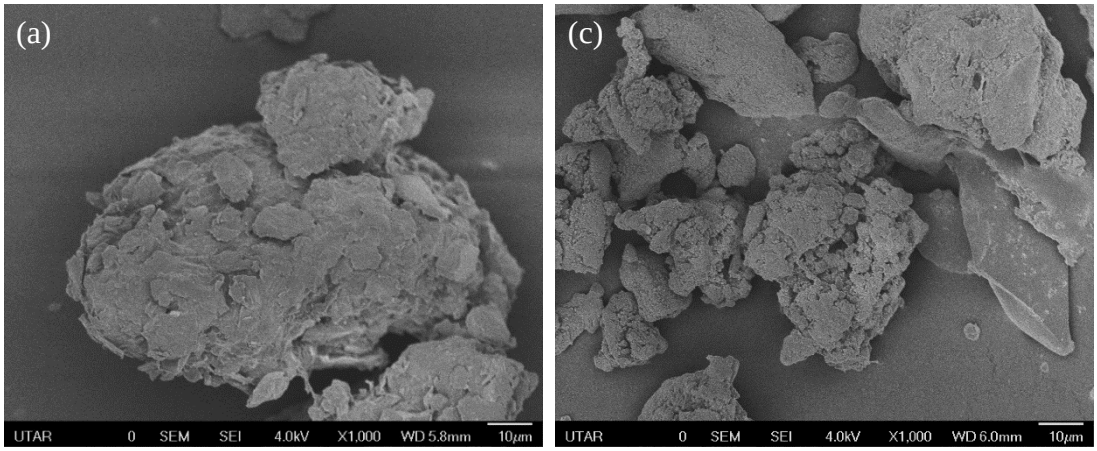

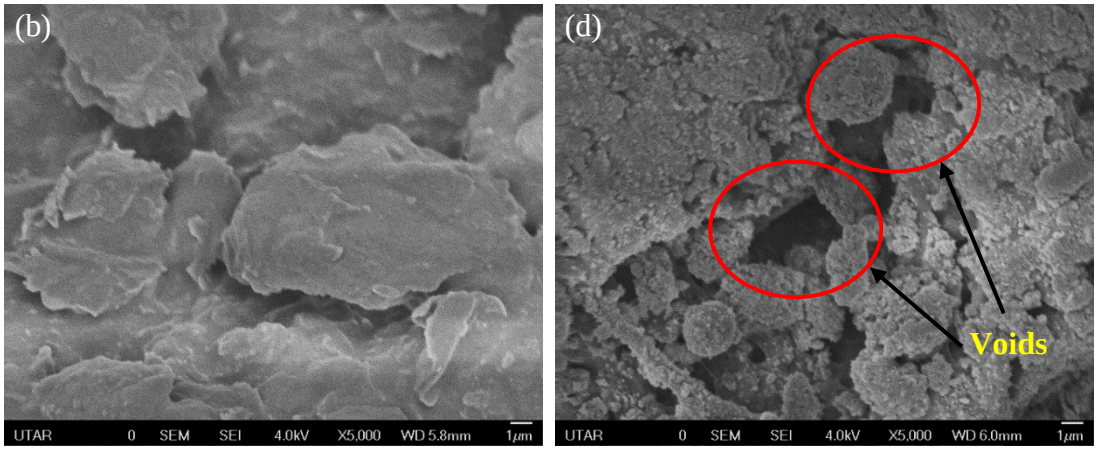

Figure 4.9: SEM Images of ALUM under (a) 1000x (b) 5000x Magnification and LeHigh under (c) 1000x (d) 5000x Magnification

4.3 Characterization and Testing of Composites

4.3.1 Fourier Transform Infrared Spectroscopy (FTIR)

FTIR analysis has been carried out for the characterization of composites to determine the functional groups in the rPVC, rPVC/ALUM and rPVC/LeHigh composites, as well as the possible chemical interactions between rPVC with ALUM or LeHigh by measuring the absorption of infrared radiation as a function of frequency. For the FTIR analysis of the rPVC composite, Table 4.5 tabulated the characteristic infrared bands of the rPVC composite of the wavelengths, functional groups and vibration types with the FTIR spectrum for the rPVC composite shown in Figure 4.11. The chemical structure of the rPVC is shown in Figure 4.10, which consists of repeating units of vinyl chloride monomers (CH_2=CHCl) that polymerize to form long chains. The rPVC used in this research also consists of dioctyl phthalate (DOP), the most widely used plasticizer in PVC that acts as an additive to soften the PVC and modify its properties or performance

characteristics to allow for a wide range of applications with the chemical structure as shown in Figure 4.10.

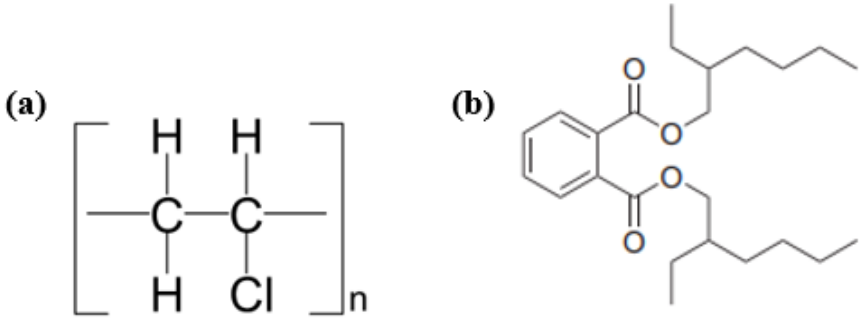

Figure 4.10: Chemical Structure of (a) Polyvinyl Chloride (b) DOP Plasticizer (Cruz et al., 2020; Burns et al., 2023)

By referring to the FTIR spectrum of rPVC composite in Figure 4.11, the sharp peak at 2958 cm^{-1} indicated the asymmetric stretching vibration of C-H in the methyl group as consisting in the chemical structure of DOP plasticizer (Nandiyanto et al., 2022). Besides that, two intense peaks at the wavelength of 2920 cm^{-1} and 2854 cm^{-1} corresponded to the asymmetric stretching vibration of C-H in the methylene group as consisting in the chemical structure of the rPVC and DOP plasticizer with the range between 2915 cm^{-1} to 2935 cm^{-1} and 2845 cm^{-1} to 2865 cm^{-1} (Nandiyanto et al., 2022). The narrow and sharp peak observed at 1723 cm^{-1} implied the presence of the DOP plasticizer in the rPVC, which assigned to the stretching vibration of the C=O double bond in the ester compound as consisting in the chemical structure of DOP plasticizer (Luo et al., 2022). In addition, the characteristic peak at 1421 cm^{-1} is attributed to the angular deformation of CH_2-Cl, while the sharp absorption peak at 1257 cm^{-1} is designated to the out-of-plane angular deformation of CH-Cl as consisting in the chemical structure of the rPVC (Chen et al., 2018).

Moreover, the absorption band at the wavelength of 1124 cm^{-1} corresponded to the symmetric stretching of the C-O-C functional group in the chemical structure of the DOP plasticizer (Machado & Webster, 2017). The intense peak at 1073 cm^{-1} indicated the stretching vibration of the C-C bond of the rPVC backbone chain that occurred in the range between 1000 cm^{-1} to 1100 cm^{-1} (Amar et al., 2019). Furthermore, the characteristic peak at 959 cm^{-1} implied the out-of-plane trans deformation of the C-H bond, while the sharp peak at 874 cm^{-1} assigned to the out-of-plane bending vibration of C-H bond in the aromatic ring as contained in the chemical structure the DOP plasticizer (Chen et al., 2018). Lastly, the absorption peaks at 743 cm^{-1}, 710 cm^{-1} and 611 cm^{-1} are designated to the stretching vibration of the C-Cl bond in the chemical structure of the rPVC, while the peak at the wavelength of 455 cm^{-1} indicated the out-of-plane bending vibration of C=C in the aromatic ring from the chemical structure of the DOP plasticizer (Amar et al., 2019).

Table 4.5: FTIR Analysis of rPVC Composite

Wavelength (cm^{-1})	Functional group	Vibration mode
2958	C-H alkyl group (methyl)	Stretching
2920, 2854	C-H alkyl group (methylene)	Stretching
1723	C=O ester	Stretching
1421	CH_2-Cl	Angular deformation
1257	Out of plane CH-Cl	Angular deformation
1124	C-O-C	Stretching
1073	C-C	Stretching
959	Out of plane C-H	Trans deformation
874	Out of plane C-H aromatic ring	Bending
743, 710, 611	C-Cl	Stretching
455	Out of plane C=C aromatic ring	Bending

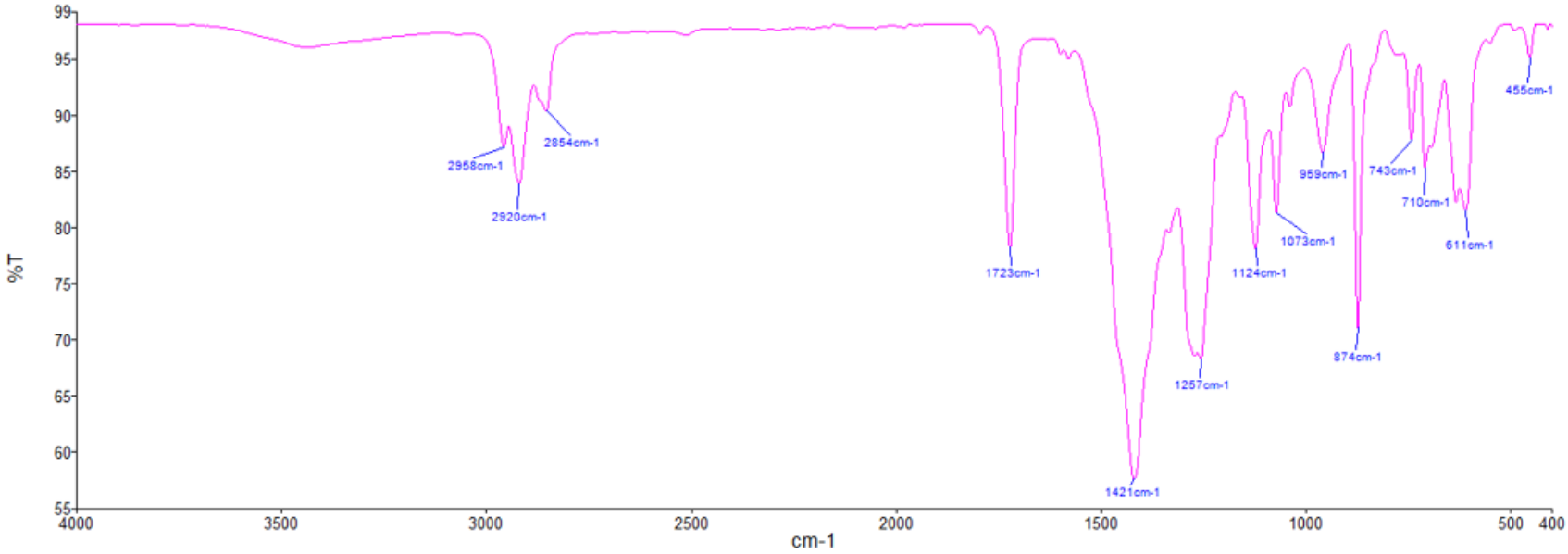

Figure 4.11: FTIR Spectrum of rPVC Composite

Based on the FTIR analyses in Table 4.6 and Figure 4.12 that compared FTIR spectra of rPVC/ALUM composites at different ALUM loadings with rPVC composite, it can be deduced that no new peak is detected, confirming that there is no chemical reaction occurred between the rPVC and ALUM during the melt mixing process with the interaction between the rPVC matrix and ALUM is solely dependent on interfacial adhesion or physical entanglement. The functional peaks of composites of rPVC/ALUM 10, rPVC/ALUM 20 and rPVC/ALUM 30 are almost similar to the rPVC composite, except there are some shifting or deviation of the peaks and some of the peaks of the rPVC/ALUM composites are not from the rPVC composite but from the filler of ALUM that interacted with the rPVC matrix. For example, the peak of the angular deformation of CH_2-Cl at 1421 cm^{-1} noted from the rPVC composite barely shifted to 1423 cm^{-1} and 1431 cm^{-1} in the rPVC/ALUM composites, the peak of the out-of-plane angular deformation of CH-Cl observed from the rPVC composite at the wavelength of 1257 cm^{-1} shifted to 1272 cm^{-1} in the rPVC/ALUM 30 composite and the peak of the out-of-plane bending vibration of C=C in the aromatic ring noted from the rPVC composite at 455 cm^{-1} slightly shifted to 465 cm^{-1} and 466 cm^{-1} in the rPVC/ALUM composites at different ALUM loadings.

In addition, the peak of the stretching vibration of the C-Cl bond observed from the rPVC composite at 710 cm^{-1} slightly shifted to 694 cm^{-1} in the rPVC/ALUM 30 composite with the appearance of the same stretching vibration of the C-Cl bond new peak at 636 cm^{-1} and 637 cm^{-1} in the composites of rPVC/ALUM 20 and rPVC/ALUM 30 as the peak was not apparent in the composites of rPVC and rPVC/ALUM 10 due to the increasing of the peak intensity with increasing ALUM loadings in the composites. It also can be observed that from Table 4.6, the peak of the out-of-plane trans deformation of the C-H bond at 959 cm^{-1} from the rPVC composite became unapparent in the rPVC/ALUM 30 composite, which may be due to the overlapping of the peak intensity that led to the weak absorption band. The functional peaks from ALUM but not from the rPVC composite that appeared in the rPVC/ALUM composites at different ALUM loadings included the peak of the asymmetric deformation vibration of methyl groups (-

CH_3) that appeared at 1377 cm^{-1} of the rPVC/ALUM 30 composite, the peak of the out-of-plane bending vibration of =C-H that appeared at 836 cm^{-1} of the rPVC/ALUM 30 composite and the peaks for the stretching vibration of zinc oxide that varied from 400 cm^{-1} to 600 cm^{-1} appeared in all the rPVC/ALUM composites of different ALUM loadings at 537 cm^{-1}, 536 cm^{-1}, 535 cm^{-1} and 426 cm^{-1} (Luna et al., 2019).

By referring to the FTIR analyses in Table 4.6 and Figure 4.13 that compared FTIR spectra of rPVC/LeHigh composites at different LeHigh loadings with rPVC composite, it can also be deduced that no new peak is detected, confirming that there is no chemical reaction occurred between the rPVC and LeHigh during the melt mixing process with only physical interaction between the rPVC matrix and LeHigh. All the functional peaks from the rPVC composite can be seen in the rPVC/LeHigh composites of different LeHigh loadings with only some slight shifting of the peaks. Moreover, it can be noted from Table 4.6 that the peak of the asymmetric stretching vibration of C-H in the methyl group at 2958 cm^{-1} from the rPVC composite became unapparent in the rPVC/LeHigh 30 composite, which may be due to the overlapping of the peak intensity that led to the weak absorption band. Although all the functional peaks of the composites of rPVC/LeHigh of different LeHigh loadings are nearly similar to the rPVC composite, there is still one peak of the asymmetric deformation vibration of methyl groups at 1372 cm^{-1} from LeHigh but not from the rPVC composite appeared in all the composites of rPVC/LeHigh of different LeHigh loadings with some shifting to 1344 cm^{-1}.

Table 4.6: FTIR Analyses of ALUM, LeHigh, rPVC Composite, rPVC/ALUM Composites and rPVC/LeHigh Composites

Functional Group	Wavelength (cm^{-1})								
	rPVC	ALUM	LeHigh	rPVC/ALUM 10	rPVC/ALUM 20	rPVC/ALUM 30	rPVC/LeHigh 10	rPVC/LeHigh 20	rPVC/LeHigh 30
O-H alcohol; Stretching	-	3677	3853, 3747, 3673, 3649, 3615	-	-	-	-	-	-
C-H alkyl group (methyl); Stretching	2958	2960	-	2958	2959	2959	2958	2958	-
C-H alkyl group (methylene); Stretching	2920, 2854	2921, 2853	2915, 2848	2922, 2856	2920, 2855	2922, 2855	2919, 2855	2919, 2852	2918, 2852
C=O ester; Stretching	1723	-	-	1723	1724	1727	1723	1723	1723
C=C alkene; Stretching	-	1663	-	-	-	-	-	-	-
C=C aromatic ring; Stretching	-	-	1536	-	-	-	-	-	-

C-H alkyl group (methylene); Bending	-	1447	-	-	-	-	-	-	-
C-H alkyl group (methyl); Bending	-	1376	1432, 1372	-	-	1377	1334	1334	1334
CH_2-Cl; Angular deformation	1421	-	-	1423	1423	1431	1422	1423	1423
Out of plane CH-Cl; Angular deformation	1257	-	-	1257	1258	1272	1257	1256	1256
C-O-C; Stretching	1124	-	-	1123	1122	1120	1123	1122	1122
C-C; Stretching	1073	1189, 1012	-	1073, 1039	1073, 1017	1192, 1073, 1014	1073	1073	1073
In plane C-H aromatic ring; Bending	-	-	1074, 960	-	-	-	-	-	-
Out of plane C-H; Trans deformation	959	-	-	960	961	-	959	959	959
Out of plane C-H aromatic ring; Bending	874	-	819, 720, 694	874	874	875	874	874	873
Out of plane =C-H	-	836	-	-	-	836	-	-	-

alkene**;** Bending									
C-Cl**;** Stretching	743, 710, 611	-	-	743, 711, 611	743, 710, 636, 610	743, 694, 637, 610	743, 710, 611	742, 710, 610	742, 710, 610
C-H alkyl group (methylene)**;** Rocking	-	753	-	-	-	-	-	-	-
C-S**;** Stretching	-	669	-	-	-	-	-	-	-
S-S**;** Stretching	-	610	-	-	-	-	-	-	-
Out of plane C=C aromatic ring**;** Bending	455	-	-	465	466	466	455	455	455
Zn-O**;** Stretching	-	532, 464, 451, 424	563, 448, 412	537	536	535, 426	-	-	-

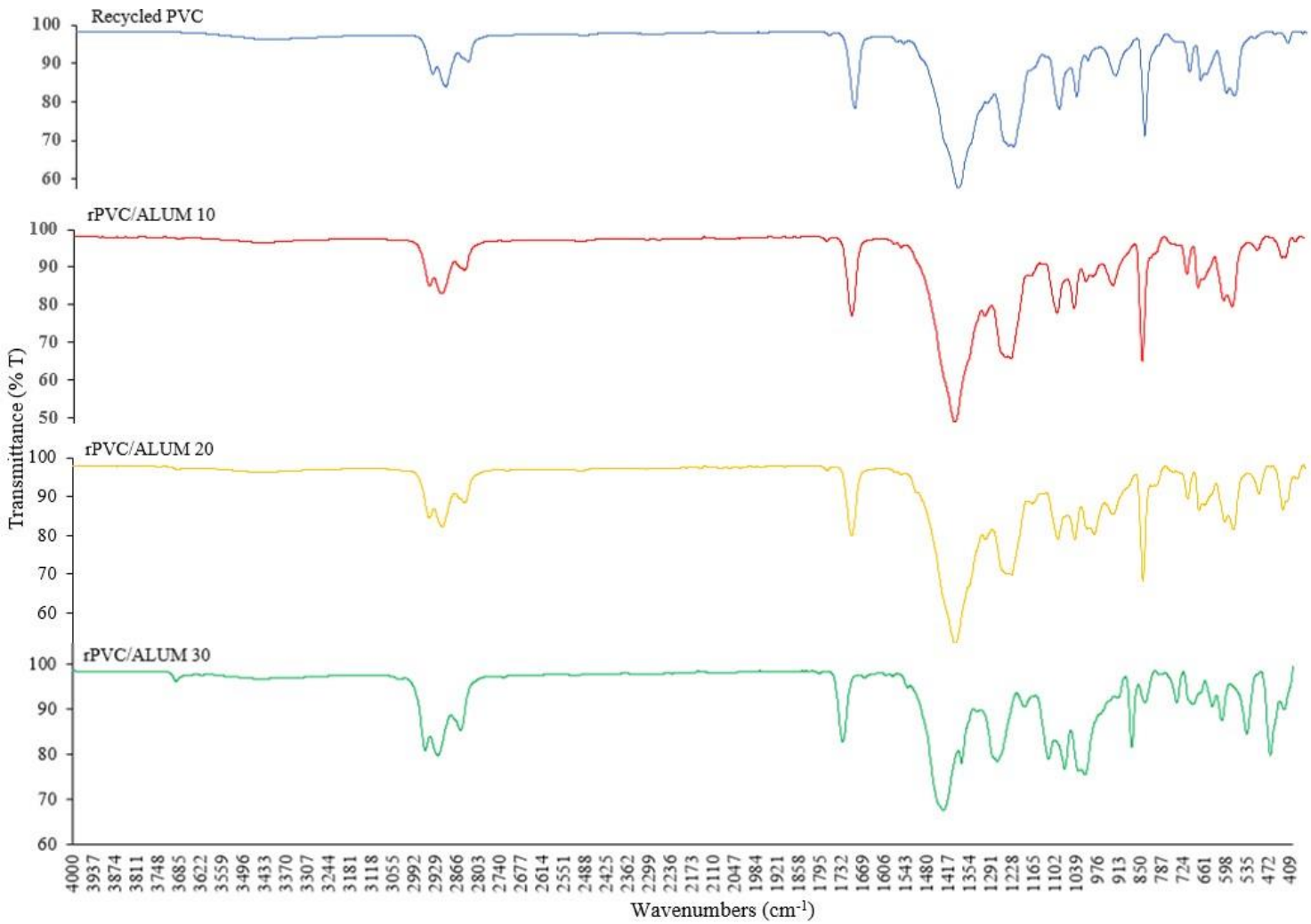

Figure 4.12: FTIR Spectra of rPVC/ALUM Composites at Different ALUM Loadings

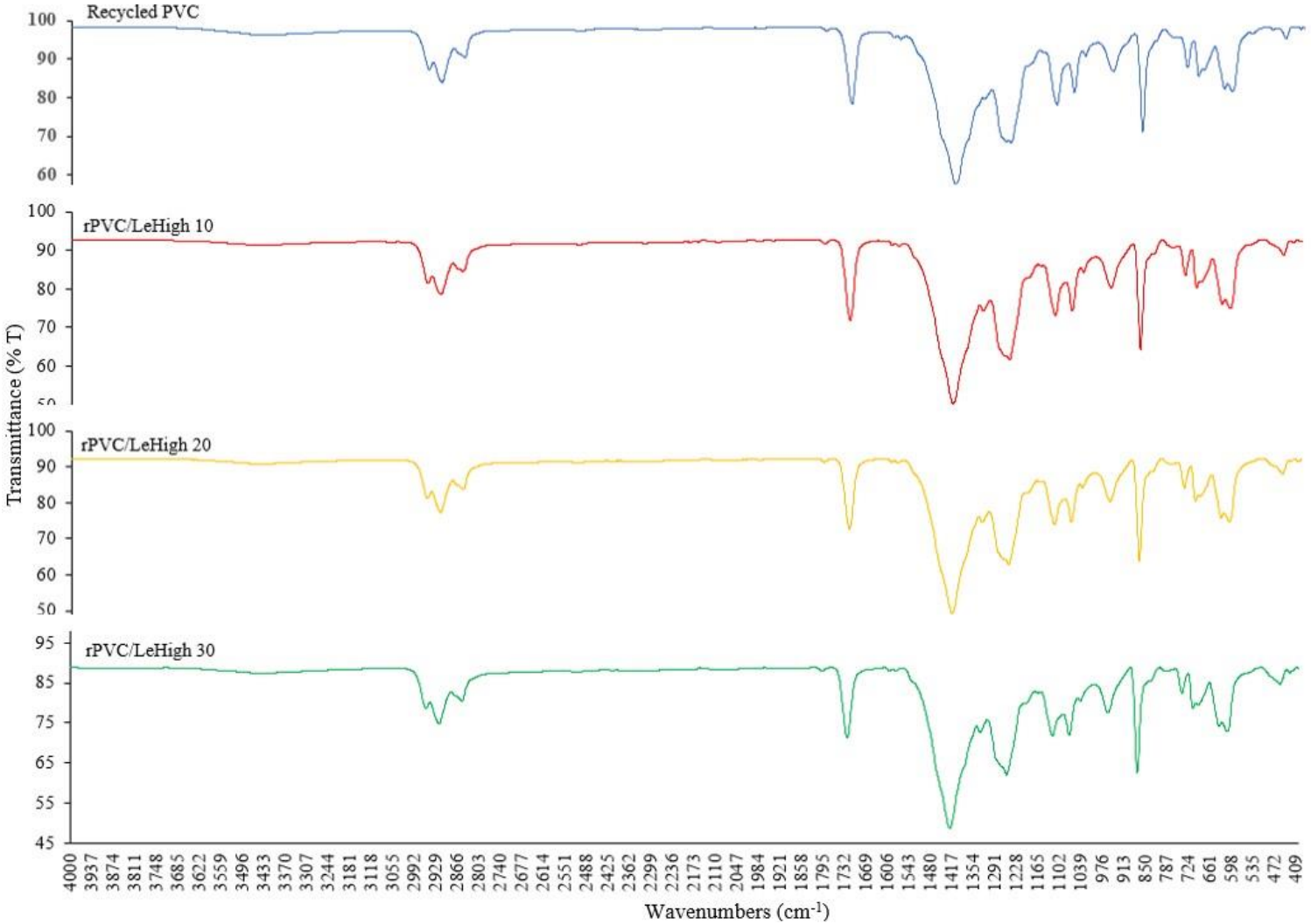

Figure 4.13: FTIR Spectra of rPVC/LeHigh Composites at Different LeHigh Loadings

4.3.2 Processing Torque

Processing torque measurement during the compounding or mixing process is a common approach used to understand the processability of any polymeric material, in which torque refers to the amount of rotational force or force required for rotation to process a material. When the polymeric materials undergo blending in an internal mixer, the resistance of materials towards shearing action during the mixing process will contribute to the generation of torque for measurement (Alias et al., 2020). Generally, the processing torque measurement plays a vital role in studying the rheological properties of the mixing compounds, such as viscosity, stiffness and processability. Besides that, the processing torque can be affected by several factors, such as the polymer properties of viscosity and melt flow behavior, processing conditions and types of filler (Vijayan et al., 2021).

The torque-time curves for the rPVC/ALUM composites at different loadings as compared to the rPVC composite are illustrated in Figure 4.14, while the torque-time curves for the rPVC/LeHigh composites at different loadings compared with the rPVC composite are displayed in Figure 4.16 with all the loading torque and stabilization torque values for the rPVC composite, rPVC/ALUM and rPVC/LeHigh composites of different loadings shown in Table 4.7. For the torque-time curves of the rPVC/ALUM composites of different loadings, the curves of processing torque for all the composites are of distinct trend against time with fluctuations due to the presence of calcium carbonate filler in the rPVC that affected the processability of the composites during the addition of ALUM of different loadings. Initially, the increase in the torque value corresponds to the initiation of the rotor and the charging of the rPVC and ALUM of different loadings into the mixing chamber at room temperature (Ling et al., 2016). The torque then continued to increase due to the presence of friction between the filler and the rPVC and also the friction between the filler and the mixing chamber of the internal mixer that contributed to the increasing resistance exerted on the internal mixer rotors by the unmelted rPVC and the filler (Koay et al., 2017). The different amounts of friction

caused by the rPVC and different loadings of ALUM with unstable processability due to the presence of calcium carbonate filler in the rPVC will then lead to dissimilar trends of the curves of processing torque with fluctuations for the rPVC/ALUM composites at different loadings.

After that, the torque will increase until it reaches a higher peak called the loading torque. Loading torque reflects polymer melt viscosity or is known as the point where the melting of the polymer starts to occur, in which the higher the loading torque, the higher the melt viscosity and increasing the difficulty for the melt mixing of the polymer (Vijayan et al., 2021). Based on Table 4.7, it can be observed that the loading torque values of rPVC/ALUM composites decreased with increasing ALUM loading from 10 wt% to 30 wt%. The decreasing loading torque values indicated that the melt mixing of the rPVC with ALUM became easier with increasing ALUM loading due to decreasing melt viscosity and lesser resistance for the rotor to rotate. The reduced loading torque value during the addition of ALUM of 10 wt% from 29.7 Nm to 16.27 Nm is attributed to the poor interfacial adhesion and bonding between the rPVC matrix and ALUM to allow the flowability of the molten mixture with a lower flow resistance, leading to lower viscosity of the composite with less shear required to overcome the lower melt viscosity (Koay et al., 2017). Hence, when increasing ALUM loadings, poorer interfacial interaction between the rPVC matrix and ALUM, as proved in the tensile test in section 4.3.6 and also the SEM images of the tensile fractured surfaces in section 4.3.7, resulting in lower flow resistance and lower melt viscosity of the composite to further decrease the loading torque values. In addition, the higher reduction of the loading torque value from 11.52 Nm to 5.92 Nm for the rPVC/ALUM 30 composite implied that the rPVC matrix could not further support the high content of ALUM particles, leading to poor melt mixing of the rPVC with ALUM as well as poor compatibility with the composite produced was not feasible as proved in the Figure 4.15 (d).

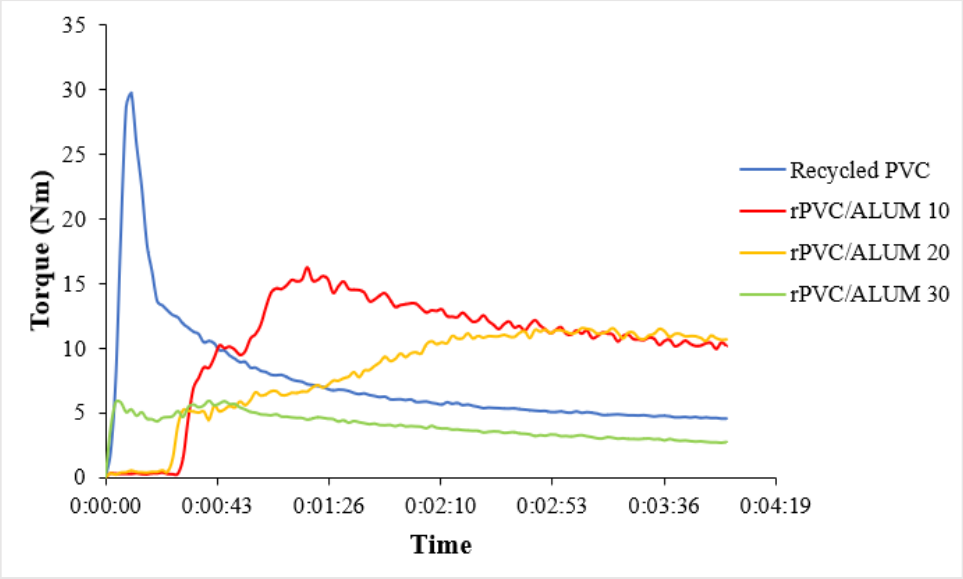

Figure 4.14: Torque-Time Curves of rPVC/ALUM Composites

When the rPVC and ALUM of different loadings started melting due to shear and temperature after reaching the loading torque, the torque gradually decreased with the increase of the mixing time. Upon accomplishing the homogeneous melting of the rPVC with ALUM to produce the composite and homogeneous dispersion of ALUM within the melted rPVC matrix, the processing torque became more stable until it reached a point called the stabilization torque at the end of the mixing time of 4 minutes (Vijayan et al., 2021). Thus, stabilization torque is the final torque value recorded at the end of the mixing process to achieve the homogeneous mixture of a polymer blend and used as a direct measurement of the polymer melt viscosity (Ling et al., 2016). High stabilization torque demonstrates high viscosity and stiffness of composites with poor filler dispersion, which makes the melt mixing of polymer very difficult. Based on Table 4.7, it can be observed that the stabilization torque values for the rPVC/ALUM composites increased with ALUM loading up to 20 wt% but decreased sharply for the ALUM loading of 30 wt %. When increasing the ALUM loading, the filler-filler interaction tends to surpass the matrix-filler interaction with a higher tendency to form filler agglomerates, resulting in the restriction of the polymer melt flow and increase of the melt viscosity of the composites, which caused the stabilization torque values to

increase with the ALUM loading as more shearing action required to overcome the internal friction caused by filler agglomerates (Koay et al., 2017). Besides that, the natural stiffness of ALUM particles would also resist the melt flow, causing a higher melt viscosity of the composites. The higher stabilization torque values at higher ALUM loading also indicated the poor homogeneous dispersion of the ALUM filler within the rPVC matrix due to a higher tendency of filler agglomerate formation. However, the stabilization torque value at ALUM loading of 30 wt% reduced sharply as the rPVC matrix could no longer support the high content of ALUM particles with poor melt mixing of the rPVC with ALUM to produce the composite in the form of small clumps with noticeable ALUM particles as shown in Figure 4.15 (d). Based on Figures 4.15 (a), (b), (c) and (d), when the recycled PVC pellets were mixed with ALUM in the powder form, the complete rPVC/ALUM composite shown in Figure 4.15 (c) was formed in a clump as the recycled PVC matrix fully wetted with the ALUM particles to coat with each other to produce a composite clump, while the Figure 4.15 (d) shown the failed rPVC/ALUM 30 composite with ALUM particles observed as the recycled PVC cannot coat the ALUM particles well to form a clump. In short, it can be concluded that the rPVC/ALUM 10 and rPVC/ALUM 20 composites showed better processability than the rPVC/ALUM 30 composite due to the failed composite produced at the ALUM loading of 30 wt%.

Table 4.7: Processing Torques of rPVC, rPVC/ALUM and rPVC/LeHigh Composites

Filler Loading (wt %)	**Loading Torque (Nm)**		**Stabilization Torque (Nm)**	
	rPVC/ALUM	rPVC/LeHigh	rPVC/ALUM	rPVC/LeHigh
0	29.7	29.7	4.54	4.54
10	16.27	17.35	10.17	12.73
20	11.52	16.57	10.65	14.83
30	5.92	4.93	2.72	4.68

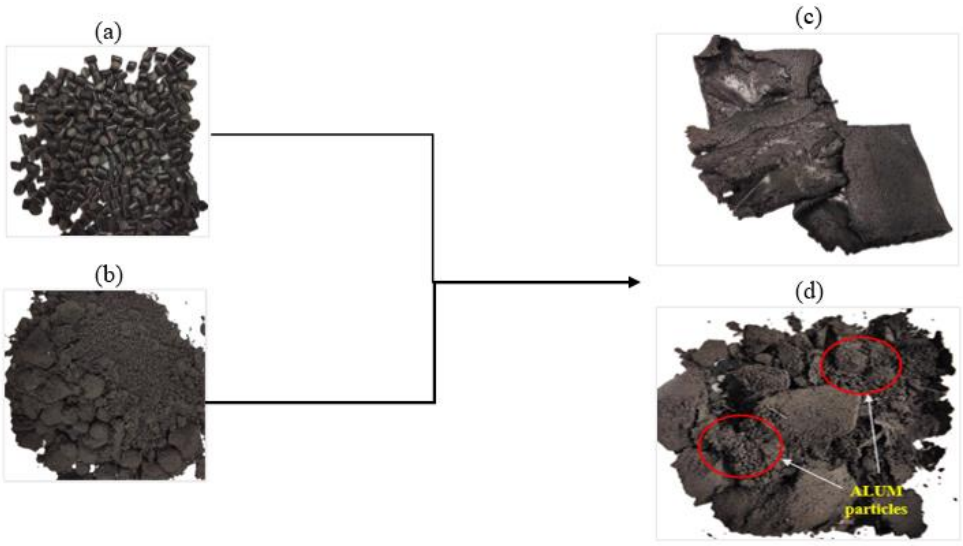

Figure 4.15: Compounding Raw Materials and Products (a) Recycled PVC Pellets (b) ALUM Powder (c) Complete rPVC/ALUM Composite (d) Failed rPVC/ALUM 30 Composite

Meanwhile, for the torque-time curves of the rPVC/LeHigh composites of different loadings, the curves of processing torque for all the composites are of barely similar trend against time to increase gradually followed by a drop, then rise again and become more stable at the end of mixing time. Initially, the increase in the torque value corresponds to the initiation of the rotor with the charging of the rPVC and LeHigh of different loadings into the mixing chamber of the internal mixer. The torque then continued to increase due to the presence of friction between the filler and the rPVC, contributing to the increasing resistance exerted on the internal mixer rotors (Koay et al., 2017). Due to the smaller size of LeHigh particles, the rPVC pellets will start to melt first to cause the torque to decrease and increase again due to the friction between the filler and the mixing chamber of the internal mixer to reach a higher peak of loading torque. After that, the LeHigh particles of different loadings also started melting and mixing with the rPVC due to shear and temperature, which caused the torque to decrease gradually with the increase of the mixing time and became more stable until it reached a point of stabilization torque at the end of the mixing time of 4 minutes to achieve the

homogeneous melting and dispersion of filler within the matrix to produce composites of rPVC/LeHigh (Vijayan et al., 2021).

By referring to Table 4.7, it can be observed that the loading torque values of rPVC/LeHigh composites decreased with increasing LeHigh loading from 10 wt% to 30 wt%. The decreasing loading torque values indicated that the melt mixing of the rPVC with LeHigh became easier with increasing LeHigh loading due to decreasing melt viscosity and lesser resistance for the rotor to rotate with the lower amount of friction generated. The reduced loading torque value during the addition of LeHigh of 10 wt% from 29.7 Nm to 17.35 Nm is also attributed to the poor interfacial adhesion and bonding between the rPVC matrix and LeHigh to allow the flowability of the molten mixture with a lower flow resistance, leading to lower viscosity of the composite with less shear required to overcome the lower melt viscosity (Koay et al., 2017). Hence, when increasing LeHigh loadings, poorer interfacial interaction between the rPVC matrix and LeHigh, as proved in the tensile test in section 4.3.6 and also the SEM images of the tensile fractured surfaces in section 4.3.7, resulting in lower flow resistance and lower melt viscosity of the composite to further decrease the loading torque values. Moreover, the higher reduction of the loading torque value from 16.57 Nm to 4.93 Nm for the rPVC/LeHigh 30 composite indicated that the rPVC matrix could not further support the high content of LeHigh particles, leading to poor melt mixing of the rPVC with ALUM to produced failed composite as proved in the Figure 4.17 (d).

Furthermore, it can be noted from Table 4.7 that the stabilization torque values for the rPVC/LeHigh composites increased with LeHigh loading up to 20 wt% but decreased sharply for the LeHigh loading of 30 wt %. When increasing the LeHigh loading, the filler-filler interaction tends to surpass the matrix-filler interaction with a higher tendency to form filler agglomerates, leading to the restriction of the polymer melt flow and increase of the melt viscosity of the composites to increase the stabilization torque values as more shearing action required to overcome the internal friction caused by filler agglomerates and the higher melt viscosity (Koay et al., 2017).

The natural stiffness of LeHigh particles would also restrict the melt flow with higher mixing resistance to increase the melt viscosity of the composites. The higher stabilization torque values at higher LeHigh loading also meant the poor homogeneous dispersion of the LeHigh filler within the rPVC matrix due to a higher tendency of filler agglomerate formation. Nevertheless, the stabilization torque value at LeHigh loading of 30 wt% decreased sharply as the rPVC matrix could no longer support the high content of LeHigh particles with poor melt mixing of the rPVC with LeHigh to produce the composite in the form of small clumps with noticeable LeHigh particles as shown in Figure 4.17 (d). Based on Figures 4.17 (a), (b), (c) and (d), when the recycled PVC pellets were mixed with LeHigh in the powder form, the complete rPVC/LeHigh composite shown in Figure 4.17 (c) was formed in a clump as the recycled PVC matrix fully wetted with the LeHigh particles to coat with each other to produce a composite clump, while the Figure 4.17 (d) shown the failed rPVC/LeHigh 30 composite with LeHigh particles observed as the recycled PVC cannot coat the LeHigh particles well to form a clump. In short, it can be concluded that the rPVC/LeHigh 10 and rPVC/LeHigh 20 composites displayed better processability than the rPVC/LeHigh 30 composite due to the failed composite produced at the LeHigh loading of 30 wt%.

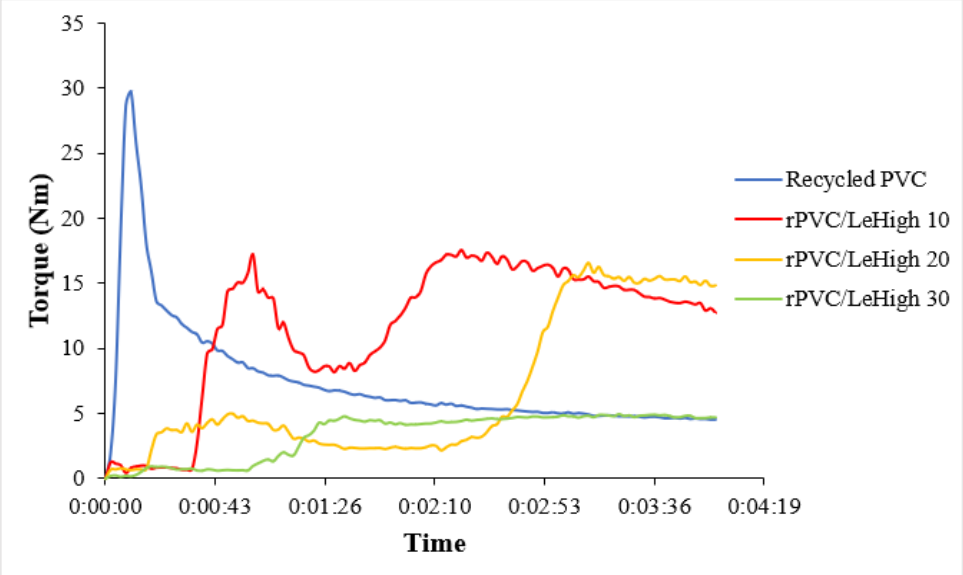

Figure 4.16: Torque-Time Curves of rPVC/LeHigh Composites

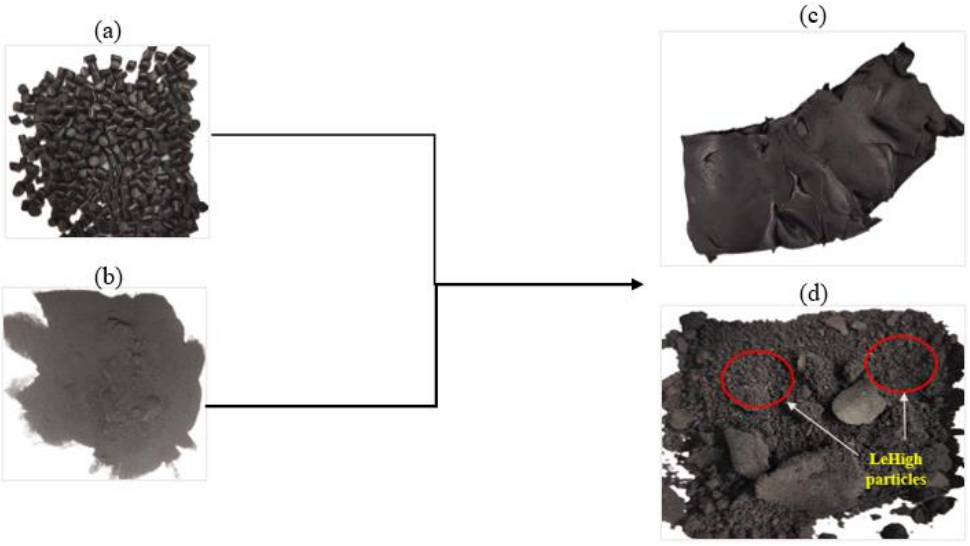

Figure 4.17: Compounding Raw Materials and Products (a) Recycled PVC Pellets (b) LeHigh Powder (c) Complete rPVC/LeHigh Composite (d) Failed rPVC/LeHigh 30 Composite

4.3.3 Thermogravimetric Analysis (TGA)

For the characterization of composites, thermogravimetric analysis (TGA) is used to study the thermal stability and decomposition behavior of the rPVC composite as compared to the rPVC/ALUM and rPVC/LeHigh composites of different loadings as it can measure the amount and rate of change in the mass of a sample as a function of temperature. For the TGA analysis of rPVC/ALUM composites, Figure 4.18 displayed the TGA thermograms of rPVC/ALUM composites at different loadings with the rPVC composite, while Table 4.8 showed the detailed variation of TGA experimental data of the rPVC and rPVC/ALUM composites. Based on Figure 4.18, it can be observed that the thermal decomposition of the rPVC composite occurred in three stages with the presence of three peaks in the DTG curve of the rPVC composite provided in Appendix A. The three stages of the thermal decomposition of the rPVC composite involved the first stage from 241.55 °C to 319.19 °C, the second stage from 393.66 °C to 527.29 °C

and the third stage from 644.54 °C to 781.34 °C. The first stage of the thermal decomposition from 241.55 °C to 319.19 °C is the fastest decomposition process, which corresponds to the decomposition of plasticizer and dehydrochlorination of PVC with the formation and stoichiometric elimination of HCl and a few chlorinated hydrocarbons (Chen et al., 2018). Besides that, the second stage of the thermal decomposition from 393.66 °C to 527.29 °C is attributed to the degradation of the complex structures resulting from aromatization and cyclization of conjugated polyene to form aromatic compounds, besides involving chain breaking and cross-linking with the release of hydrogen chloride, aromatic compounds and polyenic compounds to form smaller molecular fragments, volatile organic compounds (VOCs) and char residue (Ye et al., 2019). Meanwhile, the final decomposition stage from 644.54 °C to 781.34 °C corresponds to the further decomposition of char residues to form carbonaceous material or carbon residues (Yu et al., 2016).

In addition, from Figure 4.18, it can be observed that the rPVC/ALUM composites at different loadings showed almost similar trends of the TGA thermograms as the rPVC composite, which indicated that the addition of ALUM did not have much effect on the thermal decomposition process of the rPVC. Based on Table 4.8, it can be observed that the temperature at 50 % mass loss for the rPVC composite is 443.61 °C, which is higher than the rPVC/ALUM composites of different loadings. As the ALUM loading increased from 10 wt% to 30 wt%, the temperature at 50 % mass loss for the rPVC/ALUM composites decreased gradually from 443.61 °C to 432 °C for ALUM loading of 10 wt%, followed by a slight reduction of 432 °C to 429.78 °C for ALUM loading of 20 wt% and barely decreased from 429.78 °C to 427.29 °C for ALUM loading of 30 wt%. The decreasing trend of the $T_{50\%}$ with increasing ALUM loading indicated the decreasing thermal stability of the rPVC/ALUM composites at higher loading to withstand lower temperatures before significant decomposition occurs. When the ALUM loading increased, the amount of rPVC inside the composites reduced with more content of ALUM that possessed lower thermal decomposition characteristics with the $T_{50\%}$ of 392.73 °C, resulting in lesser heat required to penetrate and decompose the

compounds in the rPVC as the thermal decomposition temperatures of the composites are affected by the thermal stability of the filler, thus causing the $T_{50\%}$ to reduce with increasing ALUM loading (Shamsuri et al., 2015).

Moreover, based on Table 4.8, it can be observed that the total mass loss at 165 °C for the rPVC composite is 0.46 %, while the total mass loss at 165 °C for the rPVC/ALUM composites with the ALUM loading from 10 wt% to 30 wt% are 0.40 %, 0.38 % and 0.39 %. The lower total mass loss at 165 °C for all the rPVC/ALUM composites at different loadings indicated that the rPVC and ALUM showed higher thermal stability at the blend processing temperature of 165 °C without much mass loss and were able to blend well to achieve the composites with better performance and improved properties. Furthermore, from the table, it can be noted that the total mass loss at 900 °C for the rPVC composite is 75.12 %, while when increasing the ALUM loading from 10 wt% to 30 wt%, the total mass loss at 900 °C for the rPVC/ALUM composites decreased gradually from 76.47 % to 74.79 %, which implied that the residue % of the rPVC/ALUM composites increased with the ALUM loading in the composites. The increasing trend of residue % across increasing ALUM loading in the composites is attributed to the higher ALUM loading with a higher content of carbon black reinforcing filler from ALUM that remained undegraded even at a high temperature of 900 °C due to its superb thermal stability, thus contributing to the increasing residue % with increasing ALUM loading in the composites.

Table 4.8: Thermogravimetric Analysis of rPVC/ALUM Composites

ALUM loading (wt%)	Temperature at 50 % mass loss, $T_{50\%}$ (°C)	Total mass loss at 165 °C (%)	Total mass loss at 900 °C (%)
0	443.61	0.46	75.12
10	432.00	0.40	76.47
20	429.78	0.38	75.97
30	427.29	0.39	74.79
ALUM	392.73	0.96	76.02

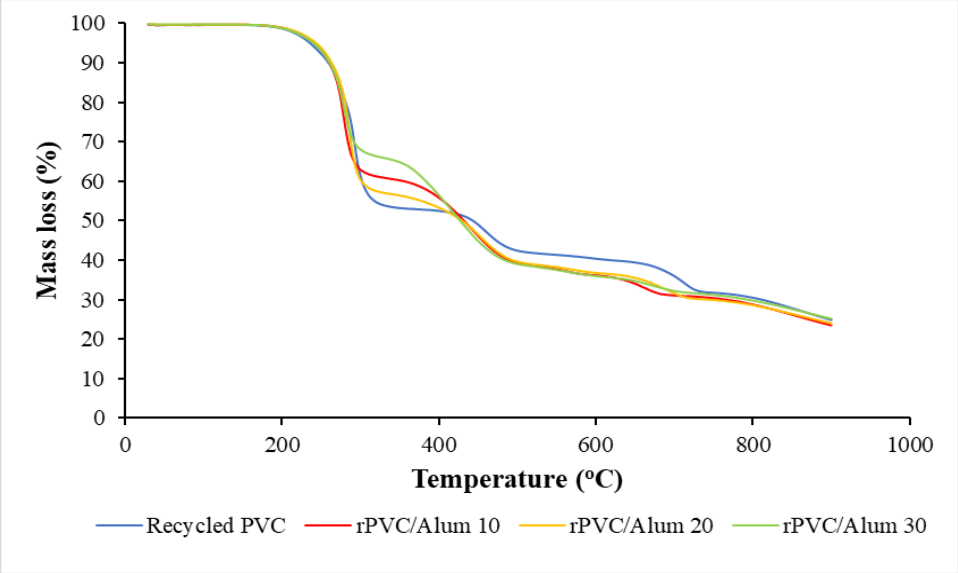

Figure 4.18: Thermogravimetric Analysis of rPVC/ALUM Composites

For the TGA analysis of rPVC/LeHigh composites of different loadings, Figure 4.19 displayed the TGA thermograms of rPVC/LeHigh composites at different loadings with the rPVC composite, while Table 4.9 showed the detailed variation of TGA experimental data of the rPVC and rPVC/LeHigh composites. Based on Figure 4.19, it can be seen that the rPVC/LeHigh composites at different loadings demonstrated almost similar trends of the TGA thermograms as the rPVC composite, which indicated that the

addition of LeHigh did not have much effect on the thermal decomposition process of the rPVC. By referring to Table 4.9, it can be noted that as the LeHigh loading increased from 10 wt% to 30 wt%, the temperatures at 50 % mass loss increased from 443.61 °C to 458.47 °C for LeHigh loading of 10 wt%, followed by a reduction to 446.76 °C for LeHigh loading of 20 wt% and further decreased to 441.02 °C for LeHigh loading of 30 wt%. The increased $T_{50\%}$ with the addition of 10 wt% of LeHigh indicated the thermal stability of the rPVC/LeHigh 10 composite is higher than the rPVC composite to withstand higher temperatures before significant decomposition occurs due to the higher thermal decomposition characteristics of LeHigh with the $T_{50\%}$ of 432.63 °C to improve the overall thermal stability of the composite. However, when the LeHigh loading increased to 20 wt% and 30 wt%, the $T_{50\%}$ slightly reduced, which may be due to the weakening of the blend system with higher loading of LeHigh to cause the heat to penetrate easily into the weakened system and occur the decomposition process at lower temperature. Although the $T_{50\%}$ reduced for the LeHigh loading of 20 wt% and 30 wt%, the temperatures at 50 % mass loss for all the rPVC/LeHigh composites are still considerably higher with better thermal stability. In addition, it also can be noted that the temperatures at 50 % mass loss for the rPVC/LeHigh composites are generally higher than the rPVC/ALUM composites, which indicated the rPVC/LeHigh composites had better thermal stability than the rPVC/ALUM composites to occur the decomposition process at higher temperature due to the higher thermal decomposition characteristics of LeHigh than ALUM with the $T_{50\%}$ of 432.63 °C.

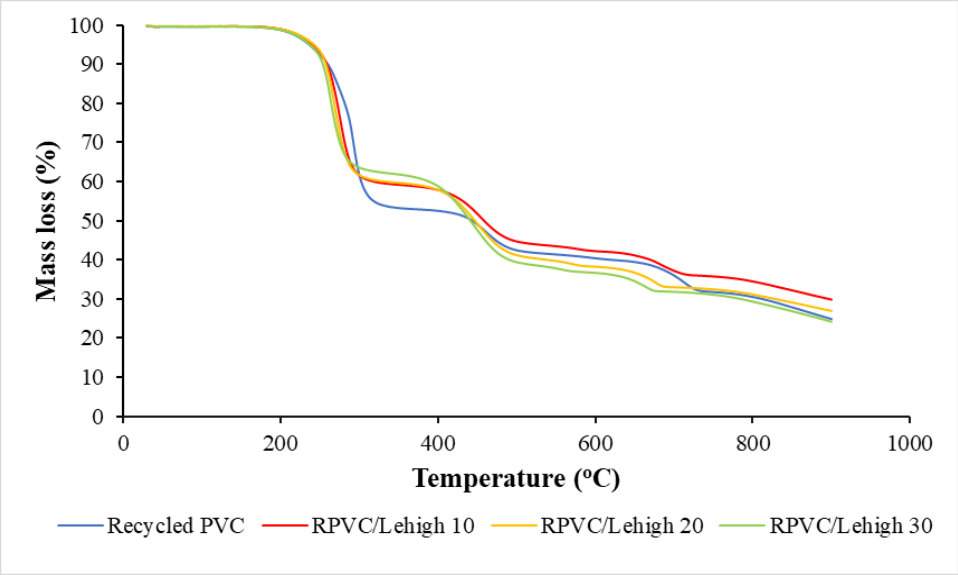

Figure 4.19: Thermogravimetric Analysis of rPVC/LeHigh Composites

Furthermore, based on Table 4.9, it can be observed that the total mass loss at 165 °C for the rPVC/LeHigh composites with the LeHigh loading from 10 wt% to 30 wt% are 0.37 %, 0.39 % and 0.54 %. The lower total mass loss at 165 °C for all the rPVC/LeHigh composites indicated that the rPVC and LeHigh displayed higher thermal stability at the blend processing temperature of 165 °C without much mass loss to mix and blend well to achieve the composites with better performance and improved properties. From the table, it can also be noted that when increasing the LeHigh loading from 10 wt% to 30 wt%, the total mass loss at 900 °C for the rPVC/LeHigh composites increased gradually from 70.16 % to 75.80 %, which implied that the residue % of the rPVC/LeHigh composites decreased when the LeHigh loading increased in the composites. Although the total mass loss at 900 °C for the rPVC/LeHigh composites displayed an increasing trend across increasing LeHigh loading, it can be noted that the total mass loss at 900 °C for the composites of rPVC/LeHigh 10 and rPVC/LeHigh 20 is lower than the rPVC composite with higher residue % due to the higher LeHigh loading with a higher content of carbon black reinforcing filler from LeHigh that remained undegraded even at a high temperature of 900 °C, contributing to the lesser mass loss than the rPVC composite. However, the rPVC/LeHigh 30 composite had a slightly

higher mass loss at 900 °C with a lower residue % than the rPVC composite, which may be due to the poor processability of the rPVC with the LeHigh loading of 30 wt% to produce the failed composite as proved in the section 4.3.2.

In short, the rPVC/LeHigh composites showed better thermal stability than the rPVC/ALUM composites with higher temperatures at 50 % mass loss and reduced total mass loss at 900 °C up to 20 wt% LeHigh loading. The complete Derivative Thermogravimetry (DTG) graphs that illustrated the thermal decomposition of rPVC, rPVC/ALUM and rPVC/LeHigh composites are included in Appendix A.

Table 4.9: Thermogravimetric Analysis of rPVC/LeHigh Composites

LeHigh loading (wt%)	Temperature at 50 % mass loss, $T_{50\%}$ (°C)	Total mass loss at 165 °C (%)	Total mass loss at 900 °C (%)
0	443.61	0.46	75.12
10	458.47	0.37	70.16
20	446.76	0.39	73.06
30	441.02	0.54	75.80
LeHigh	432.63	1.25	66.25

4.3.4 Swelling Test

The swelling test or the water absorption test is a method used to determine the resistance of rPVC, rPVC/ALUM and rPVC/LeHigh composites towards water absorption when exposed to a liquid environment. The swelling test helps assess a material's performance by determining how much water it can absorb over time to predict its behavior in real-world conditions and understand the material's water

absorption behavior for ensuring optimal performance, longevity and reliability in diverse applications when exposed to moisture or aqueous environments. The composite with a lower swelling percentage indicated a better water absorption resistance, while the composite with a higher swelling percentage indicated a weak water absorption resistance that will significantly affect the mechanical properties, dimensional stability, electrical properties and chemical resistance. The water absorption can be affected by several factors, such as the presence of void or pore, humidity, temperature, volume fraction of filler and viscosity of the matrix (Radzi et al., 2019).

Referring to the water absorption percentage of the rPVC composite and composites of the rPVC with different loadings of ALUM and LeHigh displayed in Figure 4.20, it can be observed that the rPVC composite had the lowest water absorption percentage of 0.579 % when immersed in water for 72 hours. For the composites of the rPVC with different loadings of ALUM, the initial addition of 10 wt% of ALUM increased the water absorption percentage from 0.579 % to 1.118 % and continued to rise to 1.757 % for the addition of 20 wt% of ALUM, followed by a significant increase to 3.027 % for the addition of 30 wt % of ALUM. Meanwhile, for the composites of the rPVC with different loadings of LeHigh, the initial addition of 10 wt% of LeHigh slightly increased the water absorption percentage from 0.579 % to 0.660 % and continued to grow to 0.783 % for the addition of 20 wt% of LeHigh, followed by a barely increase to 0.856 % for the addition of 30 wt % of LeHigh. Thus, it can be concluded that the water absorption percentage is affected by the loadings of ALUM and LeHigh, in which the higher the loadings of ALUM and LeHigh in the rPVC, the higher the water absorption percentage. In addition, according to the specifications given by CY Handee Rubber Mouldings Sdn. Bhd. for the car floor mat application, the rPVC/ALUM and rPVC/LeHigh composites must not exceed 2.5 % of the swelling percentage in water. Hence, it also can be concluded that all the rPVC/ALUM and rPVC/LeHigh composites at all the ALUM and LeHigh loadings meet the requirement specification with a swelling percentage of not more than 2.5 % for the car floor mat

application, except for the rPVC/ALUM 30 composite with a swelling percentage of 3.027 %, which is higher than 2.5 %.

Although rPVC is known for its hydrophobic nature due to its carbon-carbon backbone and the presence of chlorine atoms, it still can be noted that the rPVC composite absorbed 0.579 % of water during immersion in water for 72 hours, which may be due to the presence of polar group of the carbonyl group (-C=O) from the DOP plasticizer in the rPVC, which lead to some degree of polarity within the PVC molecule (M. Subitha et al., 2022). When the rPVC comes into contact with water, polar water molecules may interact with the polar sites or functional groups within the PVC molecule, leading to some degree of water absorption by PVC, particularly at the surface or near regions containing polar groups. Moreover, dipole-dipole interactions between PVC and water molecules may also occur, in which the partially negative oxygen atom of water is attracted to the partially positive carbon atom of the PVC molecule, while the partially positive hydrogen atoms of water are attracted to the partially negative chlorine atoms of the PVC molecule, contributing to the adhesion of water molecules to the surface of the rPVC and may facilitate the absorption of small amounts of water into the PVC (L Bertrand et al., 2023). Therefore, the lower water absorption percentage of the rPVC composite can be attributed to the presence of polar functional groups in the rPVC to interact with water molecules and dipole-dipole interactions between the rPVC and water molecules.

Furthermore, the higher water absorption percentage of the rPVC/ALUM and rPVC/LeHigh composites than the rPVC composite at the loading of 10 wt% is due to the poor interfacial adhesion between the fillers and the rPVC matrix, as well as poor dispersion within the rPVC matrix to create gaps or voids between them, resulting in easy penetration of water molecules and accumulate at the interface between the fillers and the matrix (Achukwu et al., 2015). As the loadings of ALUM and LeHigh increase, more voids or gaps are created due to the poorer interfacial interaction between the fillers and the rPVC matrix, with a higher tendency of the filler particles to form more

agglomeration, causing more water molecules to entrap in the voids and accumulate at the interface areas, leading to rising water absorption percentage. The increasing formation of voids with increasing loadings of ALUM and LeHigh can be further proved by the SEM images of the tensile fractured surfaces displayed in section 4.3.7, especially at the loading of 30 wt% with the occurrence of filler detachment on the surface of the rPVC/ALUM 30 composite with more voids that led to the highest water absorption percentage of 3.027 %. Therefore, the water absorption percentage is said to increase with the loadings of ALUM and LeHigh in the rPVC. From Figure 4.20, it can also be noted that the rPVC/LeHigh composites had a lower water absorption percentage than the rPVC/ALUM composites at different loadings, indicating better interfacial adhesion and binding of LeHigh than ALUM with the rPVC, as well as better dispersion of LeHigh within the matrix of the rPVC to form fewer voids or gaps with lesser amount of water molecules entrapped or accumulated.

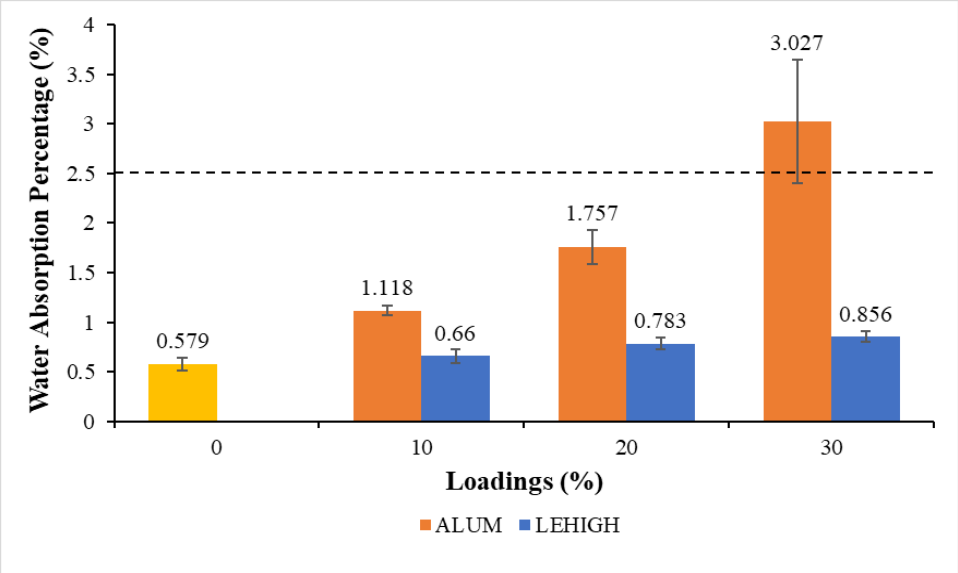

Figure 4.20: Water Absorption Percentage of rPVC, rPVC/ALUM and rPVC/LeHigh Composites

4.3.5 Hardness Test

A hardness test is a valuable method used to assess the resistance of a material to indentation, scratching or other forms of permanent deformation by pressing a standardized, rigid instrument into the material to achieve the hardness value. Hardness refers to a material's ability to resist deformation at its surface. It is an essential mechanical property that provides insights into a material's strength, wear resistance and suitability for various applications. The shore hardness test is used for this research to measure the resistance of rPVC, rPVC/ALUM and rPVC/LeHigh composites to indentation using a durometer, which typically has a blunt indenter to achieve the hardness values of the composites through the conversion of the depth of penetration to a hardness value (Xometry, 2023).

By referring to Figure 4.21 of the Shore A hardness of the rPVC composite and composites of rPVC/ALUM and rPVC/LeHigh at different loadings, all the composites had Shore A hardness values of more than or equal to 85 Shore A, in which the rPVC composite possessed Shore A hardness value of 89.21 Shore A, rPVC/ALUM 10 composite with the hardness value of 88.13 Shore A, rPVC/ALUM 20 composite with the hardness value of 86.89 Shore A, rPVC/ALUM 30 composite with the hardness value of 85 Shore A, rPVC/LeHigh 10 composite with the hardness value of 91.94 Shore A, rPVC/LeHigh 20 composite with the hardness value of 88.81 Shore A and rPVC/LeHigh 30 composite with the hardness value of 86.17 Shore A. According to the specifications given by CY Handee Rubber Mouldings Sdn. Bhd. for the car floor mat application, the rPVC/ALUM and rPVC/LeHigh composites should have a Shore A hardness value of 90 ± 5, which ranges from 85 Shore A to 95 Shore A. Thus, based on the Shore A hardness result, all the rPVC/ALUM and rPVC/LeHigh composites at different loadings had Shore A hardness values in the range of 85 Shore A to 95 Shore A, which meet the requirement specification given of the Shore A hardness value of 90 ± 5 for the car floor mat application.

As all the rPVC/ALUM and rPVC/LeHigh composites at different loadings showed a higher Shore A hardness value to meet the requirement specification, it indicated that ALUM and LeHigh acted as reinforcing fillers in the rPVC to enhance the stiffness of the composites besides reducing the flexibility of the composites, resulting in more rigid, stiffer and harder composites (Hayeemasae & Ismail, 2020). The reduction of the elongation at break with an increment of the elastic modulus in the tensile test in section 4.3.6 when adding 10 wt% of ALUM and LeHigh to the rPVC verified that ALUM and LeHigh acted as reinforcing fillers in the rPVC to enhance the elastic modulus and stiffness of the composites. Farida et al. (2019) reported that the presence of carbon black in rubber waste further reinforced the composites produced with a strengthening effect on the physical properties by increasing their hardness, tear resistance, abrasion resistance and high breaking stress, leading to a higher Shore A hardness value. Although rising the filler loading is said to stiffen and harden the composites with increasing hardness values, the figure did not show an increasing trend of the hardness values when increasing the loadings of ALUM and LeHigh in the rPVC, which may be due to the presence of carbon black in both fillers that significantly reduce the effect of filler loadings on the hardness values of the composites (Daud et al., 2016). In short, the incorporation of ALUM and LeHigh of different loadings with the rPVC can effectively improve the hardness of the composites to become stiffer and rigid with a lower elongation at break and a higher elastic modulus compared to the rPVC without ALUM and LeHigh, as proved in the tensile test in section 4.3.6.

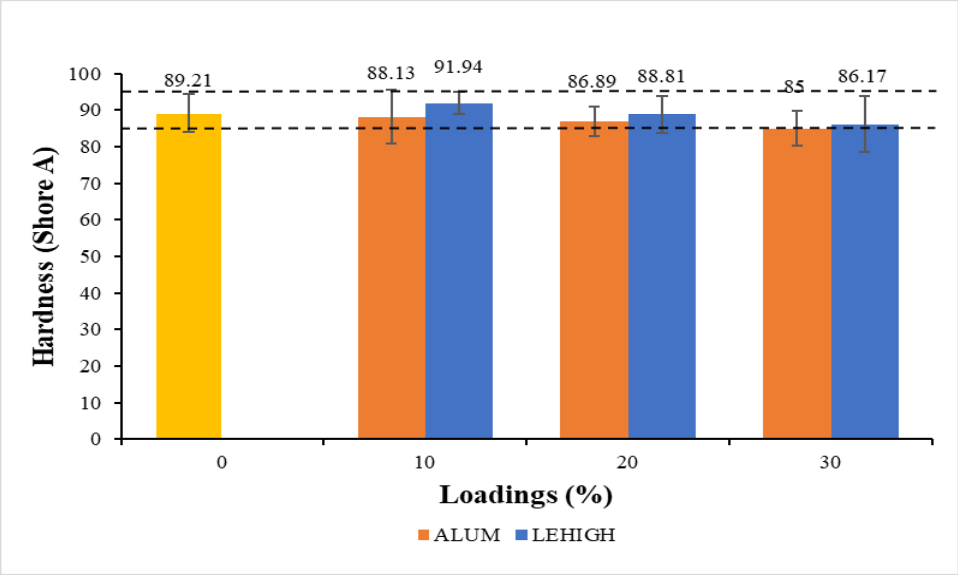

Figure 4.21: Hardness of rPVC, rPVC/ALUM and rPVC/LeHigh Composites

4.3.6 Tensile Test

A tensile test is a fundamental mechanical measurement to detect how a material withstands loaded tensile forces until it fractures. It measures the force required to break a composite or plastic specimen and the extent to which the specimen stretches or elongates to that breaking point to obtain the tensile properties of ultimate tensile strength, elastic modulus and elongation at break (Saba et al., 2019). In this research, the tensile test is performed to determine how the composites of the rPVC, rPVC/ALUM and rPVC/LeHigh behave under tension load to achieve their tensile properties of ultimate tensile strength, elastic modulus and elongation at break, which is generally affected by the interfacial adhesion between matrix and filler, filler loading, filler size and filler agglomeration (Fazli & Rodrigue, 2020). The tensile properties of elastic modulus, ultimate tensile strength and elongation at break of rPVC/ALUM composites at different ALUM loadings and rPVC/LeHigh composites at different LeHigh loadings are summarized in Table 4.10 and Table 4.11.

Table 4.10: Tensile Properties of rPVC/ALUM Composites

ALUM Loading (wt%)	Parameters		
	Elastic Modulus (MPa)	Ultimate Tensile Strength (MPa)	Elongation at break (%)
0	29.55 ± 0.67	17.6 ± 0.78	146.87 ± 6.37
10	68.69 ± 4.67	10.08 ± 0.72	52.33 ± 5.29
20	104.27 ± 2.13	5.63 ± 0.73	13.01 ± 2.97
30	30.31 ± 8.98	2.72 ± 0.13	5.59 ± 0.47

Table 4.11: Tensile Properties of rPVC/LeHigh Composites

LeHigh Loading (wt%)	Parameters		
	Elastic Modulus (MPa)	Ultimate Tensile Strength (MPa)	Elongation at break (%)
0	29.55 ± 0.67	17.6 ± 0.78	146.87 ± 6.37
10	71.50 ± 4.87	11.17 ± 0.21	71.03 ± 5.10
20	128.11 ± 2.03	8.79 ± 0.15	44.10 ± 2.50
30	157.07 ± 1.94	6.77 ± 0.14	25.15 ± 1.30

Elastic modulus quantifies the stiffness or rigidity of the rPVC, rPVC/ALUM and rPVC/LeHigh composites, indicating how much they resist elastic deformation when subjected to an applied load, in which a higher elastic modulus corresponds to a stiffer composite that requires more stress to produce a given amount of strain (Jiang & Zhou, 2023). Based on Figure 4.22, it can be noted that the rPVC composite possessed an elastic modulus of 29.55 MPa, which is the lowest elastic modulus compared to other composites of rPVC/ALUM and rPVC/LeHigh at different loadings. When adding ALUM of different loadings to the rPVC, the elastic modulus showed an increasing trend to increase from 29.55 MPa to 104.27 MPa up to 20 wt% of ALUM but decreased sharply from 104.27 MPa to 30.31 MPa for 30 wt% of ALUM. Meanwhile, when adding LeHigh of different loadings from 10 wt% to 30 wt% to the rPVC, the elastic modulus increased from 29.55 MPa to 157.07 MPa, showing an increasing trend. The increasing

elastic modulus with the addition of ALUM and LeHigh is attributed to the stiff nature of the reinforcement of ALUM and LeHigh in the rPVC to reduce the chain mobility and intermolecular motion in the rPVC matrix to increase the rigidity of the composites (Colom et al., 2013). Hence, increasing the loadings of ALUM and LeHigh in the rPVC will further stiffen and harden the composites with more reduction of the chain mobility in the rPVC matrix, leading to the increasing trend of the elastic modulus when increasing the loadings of ALUM and LeHigh in the rPVC (Daud et al., 2016). However, the rPVC/ALUM 30 composite displayed a decreasing elastic modulus, which is due to the poorer wettability of the rPVC matrix on ALUM at a high loading of 30 wt% with the matrix could no longer support the high content of filler, causing poorer interfacial adhesion with filler agglomeration and facilitating the formation of more voids due to filler detachment as proved by the SEM images in section 4.3.7, resulting in poor tensile properties with the decreased elastic modulus. Besides that, it also can be noted that the rPVC/LeHigh composites of different loadings showed a higher elastic modulus than the rPVC/ALUM composites of different loadings, which indicated that rPVC/LeHigh composites are more rigid and stiffer than the rPVC/ALUM composites due to the more stiff nature of LeHigh than ALUM to restrict the chain mobility in the matrix and increase the rigidity of the composites.

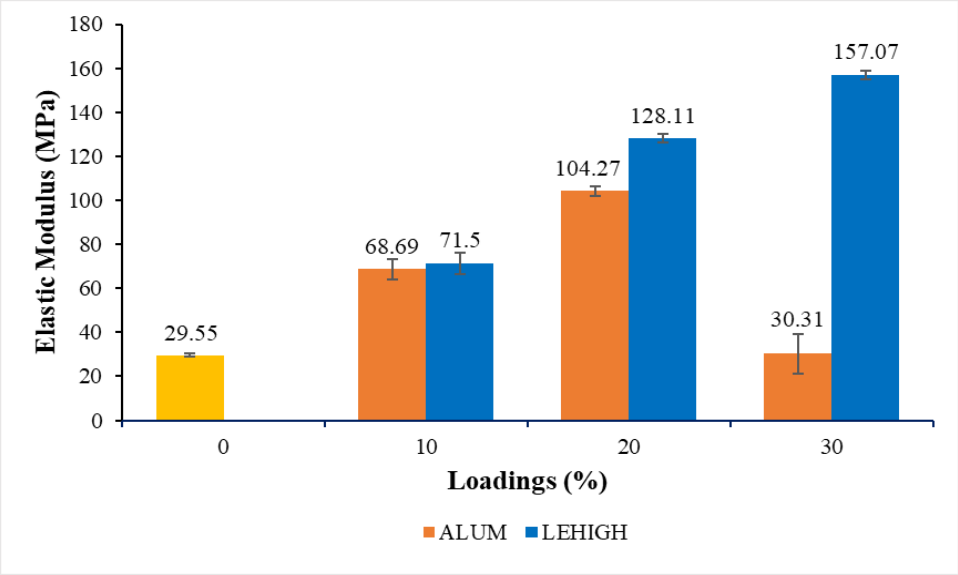

Figure 4.22: Elastic Modulus of rPVC, rPVC/ALUM and rPVC/LeHigh Composites

Ultimate tensile strength, also known simply as tensile strength, is a mechanical property of materials that measures the maximum stress a material can withstand under tensile loading before it fails or fractures. By referring to Figure 4.23, it can be seen that the rPVC composite had the highest ultimate tensile strength of 17.6 MPa and showed a decreasing trend of ultimate tensile strength when adding ALUM and LeHigh of different loadings from 10 wt% to 30 wt% to the rPVC. When adding 10 wt% of ALUM to the rPVC, the ultimate tensile strength decreased from 17.6 MPa to 10.08 MPa, followed by a reduction to 5.63 MPa for the addition of 20 wt% of ALUM and further decreased to 2.72 MPa for the addition of 30 wt% of ALUM. Meanwhile, when adding 10 wt% of LeHigh to the rPVC, the ultimate tensile strength decreased from 17.6 MPa to 11.17 MPa, followed by a reduction to 8.79 MPa for the addition of 20 wt% of LeHigh and further decreased to 6.77 MPa for the addition of 30 wt% of LeHigh. Thus, it can be concluded that the addition of ALUM and LeHigh to the rPVC will cause the ultimate tensile strength of the produced composites to reduce and the higher the filler loadings of ALUM and LeHigh, the lower the ultimate tensile strength of the produced composites.

The reduction of the ultimate tensile strength with the addition of ALUM and LeHigh to the rPVC is primarily attributed to the poor interfacial adhesion and poor physical contact between the rPVC matrix and the fillers of ALUM and LeHigh, as well as incompatibility between the rPVC matrix and the fillers due to polarity differences, resulting in a reduction in the stress transfer of the rPVC matrix to the fillers and leading to the deduction of the ultimate tensile strength of the composites (Luna et al., 2019). As the filler loadings of ALUM and LeHigh increase, the fillers of ALUM and LeHigh will no longer wetted by the rPVC matrix with a high tendency to form agglomerates, leading to poorer interfacial bonding and physical interaction between the matrix and the fillers and lower stress transfer between the matrix and the filler particles to resist detachment during the tensile test (Daud et al., 2016). Hence, the ultimate tensile strength displayed a decreasing trend from the rPVC composite during the addition of ALUM and LeHigh at different loadings. Other than that, it also can be noted that the rPVC/LeHigh composites of different loadings showed a higher ultimate tensile strength than the rPVC/ALUM composites of different loadings, which indicated that the LeHigh had better interfacial interaction with the rPVC matrix than ALUM to improve the stress transfer and increase the ultimate tensile strength. In addition, according to the specifications given by CY Handee Rubber Mouldings Sdn. Bhd. for the car floor mat application, the rPVC/ALUM and rPVC/LeHigh composites at different loadings should have a minimum ultimate tensile strength of 5 MPa. Thus, based on the ultimate tensile strength result, all the rPVC/ALUM and rPVC/LeHigh composites at different loadings had the ultimate tensile strength of more than 5 MPa to meet the requirement specification for the ultimate tensile strength, except for the rPVC/ALUM 30 composite with the ultimate tensile strength of 2.72 MPa, which is lower than the required minimum ultimate tensile strength of 5 MPa.

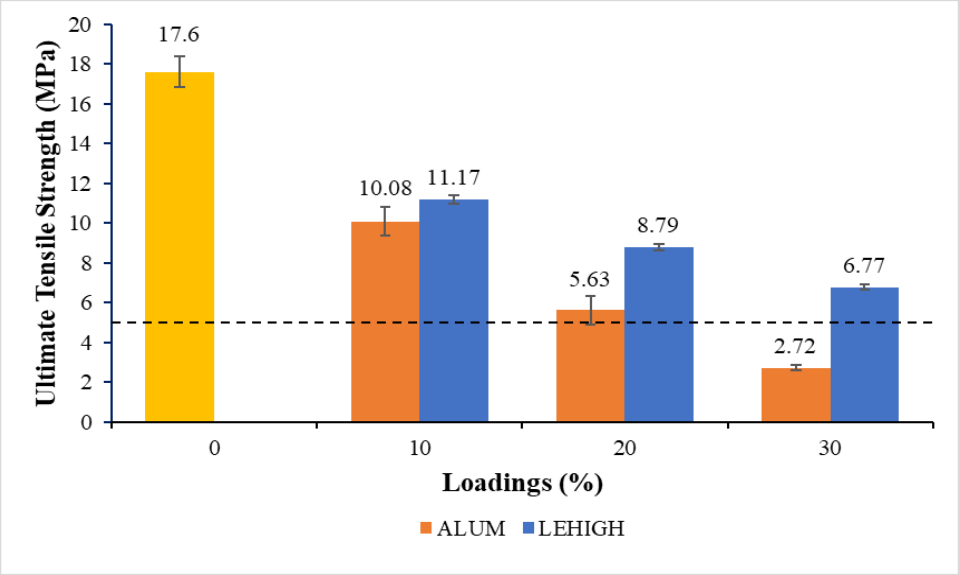

Figure 4.23: Ultimate Tensile Strength of rPVC, rPVC/ALUM and rPVC/LeHigh Composites

Elongation at break, also known as fracture strain, is the ratio between the changed length and initial length after the breakage of the test material or is defined as a mechanical property that measures the extent to which a material can stretch or deform before fracturing during a tensile test (Djafari Petroudy, 2017). Based on Figure 4.24, it can be observed that the rPVC composite had the highest percentage of elongation at break of 146.87 %, which is considered ductile to sustain large strains before reaching the breaking point, besides showing a decreasing trend of the elongation at break when adding ALUM and LeHigh of different loadings to the rPVC. When adding ALUM of different loadings from 10 wt % to 30 wt% to the rPVC, the elongation at break displayed a decreasing trend to decrease from 146.87 % to 5.59 %. Meanwhile, when adding LeHigh of different loadings from 10 wt % to 30 wt% to the rPVC, the elongation at break also illustrated a decreasing trend to drop from 146.87 % to 25.15 %. Therefore, it can be concluded that the addition of ALUM and LeHigh to the rPVC will cause the elongation at break of the produced composites to reduce to become more brittle and the higher the filler loadings of ALUM and LeHigh, the lower the elongation at break of the produced composites.

The deduction of the elongation at break with the addition of ALUM and LeHigh to the rPVC is mainly attributed to the poor compatibility between the rPVC matrix and the fillers of ALUM and LeHigh due to polarity differences, resulting in weak interfacial adhesion between the rPVC matrix and the fillers (Colom et al., 2013). The poor matrix-filler interaction with weak interfacial bonds will then cause uneven stress distribution in the rPVC matrix and stress concentrated on the filler particles, resulting in the brittle behavior of the composites with lower elongation at break (Achukwu et al., 2015). Moreover, the stiff nature of ALUM and LeHigh also caused the stiffness of the composites to increase with a reduction in flexibility to provide a brittle behavior, leading to a subsequent loss of tensile strength and elongation at break in the composites (Colom et al., 2013). As the filler loadings of ALUM and LeHigh increase, the filler particles tend to interact with each other to produce more filler-filler interactions with a high tendency to form agglomerates, leading to poorer interfacial adhesion between the matrix and the fillers and lower stress transfer between the matrix and the filler particles to break more easily with applied stress (Hayeemasae & Ismail, 2020). Thus, the elongation at break of the composites continued to decrease with increasing brittleness when the loadings of ALUM and LeHigh in the rPVC increased. It also can be noted that the rPVC/LeHigh composites of different loadings showed a higher elongation at break than the rPVC/ALUM composites of different loadings, which indicated that the LeHigh had better compatibility and interfacial adhesion with the rPVC matrix than ALUM, besides having a lower tendency to form agglomerates at higher loadings, resulting in better stress transfer and higher elongation at break. Furthermore, according to the specifications given by CY Handee Rubber Mouldings Sdn. Bhd. for the car floor mat application, the rPVC/ALUM and rPVC/LeHigh composites at different loadings should have a minimum elongation at break of 25 %. Hence, based on the elongation at break result, only the rPVC/ALUM 10 composite and all the rPVC/LeHigh composites at different loadings had the elongation at break percentage of more than 25 % to meet the requirement specification, except for the rPVC/ALUM 20 and rPVC/ALUM 30 composites with the elongation at break percentages of 13.01 % and 5.59 %.

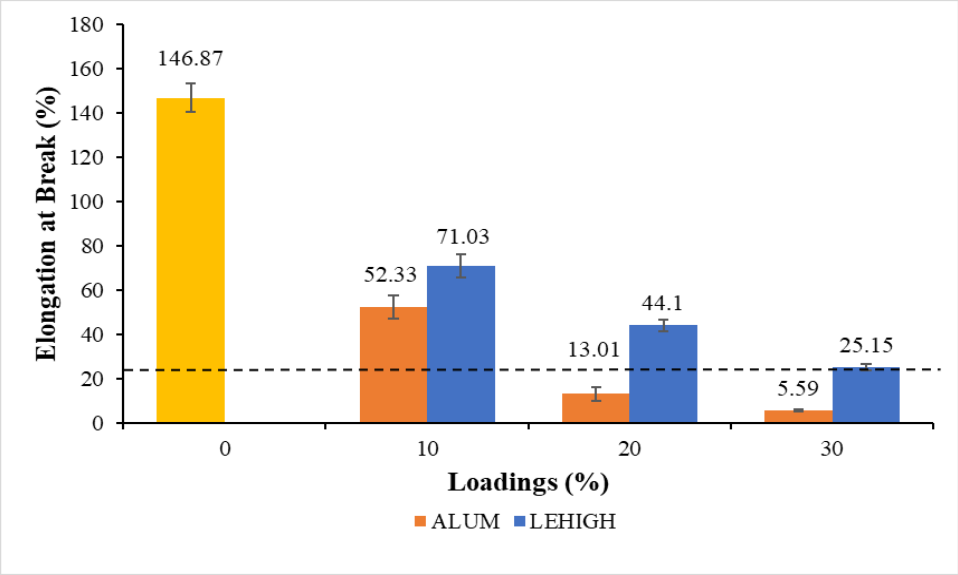

Figure 4.24: Elongation at Break of rPVC, rPVC/ALUM and rPVC/LeHigh Composites

From the tensile test evaluation, the incorporation of ALUM and LeHigh of different loadings into the rPVC matrix caused the overall tensile properties of the rPVC/ALUM and rPVC/LeHigh composites to decrease, in which the ultimate tensile strength and elongation at break showed a significant decrease at increasing ALUM and LeHigh loadings, which is mainly due to the lack of interfacial adhesion between the matrix and the fillers as well as the increasing tendency to form filler agglomeration. The increasing elastic modulus with increasing ALUM and LeHigh loadings also deduced that the composites became stiffer with lower flexibility when more ALUM or LeHigh was incorporated but more brittle to break easily, leading to lower ultimate tensile strength and elongation at break. In order to meet the required specifications given by CY Handee Rubber Mouldings Sdn. Bhd. for the car floor mat application with a minimum ultimate tensile strength of 5 MPa and minimum elongation at a break of 25 %, the rPVC/ALUM 10 composite is the optimum choice among other rPVC/ALUM composites at different loadings which satisfies both given specifications, while the 20 wt% of LeHigh will be the optimum loading although other rPVC/LeHigh composites at different loadings also fulfilled both given specifications.

4.3.7 Scanning Electron Microscopy (SEM)

SEM image of the tensile fractured surface of the rPVC composite at 500x magnification is depicted in Figure 4.25. By referring to the figure, it can be observed that the rPVC had a flat and rough fractured surface with the presence of calcium carbonate filler attached to the surface. The rough fractured surface of the rPVC composite implied that the composite possessed a higher resistance towards crack propagation, which allows the composite to deform and withstand higher stress to achieve higher ultimate tensile strength and modulus of elasticity, indicating that the composite is rigid and stiffer (Vijayan et al., 2021). Besides that, good dispersion of the calcium carbonate filler within the rPVC matrix without filler agglomeration and filler detachment on the fractured surface can also be proved from the figure to achieve better mechanical properties and performance of the composite produced (Zhu et al., 2021).

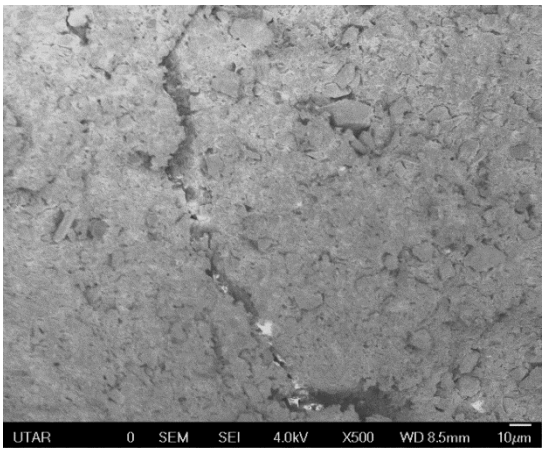

Figure 4.25: SEM Images of rPVC Composite under 500x Magnification

For the composites of rPVC/ALUM at different ALUM loadings, the SEM images of their tensile fractured surfaces under 500x magnification are shown in Figures 4.26 (a), (b) and (c), which corresponded to the composites of rPVC/ALUM 10, rPVC/ALUM 20 and rPVC/ALUM 30. For the rPVC/ALUM 10 composite with the SEM image of the tensile fractured surface displayed in Figure 4.26 (a), when added in

10 wt% of ALUM, it can be noted that the composite possessed a rougher surface as compared to other rPVC/ALUM composites at higher loadings but smoother than the surface of the rPVC composite with increasing crack propagation and from the flat surface of the rPVC composite to become a more layered structure. The increasing crack propagation on the surface of the rPVC/ALUM 10 composite indicated that the composite is softer and will crack or break easily when applying excessive stress, which led to the reduction in the ultimate tensile strength in the tensile test in section 4.3.6 as compared to the rPVC composite. In addition, the appearance of matrix tearing on the surface of the rPVC/ALUM 10 composite implied that the composite had a better elongation at break to undergo significant deformation before fracturing. However, no vivid agglomeration of ALUM particles and filler detachment was observed in the surface morphology of the rPVC/ALUM 10 composite, representing good dispersion of ALUM particles in the rPVC matrix to achieve better mechanical properties than other rPVC/ALUM composites of higher loadings (Cionita et al., 2022).

Furthermore, for the rPVC/ALUM 20 and rPVC/ALUM 30 composites with the SEM images of the tensile fractured surface displayed in Figures 4.26 (b) and (c), when added in higher loadings of ALUM, it can be observed that the surface roughness of the composites became more smooth and possessed a more flat surface with separated phases between the ALUM filler and the rPVC matrix. The more flat and smooth surface of the composites at higher ALUM loadings indicated that the composites had a lower resistance to crack propagation with a higher rigidity or stiffer, resulting in decreasing ultimate tensile strength and elongation at break but with increasing modulus as proved in the tensile test in section 4.3.6. Moreover, for the rPVC/ALUM 30 composite with the tensile fractured surface displayed in Figure 4.26 (c), the filler detachment or pull out of the ALUM particles from the surface that led to the formation of voids on the surface can be observed from the figure but not be seen in other rPVC/ALUM composites of lower ALUM loadings. The occurrence of filler detachment on the surface of the rPVC/ALUM 30 composite meant poor interfacial adhesion and weak binding between the rPVC matrix and the ALUM particles with poor dispersion of ALUM particles

within the rPVC matrix, resulting in further reduction of ultimate tensile strength and elongation at break, besides causing the increasing elastic modulus of up to 20 wt% of ALUM to decrease as proved in the tensile test in section 4.3.6 (Feng et al., 2016).

Meanwhile, for the composites of rPVC/LeHigh at different LeHigh loadings, the SEM images of their tensile fractured surfaces under 500x magnification are illustrated in Figures 4.26 (d), (e) and (f), which corresponded to the composites of rPVC/LeHigh 10, rPVC/LeHigh 20 and rPVC/LeHigh 30. For the rPVC/LeHigh 10 composite with the SEM image of the tensile fractured surface depicted in Figure 4.26 (d), when added in 10 wt% of LeHigh, it can be noted that the composite had a smoother surface than the rPVC composite with increasing crack propagation and the appearance of matrix tearing on the surface. The increasing crack propagation on the surface of the rPVC/LeHigh 10 composite also indicated that the composite is softer and will crack or break easily when applying excessive stress, which led to the deduction in the ultimate tensile strength in the tensile test in section 4.3.6 as compared to the rPVC composite. The appearance of matrix tearing on the surface of the rPVC/LeHigh 10 composite also meant that the composite had a better elongation at break to undergo significant deformation before fracturing. Besides that, no vivid agglomeration of LeHigh particles and filler detachment was observed for the rPVC/LeHigh 10 composite, representing good dispersion of LeHigh particles in the rPVC matrix to achieve better mechanical properties than other rPVC/LeHigh composites of higher loadings (Cionita et al., 2022).

When adding higher loadings of LeHigh to the rPVC, the composites seemed to possess a slightly smooth and more flat surface with the SEM images shown in Figures 4.26 (e) and (f), indicating that the composites had a lower resistance to crack propagation and became stiffer with increasing LeHigh loadings, resulting in a decreasing ultimate tensile strength and elongation at break but with increasing modulus as proved in the tensile test in section 4.3.6 for the rPVC/LeHigh 20 and rPVC/LeHigh 30 composites. Additionally, without filler detachment and noticeable agglomeration of LeHigh particles can be seen in Figures 4.26 (e) and (f), but some small voids or gaps

can be noted on the surfaces, especially for the rPVC/LeHigh 30 composite, indicating poor interfacial adhesion between the Lehigh particles and the rPVC matrix at higher loadings with poor dispersion of the Lehigh particles within the rPVC matrix (Luna et al., 2019). The poor interfacial adhesion and incompatibility between the LeHigh particles and the rPVC matrix at higher loadings corroborated with their lower tensile properties in the tensile test in section 4.3.6 of further reduction in the ultimate tensile strength and elongation at break as compared to the rPVC/LeHigh 10 composite.

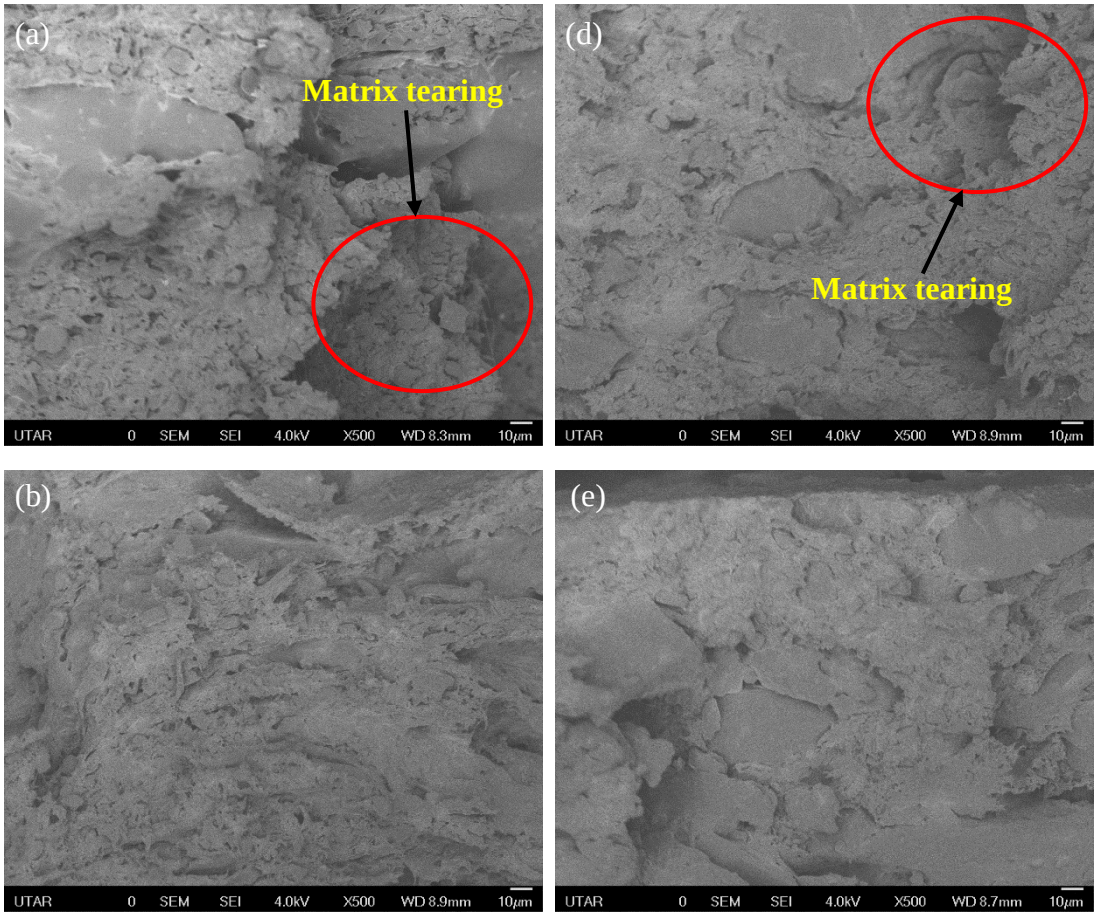

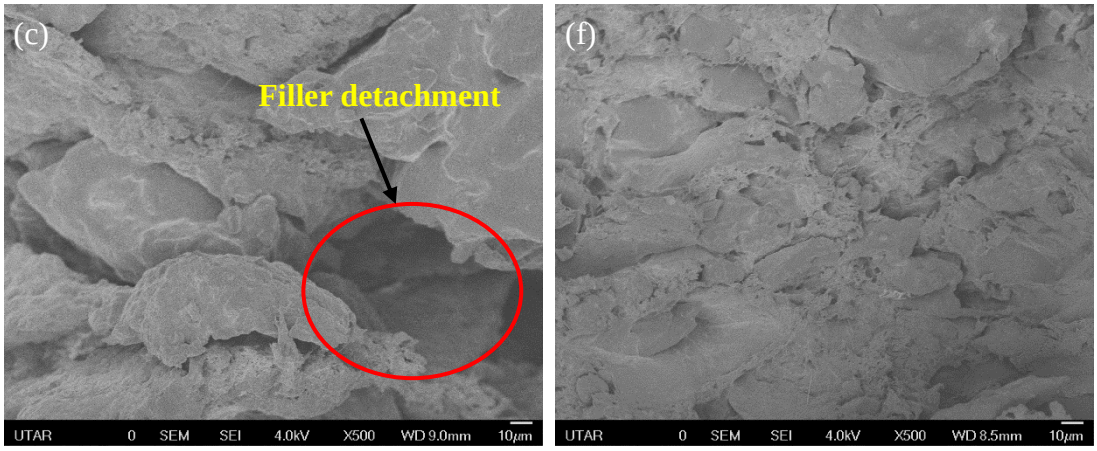

Figure 4.26: SEM Images of rPVC/ALUM and rPVC/LeHigh Composites under 500x Magnification (a) rPVC/ALUM 10 (b) rPVC/ALUM 20 (c) rPVC/ALUM 30 (d) rPVC/LeHigh 10 (e) rPVC/LeHigh 20 (f) rPVC/LeHigh 30

The SEM images of the tensile fractured surfaces of the rPVC/ALUM 30 and rPVC/LeHigh 30 composites under 1000x magnification are illustrated in Figures 4.27 (a) and (b). Under a high magnification of the SEM images of the tensile fractured surfaces of the rPVC/ALUM 30 and rPVC/LeHigh 30 composites, it can be more obviously observed that both of the composites possessed voids or gaps on their surfaces due to the filler particles pull out, indicating poor interfacial adhesion between ALUM and LeHigh particles with the rPVC matrix, as well as incompatibility with poor dispersion of ALUM and LeHigh particles within the rPVC matrix at higher loadings of 30 wt%. The poor interfacial bonding between ALUM and LeHigh particles with the rPVC matrix at higher loadings also further explained the reduction in the ultimate tensile strength and elongation at break in the tensile test in section 4.3.6 when increasing the loadings of ALUM and LeHigh in the rPVC. Besides that, when raising the filler loadings, the filler particles also will have a stronger tendency to agglomerate around the matrix due to their high aspect ratio and low surface energy, resulting in a reduction of the tensile behavior of the composites (Cionita et al., 2022).

Hence, it can be concluded that when increasing loadings of ALUM and LeHigh in the rPVC from 10 wt% to 30 wt%, there will be poorer interfacial interaction and dispersion between ALUM and LeHigh particles with the rPVC matrix, besides increasing the tendency to form filler agglomeration and more voids on the surface of the composites produced due to more filler detachment, leading to reduction in the tensile behavior of the composites.

From Figures 4.27 (a) and (b), there is a larger gap that can be seen between ALUM and rPVC as compared to LeHigh and rPVC. At higher loading, LeHigh shows slightly higher adhesion to rPVC, producing lesser filler detachment and a low tendency to agglomerate as compared to ALUM. The better interfacial adhesion of LeHigh particles with the rPVC matrix also further explained the rPVC/LeHigh composites tended to have better tensile properties than rPVC/ALUM composites, as proved in the tensile test in section 4.3.6. In short, LeHigh has a better dispersion within the rPVC matrix due to its smaller particle size. Due to the large particle size of ALUM, it has a high tendency to form agglomeration with poor dispersion within the rPVC matrix. The large particle size of ALUM can also easily detach from the matrix surface to create gaps or voids on the surface. Thus, it will then lead to the deterioration of the tensile properties of the composites produced. Overall, better interfacial interaction between LeHigh and the rPVC as compared to ALUM resulted in better tensile properties of the rPVC/LeHigh composites with higher ultimate tensile strength, elongation at break and elastic modulus than rPVC/ALUM composites even at different loadings as proved in the tensile test in section 4.3.6.

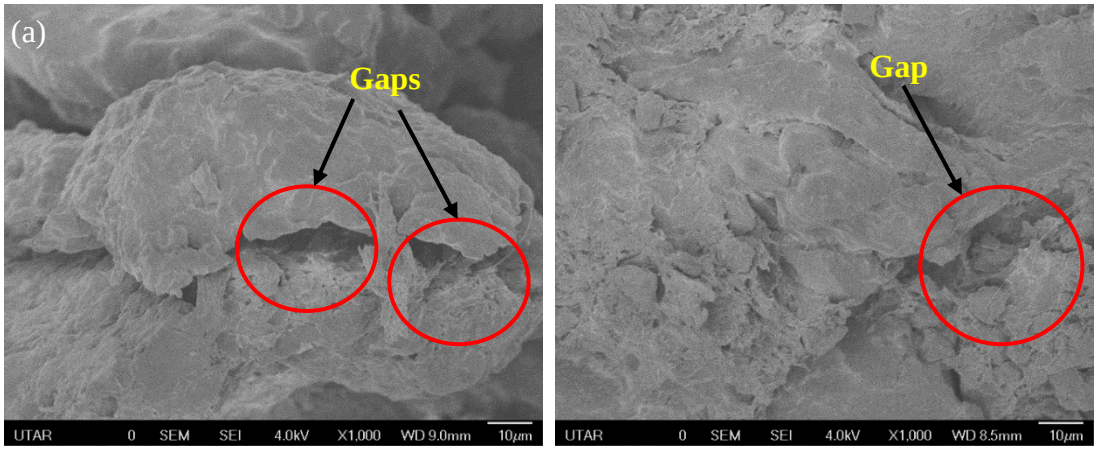

Figure 4.27: SEM Images of rPVC/ALUM and rPVC/LeHigh Composites under 1000x Magnification (a) rPVC/ALUM 30 (b) rPVC/LeHigh 30

Table 4.12: Summary Results based on Standard Specifications for Car Floor Mat Application

Specification	Required Values	rPVC	rPVC/ALUM			rPVC/LeHigh		
			10	20	30	10	20	30
Ultimate tensile strength (MPa)	>5	✓	✓	✓	✗	✓	✓	✓
Elongation at break (%)	>25	✓	✓	✗	✗	✓	✓	✓
Swelling (%)	<2.5	✓	✓	✓	✗	✓	✓	✓
Shore A hardness	90 ± 5	✓	✓	✓	✓	✓	✓	✓
Processability	Homogeneous mixture	✓	✓	✓	✗	✓	✓	✗

∴ The optimum ALUM loading for rPVC/ALUM composites is 10 wt%, while the optimum LeHigh loading for rPVC/LeHigh composites is 20 wt%. LeHigh is preferable to ALUM as it can be used at a higher loading of 20 wt%.

CHAPTER 5

CONCLUSION AND RECOMMENDATIONS

5.1 Conclusion

ALUM and LeHigh particles had been successfully characterized by FTIR, PSA, TGA and SEM. The FTIR spectrum of ALUM proved that it was mainly composed of natural rubber with zinc oxide as an activator, while the FTIR spectrum of LeHigh verified that LeHigh was mainly composed of natural rubber, styrene-butadiene rubber, butadiene rubber and EPDM rubber with zinc oxide as an accelerator. Besides that, for the particle size analysis, ALUM exhibited a mono-modal and left-skewed narrow particle size distribution, suggesting a good uniformity in the particle sizes with moderate variation of particle sizes for less prone to segregation during the melt mixing process and consisted of more fine particles than the coarse particles. However, ALUM particles were considerably coarse with a high mean diameter of 500.722 μm and a small specific surface area of 0.0218 m^2/g, thus causing poor distribution and interfacial adhesion when added to the rPVC matrix. Meanwhile, LeHigh exhibited a mono-modal and left-skewed narrower particle size distribution than ALUM, suggesting a higher degree of uniformity in the particle sizes with a lower variation of particle sizes for less segregation during the melt mixing process and consisted of more fine particles than the coarse particles. Although the LeHigh particles were considerably fine, with a mean

diameter of 51.879 μm and a specific surface area of 0.147 m^2/g, the surface area was still considerably small to cause poor interfacial interaction and poor distribution when added to the rPVC matrix. In addition, the thermogravimetric analysis proved that LeHigh was thermally more stable than ALUM with a higher temperature at 50 % mass loss of 432.63 °C than ALUM of 329.73 °C, besides attaining a higher residue of 33.75 % compared to that of 23.98 % of ALUM due to a lower decomposition rate than ALUM even at high temperature. Lastly, the SEM images of ALUM and LeHigh particles portrayed that ALUM and LeHigh particles possessed irregular particle shapes and rough surfaces with some voids to provide more surface area for better interfacial adhesion with the rPVC matrix. Nevertheless, LeHigh particles proved to have smaller particle sizes with a higher specific surface area than ALUM particles from the SEM images to have more contact surface area with the rPVC matrix to form stronger interfacial adhesion and show better physical interaction via chain interlocking.

The melt mixing process of rPVC with ALUM and LeHigh was performed at different loadings of ALUM and LeHigh to produce the composites through a Brabender Internal Mixer at the processing temperature of 165 °C for 4 minutes with a speed of 60 rpm. However, the maximum achievable ALUM and LeHigh loadings for producing the composites were up to 20 wt% only as the composites formed at 30 wt% of ALUM and LeHigh were not feasible due to the rPVC matrix could not further support the high content of ALUM and LeHigh particles, leading to poor melt mixing of the rPVC with ALUM and LeHigh as well as poor compatibility and poor wetting of ALUM and LeHigh by the rPVC matrix. Afterwards, the rPVC/ALUM and rPVC/LeHigh composites at different loadings were compressed into thin sheets through the hydraulic hot and cold press machine at 170 °C for a total of 15 minutes, including 8 minutes of pre-heat followed by 4 minutes of hot compression and 3 minutes of cooling. The processability of the rPVC/ALUM and rPVC/LeHigh composites with different loadings of ALUM and LeHigh was analyzed through the torque-time curves recorded, in which the melt viscosity of the rPVC/ALUM and rPVC/LeHigh composites increased with increasing ALUM and LeHigh loadings up to 20 wt% with higher values of stabilization

torque observed, indicating that the composites became more difficult to be processed. However, at 30 wt % of ALUM and LeHigh loadings, the values of stabilization torque were reduced as the rPVC matrix could not support the higher ALUM and LeHigh content. Thus, a non-homogeneous composite with un-melted rPVC and crumb-like powder structure is produced at higher filler loading of 30 wt%.

The tensile test of rPVC/ALUM and rPVC/LeHigh composites showed deterioration in their ultimate tensile strength and elongation at break with increasing ALUM and LeHigh loadings due to the lack of interfacial adhesion between the rPVC matrix and the fillers as well as the increasing tendency to form filler agglomeration. On the contrary, the elastic modulus of the composites increased with increasing ALUM and LeHigh loadings, signifying that the composites became stiffer with lower flexibility when more ALUM or LeHigh was incorporated into the rPVC. The incorporation of ALUM and LeHigh of different loadings with the rPVC can also effectively improve the hardness of the composites to become stiffer and more rigid by acting as reinforcing fillers with the presence of carbon black. Furthermore, the water absorption percentage of composites increased with ALUM and LeHigh loadings due to the poorer interfacial interaction with a higher tendency of the filler particles to form more agglomeration when increasing the loadings of ALUM and LeHigh. Yet, the rPVC/LeHigh composites showed a lower water absorption percentage than the rPVC/ALUM composites at different loadings. This indicates better interfacial adhesion and binding of LeHigh as compared to ALUM with the rPVC, as well as better dispersion of LeHigh within the rPVC matrix to form fewer voids with lesser amount of water molecules entrapped.

Moreover, the FTIR analyses that compared FTIR spectra of rPVC/ALUM and rPVC/LeHigh composites at different loadings with rPVC composite did not show any new peak, confirming that there was no chemical reaction occurred between the rPVC with ALUM or LeHigh during the melt mixing process with only physical interaction between the rPVC matrix with ALUM or LeHigh. For the TGA analysis, the rPVC/ALUM composites showed a decreasing trend of the $T_{50\%}$ with increasing ALUM

loading, indicating the decreasing thermal stability of the rPVC/ALUM composites at higher loading, besides displaying an increasing trend of residue % across increasing ALUM loading due to the higher ALUM loading with a higher content of carbon black reinforcing filler that remained undegraded even at a high temperature of 900 °C. Meanwhile, the TGA analysis of rPVC/LeHigh composites at different loadings proved that the incorporation of LeHigh can improve the overall thermal stability of the composites with higher $T_{50\%}$ values and higher residue % due to the higher LeHigh loading with a higher content of carbon black reinforcing filler that remained undecomposed even at a high temperature of 900 °C. The temperatures at 50 % mass loss for the rPVC/LeHigh composites were also generally higher than the rPVC/ALUM composites, indicating the rPVC/LeHigh composites had better thermal stability than the rPVC/ALUM composites. Lastly, the SEM images of the tensile fractured surfaces of the rPVC/ALUM and rPVC/LeHigh composites proved that when increasing loadings of ALUM and LeHigh in the rPVC from 10 wt% to 30 wt%, the interfacial interaction and dispersion between ALUM and LeHigh particles with the rPVC matrix will become poorer, besides increasing the tendency to form filler agglomeration and more voids on the surface of the composites produced due to more filler detachment, leading to a reduction in the water resistance and tensile behavior of the composites. The SEM images also showed that LeHigh had better dispersion within the rPVC matrix due to its smaller particle size, showing better interfacial interaction and bonding than ALUM with a larger particle size, besides resulting in better tensile properties of the rPVC/LeHigh composites than the rPVC/ALUM composites.

For the car floor mat application, the minimum required properties are minimum ultimate tensile strength of 5 MPa, minimum elongation at break of 25 %, maximum water swelling of 2.5 % and Shore A hardness of 90 ± 5. The composite with 10 wt% of ALUM loading was the optimum choice among other rPVC/ALUM composites of different loadings since it satisfied all the above requirement properties for the car floor mat application with the ultimate tensile strength of 10.08 MPa, elongation at break of 52.33 %, water absorption % of 1.118 % and Shore A hardness of 88.13. Meanwhile, the

composite with 20 wt% of LeHigh loading was the optimum choice among other rPVC/LeHigh composites of different loadings since it fulfilled all the above requirement properties for the car floor mat application with the ultimate tensile strength of 8.79 MPa, elongation at break of 44.10 %, water absorption % of 0.783 % and Shore A hardness of 88.81. However, LeHigh will be preferable to ALUM as it can be used at a higher loading of 20 wt%.

5.2 Recommendation

Several recommendations can be made for the improvement of the rPVC/ALUM and rPVC/LeHigh composites in terms of their mechanical properties:

- Introduction of compatibilizer to enhance the interfacial adhesion between the rPVC matrix and ALUM or LeHigh particles, besides improving their mechanical properties. However, usage of compatibilizer would incur higher manufacturing costs for the composites.
- Increase the mixing time and speed of the rotor during the melt mixing process to allow better dispersion of the ALUM and LeHigh particles in PVC, especially at a higher loading of >20 wt%.
- Employ different mixing methods, such as extrusion or heated two-roll mill, which allows a higher amount of material input and higher shearing action for the melt mixing process to form composite compared to the Brabender internal mixer.

REFERENCES

Achukwu, E.O. et al. (2015) 'Nigerian Journal of Materials Science and Engineering', FABRICATION OF PALM KERNEL SHELL EPOXYCOMPOSITES AND STUDY OF THEIRMECHANICAL PROPERTIES, 6(1).

Ahmad, A. et al. (2021) 'Nanomaterial Synthesis Protocols', Nanomedicine Manufacturing and Applications, pp. 73–85. doi:10.1016/b978-0-12-820773-4.00010-x.

Alban, M. (2023). Types of polyvinyl chloride (PVC) products, Chemceed. Available at: https://chemceed.com/product-news/pvc-polyvinyl-chloride-products/ (Accessed: 25 July 2023).

Alias, N.F., Ismail, H. and Ishak, K.M. (2020) 'Comparison of type of rubber in PLA/rubber/Kenaf Biocomposite: Rheological, mechanical and morphological properties', Macromolecular Symposia, 391(1). doi:10.1002/masy.201900128.

Ali Shah, A. et al. (2013) 'Biodegradation of natural and synthetic rubbers: A Review', International Biodeterioration & Biodegradation, 83, pp. 145–157. doi:10.1016/j.ibiod.2013.05.004.

Al-Subari, L., Ekinci, A. and Aydın, E. (2021) 'The utilization of waste rubber tire powder to improve the mechanical properties of cement-clay composites', Construction and Building Materials, 300, p. 124306. doi:10.1016/j.conbuildmat.2021.124306.

Amar, Z. et al. (2019) 'Structural changes undergone during thermal aging and/or processing of unstabilized, dry-blend and rigid PVC, investigated by FTIR-ATR and curve fitting', Annales de Chimie - Science des Matériaux, 43(1), pp. 59–68. doi:10.18280/acsm.430109.

Ammineni, S.P., Nagaraju, C. and Lingaraju, D. (2022) 'Thermal degradation of naturally aged nbr with time and temperature', Materials Research Express, 9(6), p. 065305. doi:10.1088/2053-1591/ac7302.

Amobonye, A.E. et al. (2023). 'Biodegradability of polyvinyl chloride', Biodegradability of Conventional Plastics, pp. 201–220. doi:10.1016/b978-0-323-89858-4.00017-8.

Bajaj, S. (2023). Structure of PVC: A comprehensive overview, PlasticRanger. Available at: https://plasticranger.com/structure-of-pvc/ (Accessed: 23 July 2023).

Barrera, C.S. and Cornish, K. (2022) 'Fly Ash as a potential filler for the rubber industry', Handbook of Fly Ash, pp. 763–792. doi:10.1016/b978-0-12-817686-3.00010-4.

Behl, A., Sharma, G. and Kumar, G. (2014). 'A sustainable approach: Utilization of waste PVC in asphalting of roads', Construction and Building Materials, 54, pp. 113–117. doi:10.1016/j.conbuildmat.2013.12.050.

Benson (2024) Various patterns of car floor mats raw material, Henan Bensen Industry Co.,Ltd. Available at: https://www.carsleather.com/various-patterns-of-car-floor-mats-raw-material-product/#:~:text=Generally%20speaking%2C%20artificial%20leather%2C%20which,also%20more%20beautiful%20and%20comfortable. (Accessed: 06 May 2024).

Bin Bakri, M.K. et al. (2022). 'Resources and energy recovery with recycled plastic biocomposites', Recycled Plastic Biocomposites, pp. 261–280. doi:10.1016/b978-0-323-88653-6.00004-3.

Blengini, G.A. et al. (2017) Assessment of the methodology for establishing the EU List of Critical Raw Materials Background Report. Luxembourg: Publications Office.

Boon, Z.H., Teo, Y.Y. and Ang, D.T.-C. (2022) 'Recent development of biodegradable synthetic rubbers and bio-based rubbers using sustainable materials from biological sources', RSC Advances, 12(52), pp. 34028–34052. doi:10.1039/d2ra06602e.

Borah, R. and Verbruggen, S.W. (2022) ‘Effect of size distribution, skewness and roughness on the optical properties of colloidal plasmonic nanoparticles’, Colloids and Surfaces A: Physicochemical and Engineering Aspects, 640, p. 128521. doi:10.1016/j.colsurfa.2022.128521.

Burns, K. et al. (2023) ‘A comparative assessment of the use of suitable analytical techniques to evaluate plasticizer compatibility’, Journal of Applied Polymer Science, 140(30). doi:10.1002/app.54104.

Chen, J. et al. (2018) ‘Thermal degradation and plasticizing mechanism of poly(vinyl chloride) plasticized with a novel cardanol derived plasticizer’, IOP Conference Series: Materials Science and Engineering, 292, p. 012008. doi:10.1088/1757-899x/292/1/012008.

Chittella, H. et al. (2021). ‘Rubber Waste Management: A review on methods, mechanism, and prospects’, Polymer Degradation and Stability, 194, p. 109761. doi:10.1016/j.polymdegradstab.2021.109761.

Cionita, T. et al. (2022) ‘The influence of filler loading and alkaline treatment on the mechanical properties of palm kernel cake filler reinforced epoxy composites’, Polymers, 14(15), p. 3063. doi:10.3390/polym14153063.

Colom, X. et al. (2013) ‘Acoustic and mechanical properties of recycled polyvinyl chloride/ground tyre rubber composites’, Journal of Composite Materials, 48(9), pp. 1061–1069. doi:10.1177/0021998313482154.

Comanita, E.-D. et al. (2020). ‘Environmental impacts of polyvinyl chloride (PVC) production process’, 2015 E-Health and Bioengineering Conference (EHB) [Preprint]. doi:10.1109/ehb.2015.7391486.

Comprehensive guide on polyvinyl chloride (PVC). (2023). Polyvinyl Chloride (PVC) Plastic: Uses, Properties, Benefits & Toxicity. Available at: https://omnexus.specialchem.com/selection-guide/polyvinyl-chloride-pvc-plastic (Accessed: 22 July 2023).

Cruz, R.L. et al. (2020) 'Advancements in soft-tissue prosthetics part B: The Chemistry of Imitating Life', Frontiers in Bioengineering and Biotechnology, 8. doi:10.3389/fbioe.2020.00147.

Daud, S., Ismail, H. and Bakar, A.A. (2016) 'The effect of 3-aminopropyltrimethyoxysilane (AMEO) as a coupling agent on curing and mechanical properties of natural rubber/palm kernel shell powder composites', Procedia Chemistry, 19, pp. 327–334. doi:10.1016/j.proche.2016.03.019.

Dincer, I. and Bicer, Y. (2018). '1.27 life cycle assessment of Energy', Comprehensive Energy Systems, pp. 1042–1084. doi:10.1016/b978-0-12-809597-3.00134-6.

Djafari Petroudy, S.R. (2017) 'Physical and mechanical properties of natural fibers', Advanced High Strength Natural Fibre Composites in Construction, pp. 59–83. doi:10.1016/b978-0-08-100411-1.00003-0.

Dobrovská, J. et al. (2024) 'Pyrolysis of natural rubber–cellulose composites: Isoconversional kinetic analysis based on thermogravimetric data', Journal of Thermal Analysis and Calorimetry [Preprint]. doi:10.1007/s10973-024-12933-y.

Elfakhri, F. et al. (2022) 'Influence of filler characteristics on the performance of Dental Composites: A comprehensive review', Ceramics International, 48(19), pp. 27280–27294. doi:10.1016/j.ceramint.2022.06.314.

Fan, H. et al. (2016) 'Kinetic analysis of the thermal decomposition of latex foam according to thermogravimetric analysis', International Journal of Polymer Science, 2016, pp. 1–7. doi:10.1155/2016/8620879.

Farida, E. et al. (2019) 'The effect of carbon black composition in natural rubber compound', Case Studies in Thermal Engineering, 16, p. 100566. doi:10.1016/j.csite.2019.100566.

Farinha, C., Brito, J. de and Veiga, M.D. (2021). 'Life cycle assessment', Eco-Efficient Rendering Mortars, pp. 205–234. doi:10.1016/b978-0-12-818494-3.00008-8.

Fazli, A. and Rodrigue, D. (2020) 'Recycling waste tires into ground tire rubber (gtr)/rubber compounds: A Review', Journal of Composites Science, 4(3), p. 103. doi:10.3390/jcs4030103.

Fazli, A. and Rodrigue, D. (2020) 'Waste rubber recycling: A review on the evolution and properties of thermoplastic elastomers', Materials, 13(3), p. 782. doi:10.3390/ma13030782.

Feng, B. et al. (2023). 'Waste PVC upcycling: Transferring unmanageable CL species into value-added Cl-Containing Chemicals', Applied Catalysis B: Environmental, 331, p. 122671. doi:10.1016/j.apcatb.2023.122671.

Feng, J., Venna, S.R. and Hopkinson, D.P. (2016) 'Interactions at the interface of polymer matrix-filler particle composites', Polymer, 103, pp. 189–195. doi:10.1016/j.polymer.2016.09.059.

Fråne, A. et al. (2019). 'PVC waste treatment in the Nordic countries', TemaNord [Preprint]. doi:10.6027/tn2019-501.

Gohatre, O.K. et al. (2020) 'Study on thermal, mechanical and morphological properties of recycled poly(vinyl chloride)/fly ash composites', Polymer International, 69(6), pp. 552–563. doi:10.1002/pi.5988.

Green, J.L. et al. (2023) 'Descriptive statistics', International Encyclopedia of Education(Fourth Edition), pp. 723–733. doi:10.1016/b978-0-12-818630-5.10083-1.

Hayeemasae, N. and Ismail, H. (2020) 'Synergistic improvement of mechanical and magnetic properties of a new magnetorheological elastomer composites based on natural rubber and powdered waste natural rubber glove', Polímeros, 30(2). doi:10.1590/0104-1428.10719.

Hlobil, M., Kumpová, I. and Hlobilová, A. (2022) 'Surface area and size distribution of cement particles in hydrating paste as indicators for the conceptualization of a cement paste representative volume element', Cement and Concrete Composites, 134, p. 104798. doi:10.1016/j.cemconcomp.2022.104798.

Ibrahim, S. et al. (2019) 'Biopolymers from crop plants', Reference Module in Materials Science and Materials Engineering [Preprint]. doi:10.1016/b978-0-12-803581-8.11573-5.

Industrial Quick Search. (2023). Polyvinyl Chloride (PVC): Types, Benefits, Applications, and Characteristics. Available at: https://www.iqsdirectory.com/articles/plastic-tubing/pvc-tubing.html (Accessed: 22 July 2023).

'Introduction to rubber' (2021). Rubber to Rubber Adhesion, pp. 1–30. doi:10.1002/9781119769354.ch1.

Irina, T. and Timo, K. (2020) 'Recycled PVC as material for natural fiber composite manufacturing—study of mechanical performance and durability', The Journal of Solid Waste Technology and Management, 46(1), pp. 36–43. doi:10.5276/jswtm/2020.36.

Isayev, A.I. (2013) 'Recycling of Rubbers', The Science and Technology of Rubber, pp. 697–764. doi:10.1016/b978-0-12-394584-6.00020-0.

Jiang, Z. and Zhou, C. (2023) 'Retracted: Predicting the elastic modulus of nanoparticle-reinforced polymer matrix composites based on digital image processing and finite elements', Advances in Materials Science and Engineering, 2023, pp. 1–1. doi:10.1155/2023/9857328.

J. Schaefer, R. (2018). CHAPTER 33 MECHANICAL PROPERTIES OF RUBBER, 8434 harris 33 B - MTEC a member of NSTDA. Available at: https://www.mtec.or.th/wp-content/uploads/2018/04/mechanical-properties_rubber.pdf (Accessed: 05 August 2023).

kadum abd-ali, N. (2017) Rubber in Engineering Applications (Experimental Series). LAP Lambert Acadimic Publishing.

Kanny, K. and Mohan, T.P. (2017) 'Rubber nanocomposites with nanoclay as the filler', Progress in Rubber Nanocomposites, pp. 153–177. doi:10.1016/b978-0-08-100409-8.00005-x.

Khan, A. et al. (2022) 'Preparation of styrene-butadiene rubber (SBR) composite incorporated with collagen-functionalized graphene oxide for Green Tire Application', Gels, 8(3), p. 161. doi:10.3390/gels8030161.

Kim, Y.N. and Jung, Y.C. (2022) 'Natural rubber-based polymer blends and Composites', Biodegradable Polymers, Blends and Composites, pp. 19–37. doi:10.1016/b978-0-12-823791-5.00002-8.

Koay, S.C. et al. (2017) 'Influence of filler loading and palm oil‐based green coupling agent on torque rheological properties of polypropylene/cocoa pod husk composites', Advances in Polymer Technology, 37(6), pp. 2246–2252. doi:10.1002/adv.21883.

Kundie, F. et al. (2018) 'Effects of filler size on the mechanical properties of polymer-filled dental composites: A review of recent developments', Journal of Physical Science, 29(1), pp. 141–165. doi:10.21315/jps2018.29.1.10.

L Bertrand, G., Johns, D. and Guess, J. (2023) Dipole-dipole interactions, Chemistry LibreTexts. Available at: https://chem.libretexts.org/Bookshelves/Physical_and_Theoretical_Chemistry_Textbook_Maps/Supplemental_Modules_(Physical_and_Theoretical_Chemistry)/Physical_Properties_of_Matter/Atomic_and_Molecular_Properties/Intermolecular_Forces/Specific_Interactions/Dipole-Dipole_Interactions (Accessed: 1 April 2024).

Leong, S.-Y. et al. (2022). '4R of Rubber Waste Management: Current and outlook', Journal of Material Cycles and Waste Management, 25(1), pp. 37–51. doi:10.1007/s10163-022-01554-y.

Lewandowski, K. and Skórczewska, K. (2022). 'A brief review of poly(vinyl chloride) (PVC) recycling', Polymers, 14(15), p. 3035. doi:10.3390/polym14153035.

Ling, P.A., Ismail, H. and Bakar, A.A. (2016) 'Influence of Kenaf (KNF) loading on processing torque and water absorption properties of KNF-filled linear low-density polyethylene/poly (vinyl alcohol) (LLDPE/PVA) composites', Procedia Chemistry, 19, pp. 505–509. doi:10.1016/j.proche.2016.03.045.

Li, X., Xu, X. and Liu, Z. (2020) 'Cryogenic grinding performance of scrap tire rubber by devulcanization treatment with ScCO2', Powder Technology, 374, pp. 609–617. doi:10.1016/j.powtec.2020.07.026.

Lo Presti, D. (2013) 'Recycled tyre rubber modified bitumens for road asphalt mixtures: A literature review', Construction and Building Materials, 49, pp. 863–881. doi:10.1016/j.conbuildmat.2013.09.007.

Lu, L. et al. (2023). 'Chemical Recycling Technologies for PVC waste and PVC-containing plastic waste: A Review', Waste Management, 166, pp. 245–258. doi:10.1016/j.wasman.2023.05.012.

Luna, C.B. et al. (2019) 'Incorporation of a recycled rubber compound from the shoe industry in polystyrene: Effect of SBS compatibilizer content', Journal of Elastomers & Plastics, 52(1), pp. 3–28. doi:10.1177/0095244318819213.

Luo, Y.M. et al. (2022) 'Effects of dioctyl phthalate on performance of Asphalt Sealant', Advances in Materials Science and Engineering, 2022, pp. 1–12. doi:10.1155/2022/5385586.

Machado, M. and Webster, T. (2017) 'Lipase degradation of plasticized polyvinyl chloride endotracheal tube surfaces to create nanoscale features', International Journal of Nanomedicine, Volume 12, pp. 2109–2115. doi:10.2147/ijn.s130608.

Miliute-Plepiene, J., Fråne, A. and Almasi, A.M. (2021). 'Overview of polyvinyl chloride (PVC) waste management practices in the Nordic countries', Cleaner Engineering and Technology, 4, p. 100246. doi:10.1016/j.clet.2021.100246.

M. Subitha et al. (2022) 'Synthesis, characterization and study on enhanced hydrophobicity of novel PVC-Mos2 composites for biomedical applications', Journal of Pharmaceutical Negative Results, 13(SO3). doi:10.47750/pnr.2022.13.s03.169.

Nagrale, A. et al. (2023) 'Influence of filler particle sizes on the physical properties of bulk-fill composites compared to conventional composites', Cureus [Preprint]. doi:10.7759/cureus.36032.

Nandiyanto, A.B., Ragadhita, R. and Fiandini, M. (2022) 'Interpretation of Fourier Transform Infrared Spectra (FTIR): A practical approach in the polymer/plastic thermal decomposition', Indonesian Journal of Science and Technology, 8(1), pp. 113–126. doi:10.17509/ijost.v8i1.53297.

Nuzaimah, M. et al. (2018). 'Recycling of waste rubber as fillers: A Review', IOP Conference Series: Materials Science and Engineering, 368, p. 012016. doi:10.1088/1757-899x/368/1/012016.

Okafor, C. et al. (2020) 'Implementation of circular economy principles in management of end-of-life tyres in a developing country (Nigeria)', AIMS Environmental Science, 7(5), pp. 406–433. doi:10.3934/environsci.2020027.

Oriplast. (2022). The advantages of PVC pipes in building and construction, Oriplast. Available at: https://oriplast.com/the-advantages-of-pvc-pipes-in-building-and-construction/ (Accessed: 25 July 2023).

ÖRÜCÜ, E. and ATILGAN TÜRKMEN, B. (2022) 'Evaluating the sustainability of Car Mat Manufacturing', Sustainable Materials and Technologies, 32. doi:10.1016/j.susmat.2022.e00402.

Osmanski, S. (2020). Why is PVC bad for the environment?, Green Matters. Available at: https://www.greenmatters.com/p/why-is-pvc-bad-environment#:~:text=and%20DDT%20pesticides.-,Hundreds%20of%20chlorine%2Dbased%20toxins%20are%20building%20up%20in%20the,dioxin%20and%20dioxin%2Dlike%20compounds (Accessed: 16 July 2023).

Parameshwaran, R. et al. (2018) 'Applications of thermal analysis to the study of phase-change materials', Recent Advances, Techniques and Applications, pp. 519–572. doi:10.1016/b978-0-444-64062-8.00005-x.

Paulthangam, K.M. et al. (2022) 'Role of zinc oxide in the compounding formulation on the growth of nonstoichiometric copper sulfide nanostructures at the brass–rubber interface', ACS Omega, 7(11), pp. 9573–9581. doi:10.1021/acsomega.1c06207.

Plinke, E. et al. (2000). Mechanical recycling of PVC Wastes: Study for DG XI of the European Commission. Basel: Prognos A.G.

Prestes, S.M. et al. (2011). ‘Construction and demolition waste as a source of PVC for recycling’, Waste Management & Research: The Journal for a Sustainable Circular Economy, 30(2), pp. 115–121. doi:10.1177/0734242x11413329.

PVC properties. (2019). Vinidex Pty Ltd. Available at: https://www.vinidex.com.au/technical-resources/material-properties/pvc-properties/ (Accessed: 21 July 2023).

Radzi, A.M. et al. (2019) ‘Water absorption, thickness swelling and thermal properties of Roselle/sugar palm fibre reinforced thermoplastic polyurethane hybrid composites’, Journal of Materials Research and Technology, 8(5), pp. 3988–3994. doi:10.1016/j.jmrt.2019.07.007.

Rahmah, M. et al. (2019) ‘Oven ageing versus UV ageing properties of natural rubber cup lump/EPDM rubber blend with Mangosteen Powder (MPP) as natural antioxidant’, IOP Conference Series: Materials Science and Engineering, 548(1), p. 012014. doi:10.1088/1757-899x/548/1/012014.

Rowhani, A. and Rainey, T. (2016) ‘Scrap tyre management pathways and their use as a fuel—a review’, Energies, 9(11), p. 888. doi:10.3390/en9110888.

Ruey Ong, H. et al. (2021) ‘The influence of waste tire powder on the properties of waste tire powder/polypropylene plastic composite’, IOP Conference Series: Materials Science and Engineering, 1092(1), p. 012003. doi:10.1088/1757-899x/1092/1/012003.

Saba, N., Jawaid, M. and Sultan, M.T.H. (2019) ‘An overview of mechanical and physical testing of composite materials’, Mechanical and Physical Testing of Biocomposites, Fibre-Reinforced Composites and Hybrid Composites, pp. 1–12. doi:10.1016/b978-0-08-102292-4.00001-1.

Sadat-Shojai, M. and Bakhshandeh, G.-R. (2011). ‘Recycling of PVC Wastes’, Polymer Degradation and Stability, 96(4), pp. 404–415. doi:10.1016/j.polymdegradstab.2010.12.001.

Sathiskumar, C. and Karthikeyan, S. (2019) 'Recycling of waste tires and its energy storage application of by-products –A Review', Sustainable Materials and Technologies, 22. doi:10.1016/j.susmat.2019.e00125.

Senhadji, Y. et al. (2019) 'Physical, mechanical and thermal properties of lightweight composite mortars containing recycled polyvinyl chloride', Construction and Building Materials, 195, pp. 198–207. doi:10.1016/j.conbuildmat.2018.11.070.

Shamsuri, A.A. et al. (2015) 'A preliminary investigation on processing, mechanical and thermal properties of polyethylene/kenaf biocomposites with dolomite added as secondary filler', Journal of Composites, 2015, pp. 1–7. doi:10.1155/2015/760909.

Siraj, S. et al. (2022) 'Impact of micro silica filler particle size on mechanical properties of polymeric based composite material', Polymers, 14(22), p. 4830. doi:10.3390/polym14224830.

Sisanth, K.S. et al. (2017) 'General introduction to rubber compounding', Progress in Rubber Nanocomposites, pp. 1–39. doi:10.1016/b978-0-08-100409-8.00001-2.

Smith, B.C. (2022) 'The infrared spectra of polymers IV: Rubbers', Spectroscopy, pp. 8–12. doi:10.56530/spectroscopy.mz6968v1.

Soomro, N. and Sohaib, Q. (2015) 'Comparative Analysis of Recycled PVC composites reinforced with nonmetals of printed Circuit Boards', SINDH UNIVERSITY RESEARCH JOURNAL (SCIENCE SERIES), 47(3), pp. 431–436.

Sowcharoensuk, C. (2023) Industry outlook 2023-2025: Rubber Processing, Industry Outlook 2023-2025: Rubber Processing. Available at: https://www.krungsri.com/en/research/industry/industry-outlook/agriculture/rubber/io/rubber-2023-2025 (Accessed: 23 April 2024).

Staff, C.M. (2016). Everything you need to know about PVC plastic, Everything You Need To Know About PVC Plastic. Available at: https://www.creativemechanisms.com/blog/everything-you-need-to-know-about-pvc-plastic (Accessed: 19 July 2023).

Sun, H. et al. (2023) 'Influence of the physical morphological characteristics of mineral fillers on the bitumen-filler interfacial interaction', Construction and Building Materials, 378, p. 131206. doi:10.1016/j.conbuildmat.2023.131206.

Surya, I., Maulina, S. and Ismail, H. (2018) 'Effects of alkanolamide and epoxidation in natural rubber and epoxidized natural rubbers compounds', IOP Conference Series: Materials Science and Engineering, 299, p. 012061. doi:10.1088/1757-899x/299/1/012061.

Tang, G., Hu, Y. and Song, L. (2013) 'Study on the flammability and thermal degradation of a novel intumescent flame retardant EPDM composite', Procedia Engineering, 62, pp. 371–376. doi:10.1016/j.proeng.2013.08.078.

The PVC production process explained. (2023). PVC Forum. Available at: http://www.seepvcforum.com/en/content/8-the-pvc-production-process-explained (Accessed: 25 July 2023).

Tuladhar, R., Marshall, A. and Sivakugan, N. (2020) 'Use of recycled concrete aggregate for pavement construction', Advances in Construction and Demolition Waste Recycling, pp. 181–197. doi:10.1016/b978-0-12-819055-5.00010-3.

Valavanidis, A. (2023). Plastic Waste Biodegradation. Bio-recycling by microbial enzymes can be a potential solution to plastic waste management?. [online] Available at: https://www.researchgate.net/publication/370985315_Plastic_Waste_Biodegradation_Bio-recycling_by_microbial_enzymes_can_be_a_potential_solution_to_plastic_waste_management [Accessed 13 July 2023].

Vijayan, K., Muniyadi, M. and Munusamy, Y. (2021) 'Impact modified polyvinyl chloride based thermoplastic elastomers: Effect of nitrile butadiene rubber and graphene oxide loading', Journal of Engineering Science, 17(1), pp. 51–74. doi:10.21315/jes2021.17.1.4.

Waghmare, J. (2023) Plastics industry to grow up because of the increasing demand for plastic polymers across the Globe, LinkedIn. Available at: https://www.linkedin.com/pulse/plastics-industry-grow-up-because-increasing-demand-plastic-waghmare/ (Accessed: 23 April 2024).

Wan, L. et al. (2020) ‘Flame retardation of natural rubber: Strategy and recent progress’, Polymers, 12(2), p. 429. doi:10.3390/polym12020429.

Wheeler, R.N. (1981). ‘Poly (vinyl chloride) processes and products.’, Environmental Health Perspectives, 41, pp. 123–128. doi:10.1289/ehp.8141123.

Wypych, G. (2016) ‘Physical properties of fillers and filled materials’, Handbook of Fillers, pp. 303–371. doi:10.1016/b978-1-895198-91-1.50007-5.

Xometry, T. (2023) Hardness testing: Definition, how it works, types, and benefits, Xometrys RSS. Available at: https://www.xometry.com/resources/materials/hardness-testing/ (Accessed: 22 April 2024).

Yamamoto, Y. et al. (2018) ‘Thermal degradation of deproteinized natural rubber’, Polymer Degradation and Stability, 156, pp. 144–150. doi:10.1016/j.polymdegradstab.2018.08.003.

Ye, F. et al. (2019) ‘Synthesis and study of zinc orotate and its synergistic effect with commercial stabilizers for stabilizing poly(vinyl chloride)’, Polymers, 11(2), p. 194. doi:10.3390/polym11020194.

Yehia, A.A. (2004) ‘Recycling of Rubber Waste’, Polymer-Plastics Technology and Engineering, 43(6), pp. 1735–1754. doi:10.1081/ppt-200040086.

Yu, J. et al. (2016) ‘Thermal degradation of PVC: A Review’, Waste Management, 48, pp. 300–314. doi:10.1016/j.wasman.2015.11.041.

Zhu, J., Abeykoon, C. and Karim, N. (2021) ‘Investigation into the effects of fillers in polymer processing’, International Journal of Lightweight Materials and Manufacture, 4(3), pp. 370–382. doi:10.1016/j.ijlmm.2021.04.003.

APPENDICES

APPENDIX A: Derivative Thermogravimetry

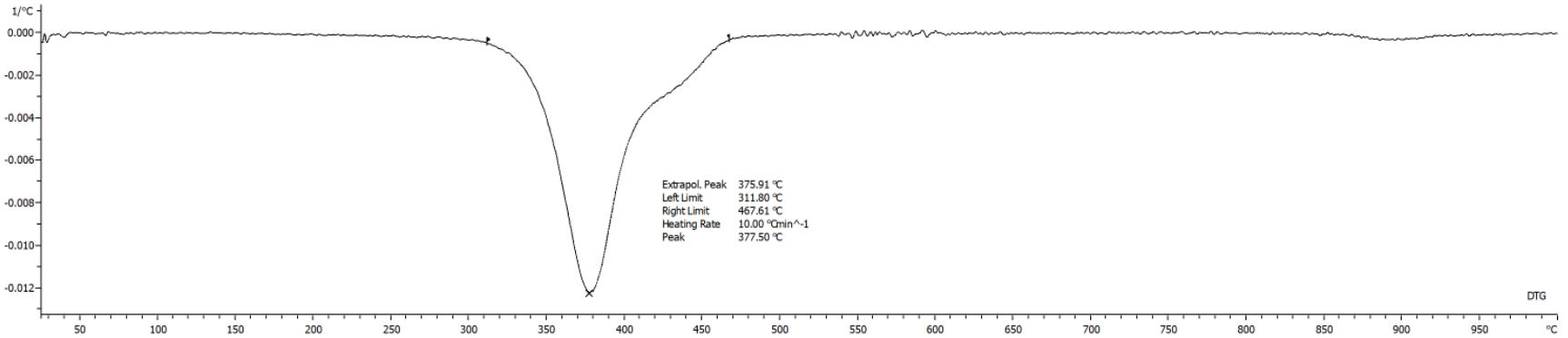

DTG of ALUM

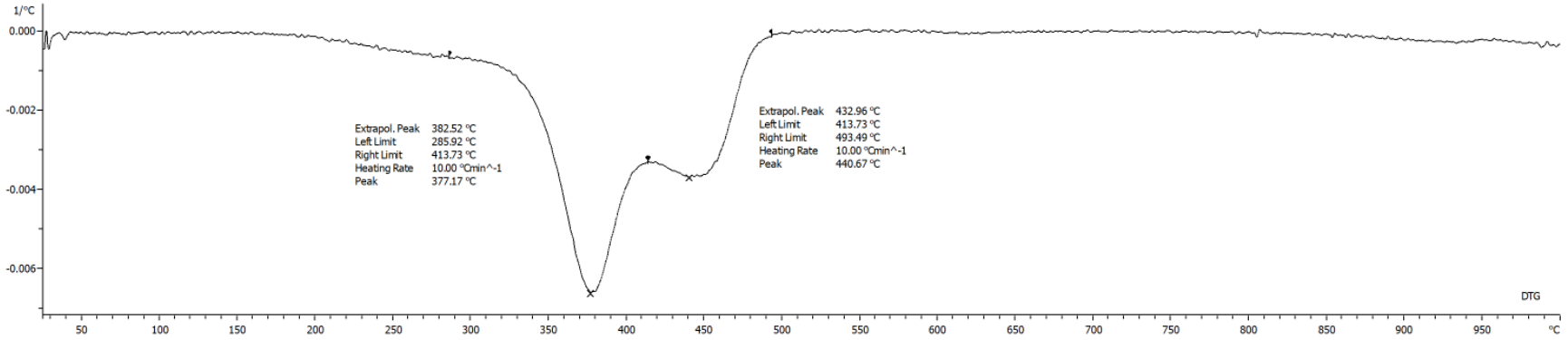

DTG of LeHigh

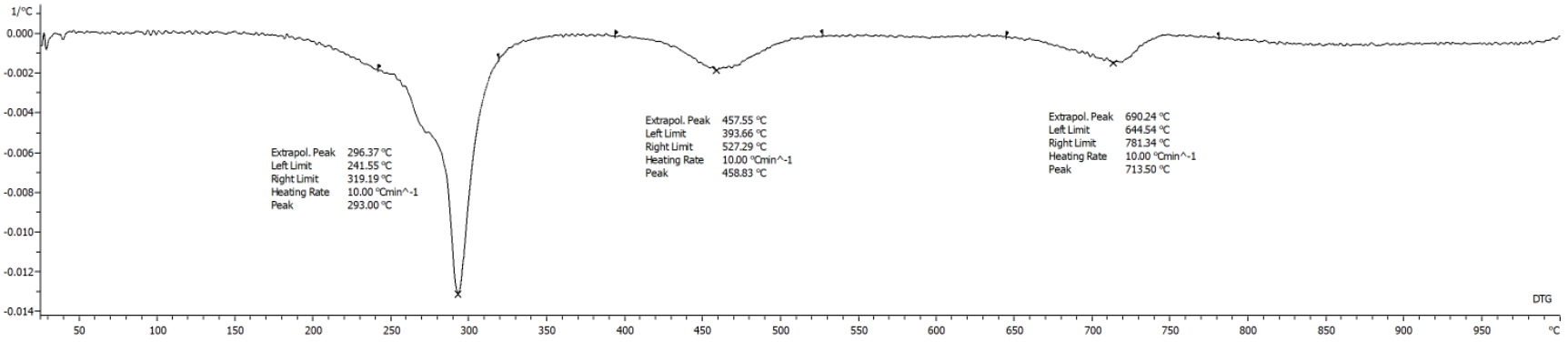

DTG of Recycled PVC Composite

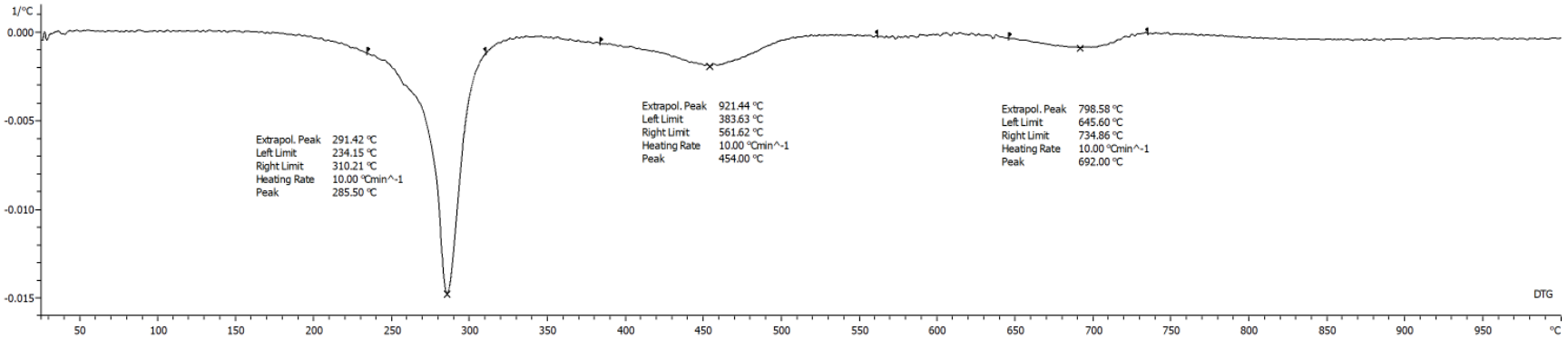

DTG of rPVC/ALUM 10 Composite

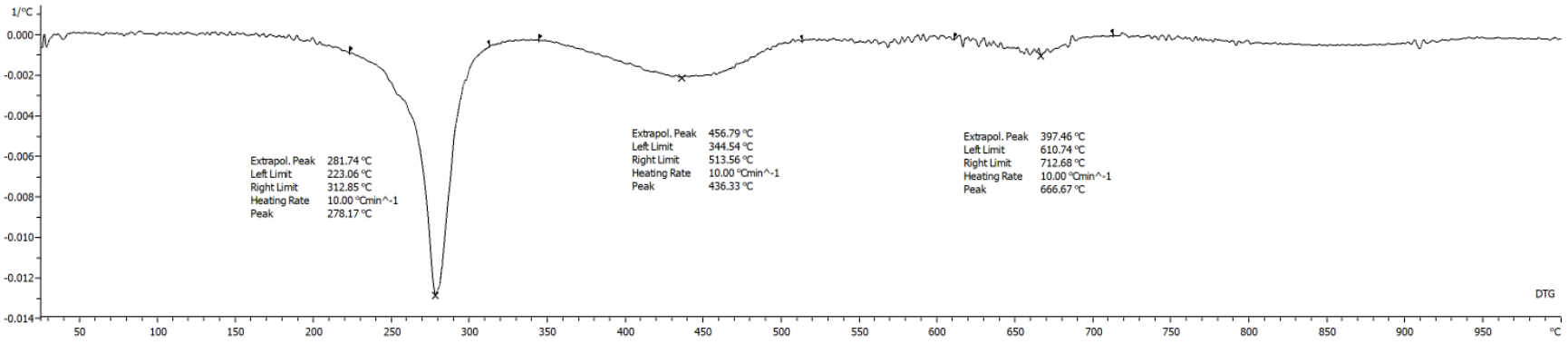

DTG of rPVC/ALUM 20 Composite

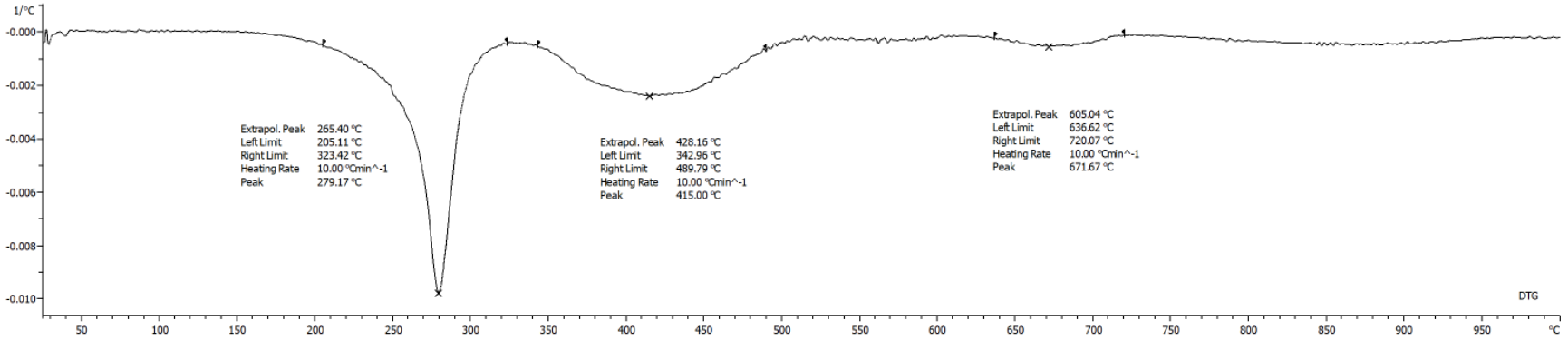

DTG of rPVC/ALUM 30 Composite

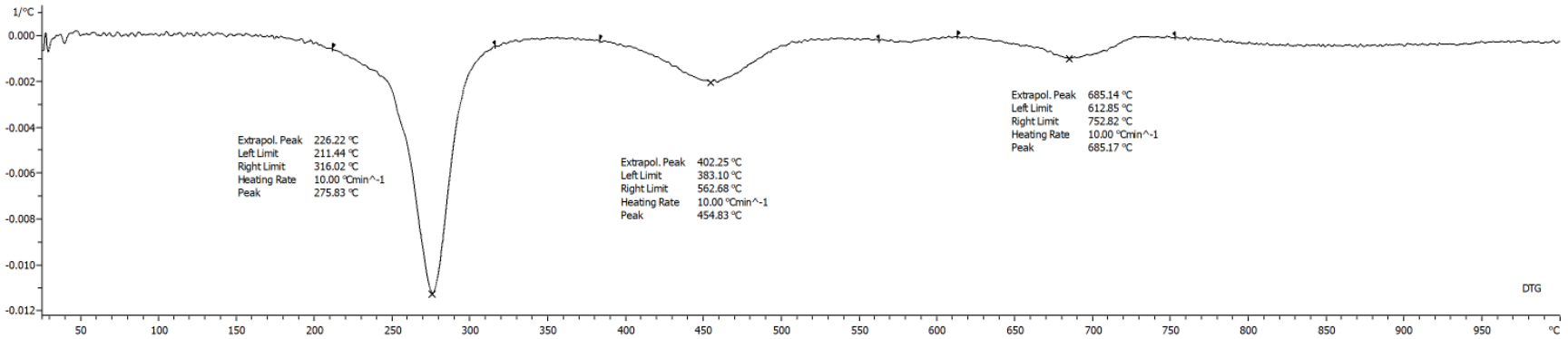

DTG of rPVC/LeHigh 10 Composite

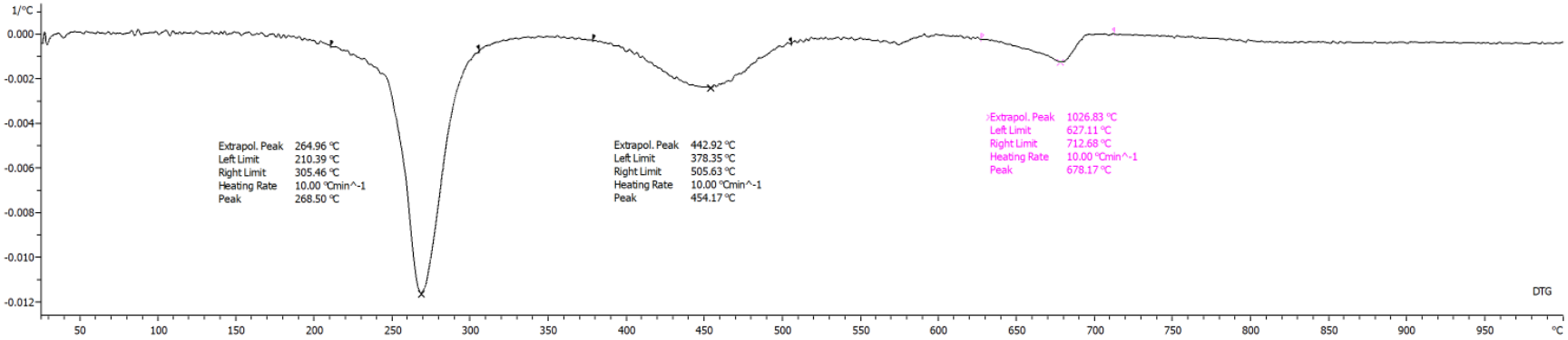

DTG of rPVC/LeHigh 20 Composite

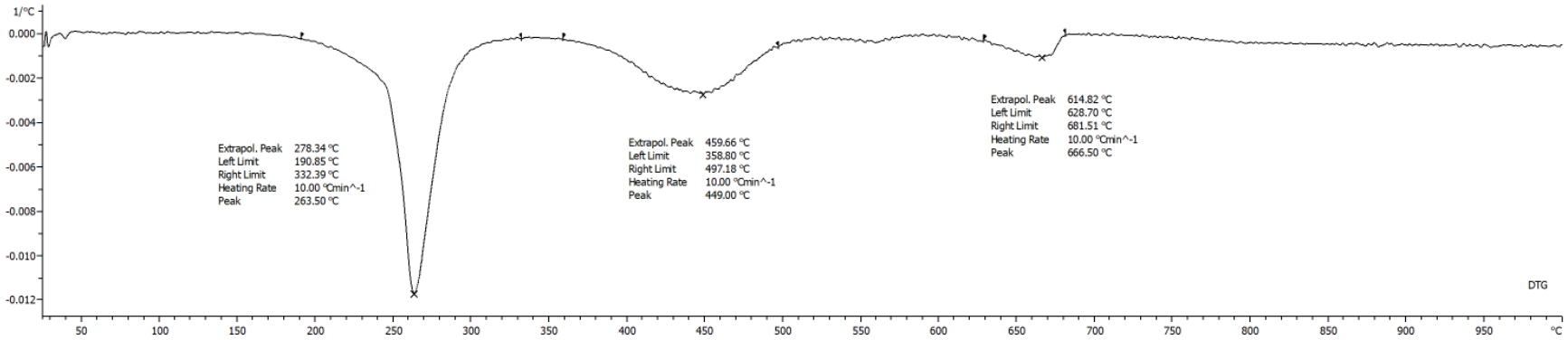

DTG of rPVC/LeHigh 30 Composite